



UNIwersYTET MEDYCZNY
IM. PIASTÓW ŚLĄSKICH WE WROCLAWIU

Katedra i Zakład Biofizyki i Neurobiologii

Katarzyna Terejko

**„Wpływ wybranych mutacji w domenie zewnątrzkomórkowej na
wiązanie neuroprzekaźnika i bramkowanie rekombinowanego
receptora GABA_A typu $\alpha_1\beta_2\gamma_2$ ”**

Praca doktorska przygotowana pod kierunkiem

Prof. dr hab. Jerzego W. Mozrzymasa

Wrocław, 2021

Niniejsza rozprawa doktorska stanowi cykl trzech publikacji naukowych opisujących badania zrealizowane w Katedrze i Zakładzie Biofizyki i Neurobiologii Uniwersytetu Medycznego im. Piastów Śląskich we Wrocławiu.

Badania zostały przeprowadzone w ramach grantów przyznanych przez Narodowe Centrum Nauki:

- MAESTRO pt. „Interdyscyplinarne badania molekularnych mechanizmów zmian konformacyjnych związanych z aktywacją receptora GABA_A”, nr grantu: DEC-2015/18/A/NZ1/00395
- OPUS pt. „Molekularne mechanizmy aktywacji i modulacji rekombinowanych receptorów GABA_A przez wybranych agonistów i modulatory”, nr grantu: DEC-2013/11/B/NZ3/00983

Składam serdeczne podziękowania mojemu promotorowi, Panu Prof. dr hab. Jerzemu W. Mozrzymasowi za umożliwienie mi zdobywania cennego doświadczenia naukowego poprzez obfitującą w ambitne wyzwania pracę w swoim zespole. Szczególnie dziękuję za możliwość uczestniczenia w wielu interesujących projektach badawczych i konferencjach naukowych dzięki którym mogłam rozwijać swoje umiejętności i wiedzę oraz budować swój dorobek naukowy. Dziękuję również za pomoc i wsparcie okazywane na przestrzeni okresu studiów doktoranckich oraz za cenne uwagi podczas przygotowywania publikacji naukowych, których jestem współautorem oraz niniejszej rozprawy doktorskiej.

Chciałabym również podziękować moim Najbliższym, w szczególności Mamie i siostrze Magdzie z mężem Mario, za ogromne wsparcie, cierpliwość i wyrozumiałość.

Dziękuję również wszystkim pracownikom i doktorantom Katedry i Zakładu Biofizyki i Neurobiologii za przyjazną atmosferę, życzliwość, udzielane pomoc i doświadczenie, a także za długie i owocne dyskusje naukowe.

SPIS TREŚCI

STRESZCZENIE	5
ABSTRACT	6
WPROWADZENIE	7
1. Receptory GABA _A w układzie nerwowym dorosłych ssaków	7
2. Struktura receptora GABA _A	8
3. Proces aktywacji receptorów GABA _A	9
4. Kinetyka procesu aktywacji receptorów GABA _A	10
5. Modulacja aktywności receptorów GABA _A przez benzodiazepiny	15
CEL I ZAŁOŻENIA PRACY	16
MATERIAŁY I METODY	19
WYKAZ PUBLIKACJI STANOWIĄCYCH ROZPRAWĘ DOKTORSKĄ	22
PUBLIKACJE	23
1. Distinct Modulation of Spontaneous and GABA-Evoked Gating by Flurazepam Shapes Cross Talk Between Agonist-Free and Liganded GABA _A Receptor Activity	23
2. The C loop at the orthosteric binding site is critically involved in GABA _A receptor gating ...	42
3. Interaction between GABA _A receptor α_1 and β_2 subunits at the N-terminal peripheral regions is crucial for receptor binding and gating	58
PODSUMOWANIE I WNIOSKI	71
BIBLIOGRAFIA	74
WYKAZ RYCIN	83
ZAŁĄCZNIKI	84
1. Dorobek naukowy	84
2. Oświadczenia współautorów	86

STRESZCZENIE

Receptory GABA_A to kanały chlorkowe o pentamerycznej budowie do których wiążą się cząsteczki neuroprzekaźnika – kwasu γ -aminomasłowego (GABA) i które pełnią kluczową rolę w szybkiej synaptycznej transmisji hamującej w mózgach dorosłych ssaków. Zaburzenia transmisji GABA-ergicznej mogą prowadzić do poważnych schorzeń neurologicznych, m. in. padaczki, autyzmu, zaburzeń lękowych oraz schizofrenii. Ponadto, aktywność receptorów GABA_A modulowana jest przez związki farmakologiczne takie jak benzodiazepiny, anestetyki i barbiturany, powszechnie stosowane w praktyce klinicznej. Transdukcja sygnału, który prowadzi do aktywacji, obejmuje duże obszary makromolekuły i jest indukowana przez wiązanie agonisty do miejsc wiązania w domenie zewnątrzkomórkowej. Stamtąd dociera do zlokalizowanej w domenie transbłonowej bramki kanału jonowego, powodując jej otwarcie. Co interesujące, sygnał aktywacji rozprzestrzenia się nie tylko wzdłuż osi receptora, lecz również lateralnie – pomiędzy podjednostkami poprzez występowanie lokalnych oddziaływań w strukturze. Jednakże molekularne mechanizmy leżące u podstaw procesu aktywacji receptora GABA_A oraz jego modulacji przez związki farmakologiczne wciąż nie są w pełni poznane.

Niniejsza rozprawa doktorska dotyczy określenia funkcji wybranych aminokwasów zlokalizowanych w obrębie szczytu domeny zewnątrzkomórkowej receptora GABA_A: α_1 F14 i β_2 F31 oraz w miejscu wiązania: β_2 F200, we wspomnianym procesie aktywacji, ze szczególnym uwzględnieniem ich udziału w etapach wiązania neuroprzekaźnika i bramkowania kanału jonowego. Zbadana została także wrażliwość receptorów GABA_A zmutowanych w pozycjach α_1 F64 i β_2 F200 na modulację przez benzodiazepinę, flurazepam. Poprzez zastosowanie punktowej mutagenyzy oraz wykorzystanie techniki elektrofizjologicznej *patch-clamp*, możliwe było rejestrowanie prądów przewodzonych przez rekombinowane receptory GABA_A ekspresjonowane w komórkach linii HEK 293. Analiza oraz modelowanie kinetyczne uzyskanych przebiegów prądowych dostarczyły jednoznacznej informacji na temat roli badanych aminokwasów w wyżej opisanych procesach. Wykazano także w ten sposób występowanie dalekozasięgowych oddziaływań pomiędzy różnymi rejonami struktury receptora, ale także istnienie funkcjonalnego oddziaływania o krótkim zasięgu pomiędzy sąsiadującymi podjednostkami α_1 i β_2 . Badanie wpływu flurazepamu na proces aktywacji wskazało na mechanizm działania tego związku poprzez modulację kluczowego etapu bramkowania, zwanego preaktywacją. Uzyskane wyniki dostarczyły nowych informacji z zakresu relacji pomiędzy strukturą i funkcją receptora GABA_A, które potencjalnie mogą mieć zastosowanie w projektowaniu nowych leków oddziałujących z tym receptorem.

ABSTRACT

GABA_A receptors are pentameric chloride channels that bind the neurotransmitter molecules – γ -aminobutyric acid (GABA) and play a key role in fast synaptic inhibitory transmission in the adult mammalian brain. Dysfunction of the GABA-ergic drive leads to severe neurological disorders such as epilepsy, autism, anxiety and schizophrenia. Moreover, the activity of GABA_A receptors is modulated by many pharmacological compounds, such as benzodiazepines, anesthetics and barbiturates, that are commonly used in the clinical practice. The activation process is initiated with agonist binding to the binding sites located in the extracellular domain. Transduction of the activation signal comprises the whole receptor structure and eventually leads to the opening of channel gate in the transmembrane domain. Additionally, the activation signal can also spread in the lateral direction, between the adjacent receptor subunits due to some local interactions within the structure. However, molecular mechanisms of the GABA_A receptor activation process, as well as the mechanisms of its modulation by pharmacological compounds, remain elusive.

The present doctoral thesis concerns determination of the function of selected amino acid residues, localized at the top of the GABA_A receptor extracellular domain: α_1 F14 and β_2 F31, or in the binding site region: β_2 F200, in the aforementioned processes, with emphasis on their specific role in binding of the neurotransmitter and gating of the ion channel. Sensitivity to benzodiazepine, flurazepam, of GABA_A receptors mutated in the positions α_1 F64 and β_2 F200 was also investigated. Using site-directed mutagenesis and electrophysiological technique *patch clamp*, current traces mediated by recombinant GABA_A receptors expressed in HEK 293 cells were recorded. Kinetic analysis and modeling of the experimental data provided unequivocally the information about the role of the considered residues in the studied processes. Long-distance interactions between different protein regions were proved but also a short-range functional intersubunit interaction between the α_1 and β_2 subunits was also discovered. The investigation of the impact of flurazepam on the GABA_A receptor activation indicated a mechanism of action of this compound that largely modulated a crucial step of gating, known as preactivation. The results shed new light on the issue of the relationship between the structure and the function of GABA_A receptor, an insight that could potentially be relevant in designing new drugs that target the receptor.

WPROWADZENIE

1. Receptory GABA_A w układzie nerwowym dorosłych ssaków

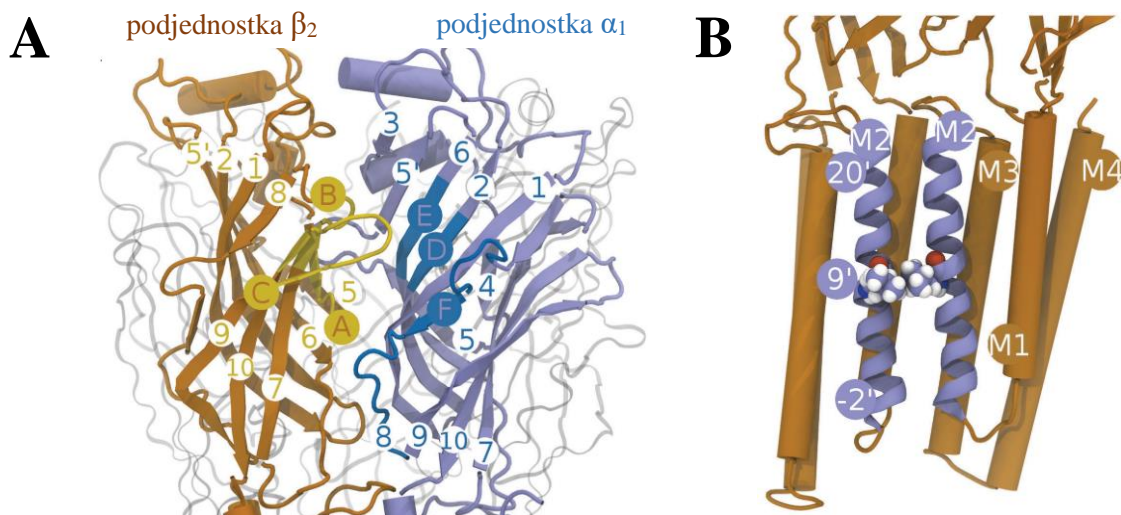
W układzie nerwowym dorosłych ssaków niezwykle ważna jest równowaga pomiędzy pobudzeniem i hamowaniem jego aktywności. Za możliwość szybkiego i precyzyjnego hamowania w mózgu odpowiadają przede wszystkim jonotropowe receptory GABA_A (GABA_AR), poprzez uczestnictwo w szybkiej hamującej transmisji synaptycznej (Cherubini i Conti, 2001; Farrant i Nusser, 2005), podczas gdy w rdzeniu kręgowym dominują receptory glicyny (Du i wsp., 2015; Rajendra i wsp., 1997). Receptory GABA_A to pentameryczne kanały jonowe bramkowane ligandem (pLGICs – ang. „*pentameric Ligand-Gated Ion Channels*”), które należą do rodziny receptorów pętli cysteiny (ang. „*Cys-loop*”) wraz z receptorami acetylocholinylu typu nikotynowego (nAChR), receptorami serotoniny typu 3 (5-HT₃R) i receptorami glicyny (GlyR) (Cederholm i wsp., 2009; Miller i Smart, 2010; Thompson i wsp., 2010), z którymi łączy je także wysokie podobieństwo strukturalne. Receptory GABA_A charakteryzują się niezwykłą różnorodnością funkcjonalną, co spowodowane jest występowaniem aż 19 typów różnych podjednostek (α_{1-6} , β_{1-3} , γ_{1-3} , δ , ϵ , θ , π , ρ_{1-3}), które mogą wchodzić w skład pentameru i tym samym determinować jego właściwości (McKernan i Whiting, 1996; Sieghart, 2000; Sieghart i Savić, 2018). Przykładowo, receptory GABA_A o składzie $\alpha_1\beta\gamma_2$, $\alpha_2\beta\gamma_2$, $\alpha_3\beta\gamma_2$ w przeważającym stopniu są zlokalizowane synaptycznie i uczestniczą w inhibicji fazowej, czyli hamowaniu aktywności sieci neuronalnej poprzez szybką aktywność synaps chemicznych, podczas gdy receptory o składzie $\alpha_4\beta\gamma_2$, $\alpha_5\beta\gamma_2$, $\alpha_6\beta\gamma_2$ lub $\alpha\beta\epsilon$ mogą znajdować się także pozasynaptycznie i uczestniczyć dodatkowo w tonicznej formie inhibicji, która działając w dużo wolniejszej skali czasowej, powoduje obniżenie pobudliwości błony neuronu (Chen i wsp., 2017; Glykys i Mody, 2007; Mody i Pearce, 2004). Jednakże najczęściej występującą postacią receptora w ośrodkowym układzie nerwowym jest forma o składzie podjednostkowym $\alpha_1\beta_2\gamma_2$ i receptor ten zlokalizowany jest głównie synaptycznie. Na dwóch stykach podjednostek α i β są zlokalizowane odpowiednio dwa miejsca wiązania dla agonisty, kwasu γ -aminomasłowego (GABA). Podjednostka β określana jest mianem podjednostki głównej, natomiast podjednostka α określana jest jako uzupełniająca (Farrar i wsp., 1999; Sieghart i Savić, 2018; Smith i Olsen, 1995).

Obecność konkretnych typów podjednostek w danym receptorze GABA_A określa także jego podatność na modulację przez związki farmakologiczne oddziałujące na układ nerwowy (Brickley i Mody, 2012; Jacob i wsp., 2012; Rudolph i Mohler, 2014). Do takich związków należą benzodiazepiny, wykorzystywane w leczeniu epilepsji, bezsenności i zaburzeń

lękowych, barbiturany, dożylnie anestetyki i neurosteroidy (Rudolph i Möhler, 2004, 2006; Berezhnoy i wsp., 2004). Możliwość modulacji receptorów GABA_A przez związki farmakologiczne wynika przede wszystkim z występowania w ich strukturze odpowiednich miejsc wiązania, z którymi się mogą wiązać. Miejsce wiązania dla benzodiazepin znajduje się na styku podjednostek α i γ w domenie zewnątrzkomórkowej receptora (Berezhnoy i wsp., 2004; Hanson i Czajkowski, 2008), pozostałe miejsca wiązania dla barbituranów, anestetyków i neurosteroidów znajdują się w domenie transbłonowej (Kim i wsp., 2020; Seljeset i wsp., 2015).

2. Struktura receptora GABA_A

Jak zostało już wspomniane, receptory GABA_A są kanałami jonowym zbudowanym z pięciu różnych podjednostek (heteropentamery), ale mogą składać się także z podjednostek tego samego rodzaju (homopentamery). Są to duże białka, w których wyodrębnia się kilka domen. Domenę zewnątrzkomórkową stanowi ok. 200-250 aminokwasów przyjmujących formę 10 łańcuchów o strukturze β -kartki. Natomiast strukturę miejsc wiązania znajdujących się w tej domenie tworzą fragmenty białka zwyczajowo określane mianem pętli. Pętłe A, B i C formujące miejsce wiązania pochodzą od jednostki głównej β , podczas gdy pętłe D, E i F od podjednostki komplementarnej α (Ryc. 1A).



Ryc. 1 *Wizualizacja wybranych elementów strukturalnych receptora GABA_A typu $\alpha_1\beta_2\gamma_2$.*
A. Łańcuchy białkowe numerowane 1-10 od N-końca, odpowiednio w podjednostce α_1 i β_2 , wraz z zaznaczeniem pętli A-F tworzących miejsce wiązania w domenie zewnątrzkomórkowej. **B.** Fragment struktury receptora obrazujący wnętrze poru w domenie transbłonowej. Opracowano na podstawie Michałowski i wsp., 2017.

Domenę transbłonową stanowią cztery α -helisy M1, M2, M3 i M4. Helisy M2 tworzą wnętrze poru jonowego, a jego bramkę stanowi przewężenie utworzone przez pięć reszt leucynowych w pozycji 9', gdzie numeracja pozycji odnosi się do kolejności poszczególnych reszt aminokwasowych tworzących por jonowy (Ryc. 1B; Michałowski i wsp., 2017; Miller i Aricescu, 2014; Sigel i Steinmann, 2012). Receptory GABA_A posiadają także niewielką domenę wewnątrzkomórkową, która z reguły jest pomijana w badaniach strukturalnych z uwagi na trudność obrazowania i brak jednoznacznych informacji na temat funkcji w procesie aktywacji.

3. Proces aktywacji receptorów GABA_A

Proces aktywacji receptorów GABA_A oparty jest na sprzężeniu przyłączenia cząsteczki agonisty do miejsc wiązania, z otwarciem bramki kanału jonowego, które umożliwia transport bierny ujemnie naładowanych jonów do wnętrza komórki nerwowej i obniżenie napięcia błonowego (Cederholm i wsp., 2009; Mortensen i wsp., 2004). Jak już wspomniano, receptory GABA_A w swojej strukturze posiadają dwa miejsca wiązania i w warunkach niewysycających mogą pozostawać w stanie nie w pełni związanym, podczas gdy obsadzenie obu tych miejsc określane jest jako stan podwójnie związany. Cząsteczkę agonisty stabilizują w miejscu wiązania głównie oddziaływania π -kationowe, powstające w kontakcie z resztami aminokwasowymi tworzącymi miejsce wiązania (Padgett i wsp., 2007) pochodzące od pętli A-C, z dodatnio naładowanymi grupami aminowymi neuroprzekaźnika (Corringer i wsp., 2012; Nemeč i wsp., 2016). W doświadczeniach z wykorzystaniem dynamiki molekularnej obserwuje się, że pod wpływem związania agonisty, pętla C wykonuje obszerny ruch w kierunku do wnętrza struktury. Z tego powodu opisana zmiana położenia pętli C nazywana jest „nakrywaniem” miejsca wiązania (ang. „*capping*”) (Cheng i wsp., 2006; Michałowski i wsp., 2017; Venkatachalan i Czajkowski, 2008; Wagner i Czajkowski, 2001).

Po związaniu agonisty, receptor GABA_A ulega złożonym zmianom strukturalnym skutkującym ostatecznie otwarciem poru jonowego. Jednym ze wstępnych etapów tego procesu jest tak zwana preaktywacja. (Gielen i wsp., 2012; Kisiel i wsp., 2018; Lape i wsp., 2008; Szczot i wsp., 2014). W jej przebiegu, pomimo wcześniejszego przyłączenia neuroprzekaźnika, bramka kanału jonowego pozostaje zamknięta jednakże zachodzące zmiany konformacyjne w obrębie obszernych fragmentów struktury czynią aktywację receptora bardziej prawdopodobną. Jest to istotne ze względu na fakt, że miejsca wiązania agonisty w domenie zewnątrzkomórkowej znajdują się w znaczącej odległości (ok. 50 Å; Miller i Smart, 2010) od bramki kanału jonowego w domenie transbłonowej, zatem ostateczne otwarcie się bramki

kanału umożliwiające transport jonów, determinowane jest przez skuteczne zajście poprzedzających je zdarzeń – etapu preaktywacji. Jednakże molekularne mechanizmy leżące u podłoża tych zjawisk wciąż nie zostały w pełni poznane.

Rosnąca liczba badań dowodzi, że różne obszary struktury receptora GABA_A mogą być zaangażowane w procesy zachodzące w znacznie oddalonych rejonach białka, np. reszta aminokwasowa α_1 F64 znajdująca się w pętli D i bezpośrednio w miejscu wiązania, bierze udział w wiązaniu agonisty ale pełni także kluczową rolę w procesie preaktywacji (Szczołt i wsp., 2014). Podobnie mutacja w pozycji α_1 F45 w pętli G powoduje zmianę powinowactwa kwasu γ -aminomasłowego do receptora GABA_A ale także wpływa na jego zdolność do otwierania i zamykania się (Brodzki i wsp., 2020). Przykłady te świadczą o występowaniu długodystansowych oddziaływań funkcjonalnych pomiędzy różnymi obszarami struktury tego receptora.

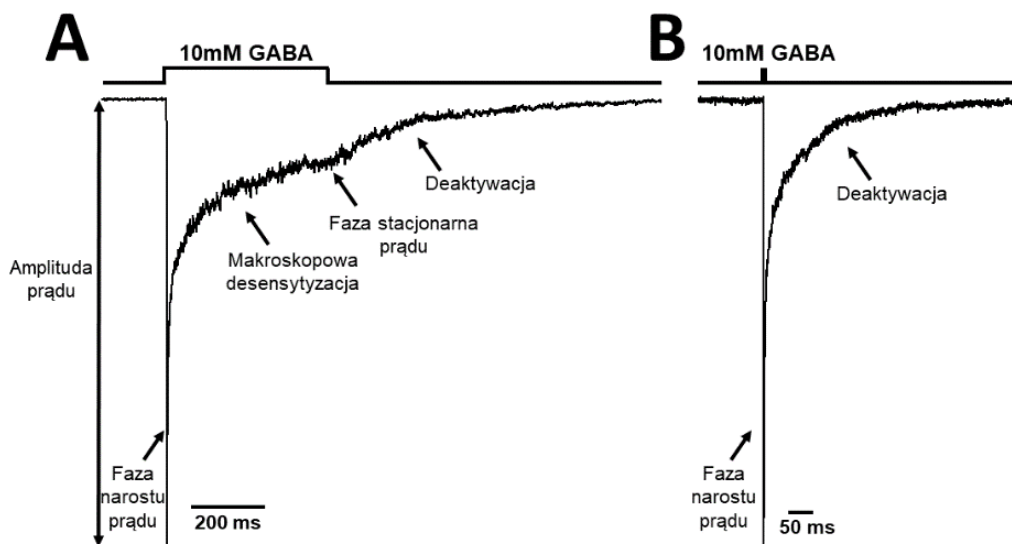
Nie są to jednak jedyne rodzaje oddziaływań zachodzących podczas procesu aktywacji receptorów pLGIC. Wspomniane wcześniej zmiany konformacyjne mogą obejmować także skoordynowaną czwartorzędową rotację położenia podjednostek, prowadzącą do zmiany objętości struktury receptora (ang. „*un-blooming*”, Althoff i wsp., 2014; Martin i wsp., 2017; Nemečz i wsp., 2016; Sauguet i wsp., 2014). Tego rodzaju mobilność podjednostek musi wymagać występowania oddziaływań pomiędzy nimi, które także mogą pełnić istotne funkcje w samym procesie aktywacji. Przykładowo, oddziaływanie pomiędzy α_1 Arg120 i β_2 Asp163 u szczytu miejsca wiązania powoduje stabilizację stanów zamkniętych receptorów GABA_A po związaniu agonisty (Laha i Wagner, 2011).

4. Kinetyka procesu aktywacji receptorów GABA_A

Jak wspomniano, wyróżnia się dwie formy inhibicji GABA-ergicznej opartej na działaniu jonotropowych receptorów GABA_A: inhibicję fazową, czyli synaptyczną oraz toniczną. Obie formy regulują pobudliwość sieci neuronalnej, jednakże zachodzą w różnych skalach czasowych i przestrzennych. Inhibicja fazowa związana jest bezpośrednio z szybką aktywnością synaps chemicznych. Uwolnione do szczeliny synaptycznej wysokie stężenie (do 1 mM) neuroprzekaźnika GABA prowadzi do przyłączenia tych cząsteczek do receptorów zlokalizowanych w błonie postsynaptycznej neuronu, co z kolei powoduje otwarcie kanałów jonowych i tym samym wzrost przepuszczalności błony dla jonów chlorkowych Cl⁻ oraz wodorowęglanowych HCO₃⁻. W neuronach w dojrzałym układzie nerwowym ssaków dokomórkowy napływ ujemnie naładowanych jonów powoduje powstawanie postsynaptycznych prądów hamujących (IPSCs, ang. „*Inhibitory Post-Synaptic Currents*”).

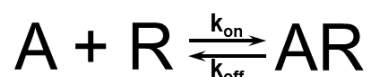
Czas przebywania GABA w synapsie po wydzieleniu jest krótki (ok. 100 μ s), co spowodowane jest szybką dyfuzją neuroprzebieźnika ze szczeliny synaptycznej. Niskie stężenie dyfundujących cząsteczek GABA z przestrzeni synaptycznej do przestrzeni zewnątrzkomórkowej może natomiast aktywować pozasynaptyczne receptory GABA_A w błonach okolicznych neuronów, co stanowi podstawę mechanizmu wolniejszej i mniej ograniczonej przestrzennie inhibicji tonicznej (Mody i Pearce, 2004; Farrant i Nusser, 2005; Cherubini, 2012).

Przebieg czasowy postsynaptycznych prądów hamujących IPSCs, wynikających z zachodzenia szybkiej inhibicji fazowej, zależy od właściwości kinetycznych receptorów GABA_A znajdujących się w błonie postsynaptycznej neuronów (Mozrzymas i wsp., 2003, 1999). Szczegółowe badanie mechanizmów zachodzących podczas przebiegu IPSCs możliwe jest dzięki zastosowaniu modelu eksperymentalnego jakim jest sterowany przez piezoelektryk system do ultraszybkiej perfuzji w połączeniu z techniką elektrofizjologiczną – *patch clamp*. Technika pozwala na bezpośrednią rejestrację przewodzonych przez receptory jonotropowe prądów, które zostały wywołane podaniem roztworu agonisty (Jonas, 1995; Mozrzymas i wsp., 2003, 2007; Szczot i wsp., 2014). Rozdzielczość czasowa badanych w ten sposób zjawisk w bardzo dobrym przybliżeniu naśladuje warunki występujące w synapsie. Kinetyka wywołanych odpowiedzi prądowych przewodzonych przez rekombinowane receptory GABA_A została przedstawiona na Rycinie 2.



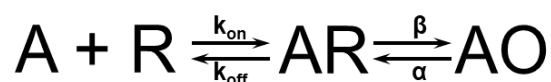
Ryc. 2 Przykładowe przebiegi czasowe prądów przewodzonych przez receptory GABA_A typu $\alpha_1\beta_2\gamma_2$, wywołane podaniem wysycającego stężenia agonisty (10 mM GABA) **A**. Długie podanie agonisty pokazujące poszczególne fazy kinetyki receptora **B**. Krótkie podanie wysycającego stężenia agonisty, w którym widoczna jest jedynie faza narostu prądu i kinetyka deaktywacji.

Analiza kinetyczna przebiegów czasowych prądów rejestrowanych techniką *patch clamp* pozwala na precyzyjne badanie etapów procesu aktywacji związanych z przyłączeniem neuroprzekaźnika, jego dysocjacją oraz bramkowaniem, które obejmuje preaktywację, otwarcie się receptora i desensytyzację. Podstawę analizy kinetycznej stanowi wykorzystanie teoretycznych modeli kinetyki I rzędu dla procesów odwracalnych, które zostały opracowane na podstawie danych eksperymentalnych. (Colquhoun, 1998; Jones i Westbrook, 1995; Mozrzymas i wsp., 1999, 2003). Receptor GABA_A może występować w różnych stanach konformacyjnych, natomiast model kinetyczny aktywności kanału jonowego opiera się na schemacie procesu Markova - połączonych między sobą oddzielnych stanach, a szybkości przejść pomiędzy poszczególnymi stanami opisywane są za pomocą kinetycznych stałych czasowych. Tak oto wiązanie agonisty A do receptora R opisuje schemat:



Ryc. 3 Schemat opisujący wiązanie cząsteczki agonisty do receptora. Przedstawione są dwa stany w procesie wiązania agonisty A do receptora w stanie spoczynkowym R, drugi stan to związany stan receptora AR oraz przejścia pomiędzy nimi: stała szybkości wiązania, k_{on} oraz stała szybkości oddysocjowania agonisty, k_{off} . Stałą równowagi (K) dla tej reakcji opisuje relacja: $K = k_{\text{on}}/k_{\text{off}}$

Dla opisu aktywacji kanału jonowego, najprostszy scenariusz przejścia z konformacji stanu zamkniętego związanego w konformację stanu otwartego zaproponowany został w 1957 roku przez del Castillo i Katz, równocześnie po raz pierwszy postulował wyraźne oddzielenie procesu wiązania agonisty od następującej po nim zmiany konformacyjnej związanej z otwarciem poru (Ryc. 4). W procesach Markova, efektywność obsadzania wybranych stanów konformacyjnych zależy od szybkości wszystkich przejść pomiędzy pozostałymi stanami konformacyjnymi w modelu oraz od stopnia obsadzenia tych stanów. Oznacza to, że ponieważ wszystkie stany w modelu są funkcjonalnie powiązane, dowolna cecha kinetyczna prądu makroskopowego (odzwierciedlającego niejako statystykę obsadzenia poszczególnych stanów konformacyjnych przy wielu jednocześnie funkcjonujących kanałach), będzie kształtowana przez skomplikowany proces na przebieg którego wpływ mają wszystkie występujące w nim stany konformacyjne (Kisiel i wsp., 2018; Mozrzymas i wsp., 2003).

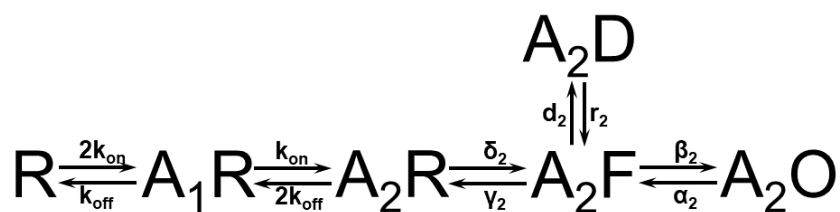


Ryc. 4 Schemat klasycznego mechanizmu aktywacji receptora, proponowany przez del Castillo i Katz (1957). Oprócz omówionego na Ryc. 2 etapu wiązania, schemat został rozbudowany o stan otwarty AO receptora oraz odpowiednio przejścia pomiędzy stanami: otwarcie β oraz zamknięcie α . Zdolność agonisty do otwarcia receptora jest charakteryzowana jako jego efektywność (ang. „*efficacy*”), która określana jest poprzez stałą równowagi E dla przejść: $E = \beta/\alpha$.

Jak prezentuje Rycina 2A, wydłużone podanie agonisty (500 ms) charakteryzuje się stopniowym zanikiem prądu po osiągnięciu maksymalnej amplitudy, co określane jest jako makroskopowa desensytyzacja. W przypadku kanałów jonowych związane jest to z fizjologicznym stanem nieprzewodzącym po przyłączeniu agonisty, będącym konsekwencją wydłużonej stymulacji tego receptora. (Papke i wsp., 2011). W 1995 roku Jones i Westbrook, badali wpływ makroskopowej desensytyzacji na kinetykę fazy relaksacji prądu po zakończeniu podania agonisty, zwanej deaktywacją i dokonali ważnej obserwacji świadczącej o tym, że deaktywacja jest kształtowana poprzez zachodzenie kilku procesów: oddysocjowywanie agonisty, desensytyzację/resensytyzację oraz otwieranie/zamykanie. Wynika to z faktu, że desensytyzacja jest stanem utrzymującym kanał jonowy w warunkach wysokiego prawdopodobieństwa przejścia w ponowne otwarcie, nim nastąpi odłączenie się agonisty od miejsca wiązania. Tym samym badacze udowodnili, że proces desensytyzacji receptorów GABA_A pełni ważną rolę w kształtowaniu postsynaptycznych prądów IPSCs poprzez wydłużenie ich trwania. Zaproponowano również uwzględnienie stanu pojedynczo związanej desensytyzacji (AD) w obowiązującym ówczynie modelu kinetycznym dla receptora GABA_A (Jones i Westbrook, 1995).

Kolejnym krokiem w pogłębianiu wiedzy w zakresie procesu aktywacji receptora GABA_A było wyodrębnienie i scharakteryzowanie stanu zwanego preaktywacją (również określanej przez D. Colquhouna, odkrywcy zjawiska, ang. „*flipping*”). Informacja o tym, że stan związany zamknięty receptora, który wykazuje zwiększone prawdopodobieństwo przejścia do stanu związanego otwartego, to także odrębny i funkcjonalnie istotny stan konformacyjny, niejako zrewolucjonizowała dotychczasowe założenia (Plested, 2014). Występowanie stanu preaktywacji dowiedziono początkowo dla receptora glicyny (Lape i wsp., 2008), jednak jego obecność potwierdzono także w pozostałych receptorach z rodziny pętli cysteiny (Mukhtasimova i wsp., 2009; Plested, 2014), w tym również receptorze GABA_A (Gielen i wsp., 2012) poprzez przeprowadzenie badań wykorzystujących zjawisko częściowego agonizmu (Colquhoun i Lape, 2012; Zhu i wsp., 2019). Początkowo sądzono, że częściowi agonści

wykazują obniżoną zdolność do zmiany równowagi przejścia receptora w stan otwarty na rzecz stanu zamkniętego, udowodniono jednak, że różnica ta dotyczy zmiany efektywności wejścia w stan preaktywowany (AF). Ponieważ preaktywacja opisuje przejściowy stan zamknięty związanego receptora o wyższym prawdopodobieństwo otwarcia się poru lub wejścia receptora w stan desensytyzacji, pełni kluczową rolę w przebiegu procesu bramkowania. Uwzględnienie tego etapu w schemacie modelu kinetycznego dla aktywności receptora GABA_A (Kisiel i wsp., 2018; Szczot i wsp., 2014) doprowadziło to powstania współcześnie stosowanych modeli. W warunkach wysycenia, gdy oba miejsca wiązania są obsadzone cząsteczkami agonisty, proces aktywacji w najprostszej postaci opisuje schemat:



Ryc. 5 Schemat modelu kinetycznego uwzględniający wszystkie kluczowe stany, w których może przebywać receptor GABA_A podczas procesu aktywacji w warunkach wysycenia, wraz ze stałymi kinetycznymi definiującymi szybkości przejść pomiędzy nimi. Po etapie wiązania wyróżnia się stan A₂F preaktywację/"flipping" wraz ze stałymi: δ_2 - stała szybkości wejścia w preaktywację, γ_2 - stała szybkości wyjścia z preaktywacji oraz następujące stany, które mogą być równoczesne: stan zdesensytyzowany A₂D ze stałymi kinetycznymi wejścia w desensytyzację d_2 oraz wyjścia, czyli resensytyzację r_2 , a także opisane poprzednio na Ryc. 3 i 4 stany związane i stan otwarty. Indeks dolny „2” dla stałych kinetycznych odnosi się do receptorów podwójnie związanych. Schemat uwidacznia złożoność procesów kształtujących kinetykę odpowiedzi prądowych.

Do opisanej powyżej analizy opartej na modelach kinetycznych wykorzystuje się także rejestracje stacjonarnej aktywności pojedynczych kanałów jonowych (ang. „*single-channel recordings*”), uzyskane wspomnianą wcześniej techniką elektrofizjologiczną *patch clamp*. W warunkach wysycenia rejestrowana aktywność dotyczy wyłącznie receptora w stanie podwójnie związanym, zatem stany R oraz A₁R nie są uwzględniane w schemacie. Ze względu na specyfikę danych, estymacja stałych kinetycznych w analizie kinetycznej aktywności pojedynczych kanałów jonowych uważana jest za bardziej wiarygodną, nawet w przypadku modeli o wysokim stopniu złożoności (Kisiel i wsp., 2018; Colquhoun i Lape, 2012).

Wykorzystywanie modelowania kinetycznego, pomimo dostępności nowych rozwiązań badawczych takich jak obrazowanie struktury receptora GABA_A metodami krystalograficznymi lub mikroskopii krioelektronowej (Kim i wsp., 2020; Lavery i wsp., 2019;

Masiulis i wsp., 2019; Miller i Aricescu, 2014), ma wciąż duże uzasadnienie, ponieważ wiele konformacji jest zbyt niestabilnych, by możliwe było ich zobrazowanie wspomnianymi metodami. Ponadto, opracowanie wszechstronnego modelu pozwala na symulowanie odpowiedzi receptora w dowolnych warunkach aktywacji oraz także z uwzględnieniem efektów wywołanych przez modulację związkami farmakologicznymi (Jatczak-Śliwa i wsp., 2018; Rüschi i Forman, 2005; Terejko i wsp., 2020)

5. Modulacja aktywności receptorów GABA_A przez benzodiazepiny

Benzodiazepiny to grupa związków farmakologicznych uważanych za pozytywne modulatory aktywności receptora GABA_A, które są powszechnie wykorzystywane w psychiatrii i neurologii w leczeniu m.in. autyzmu lub zaburzeń lękowych (Möhler, 2015; Rudolph i Möhler, 2014). Badania elektrofizjologiczne pokazują, że obecność benzodiazepiny powoduje istotny wzrost amplitudy prądów wywołanych podaniem niskiego stężenia agonisty GABA. Nie obserwuje się tego efektu w przypadku prądów wywołanych w warunkach wysycającego stężenia GABA. Z tego powodu początkowo sądzono, że mechanizm działania benzodiazepin opiera się zasadniczo na modulacji wiązania cząsteczek agonisty do receptora GABA_A (Krampfl i wsp., 1998; Lavoie i Twyman, 1996). Jednakże dalsze badania wykazały, że mechanizm ten obejmuje także bramkowanie receptora (Downing i wsp., 2005; Rüschi i Forman, 2005; Mercik i wsp., 2007) i dotyczy zarówno fazowej jak i tonicznej aktywności hamującej receptorów GABA_A (Mozrzymas i wsp., 2007). Co istotne, jak pokazują wyniki badań prezentowanych także w tej rozprawie, wykazano również, że mechanizmowi modulacji przez benzodiazepiny podlega etap preaktywacji (Jatczak-Śliwa i wsp., 2018; Terejko i wsp., 2020; Dixon i wsp., 2015). Ponadto, związki te mają zdolność modulowania także aktywności spontanicznej w niezwiązanych receptorach, co zostało zaobserwowane w badaniach z użyciem punktowej mutacji receptora GABA_A, powodującej wzrost amplitudy prądów wywołanych zachodzeniem spontanicznych otwarć (Jatczak-Śliwa i wsp., 2018).

CEL I ZAŁOŻENIA PRACY

Publikacje naukowe, które są podstawą niniejszej pracy doktorskiej stanowią spójny cykl badań realizowanych w celu zgłębienia tytułowego zagadnienia: *wpływu wybranych mutacji w domenie zewnątrzkomórkowej na wiązanie neuroprzekaźnika i bramkowanie rekombinowanego receptora GABA_A typu $\alpha_1\beta_2\gamma_2$* . Przeprowadzone badania miały na celu weryfikację hipotezy mówiącej o tym, że aminokwasy zlokalizowane w różnych rejonach domeny zewnątrzkomórkowej receptora GABA_A, tj. kluczowe aminokwasy aromatyczne: α_1 F14, β_2 F31 i β_2 F200, są zaangażowane zarówno we wczesny etap aktywacji – wiązanie neuroprzekaźnika, jak i etap bramkowania – preaktywację, otwarcie i zamknięcie kanału jonowego oraz desensytyzację. Założeniem projektu badawczego była również ocena wpływu benzodiazepin (flurazepamu) na bramkowanie receptora GABA_A, na przykładzie mutacji aminokwasów zlokalizowanych w miejscu wiązania dla agonisty: α_1 F64 i β_2 F200.

Celem pierwszej publikacji z cyklu, zatytułowanej „*Distinct Modulation of Spontaneous and GABA-Evoked Gating by Flurazepam Shapes Cross-Talk Between Agonist-Free and Liganded GABA_A Receptor Activity*” (Frontiers in Cellular Neuroscience 12:1–18, 2018) było zbadanie wpływu modulacji przez flurazepam zmutowanych receptorów GABA_A w pozycji α_1 F64 w warunkach wysycenia, ze względu na poznaną wcześniej rolę tego aminokwasu w kluczowym etapie aktywacji receptora, jakim jest preaktywacja. Badania miały na celu weryfikację hipotezy dotyczącej bezpośredniego wpływu tego związku nie tylko na wiązanie neuroprzekaźnika, ale także na różne etapy bramkowania receptora.

Celem drugiej publikacji z cyklu, zatytułowanej „*The C loop at the orthosteric binding site is critically involved in GABA_A receptor gating*” (Neuropharmacology 166:107903, 2020) było precyzyjne określenie roli pętli C, znajdującej się w miejscu wiązania receptora, w poszczególnych etapach jego aktywacji, poprzez zastosowanie mutacji reszty aminokwasowej β_2 F200 w obrębie tej pętli. Założeniem pracy było również wykazanie zmiany wrażliwości badanych receptorów na modulację przez flurazepam pod wpływem wprowadzonych mutacji.

Celem trzeciej publikacji z cyklu, zatytułowanej „*Interaction between GABA_A receptor α_1 and β_2 subunits at the N-terminal peripheral regions is crucial for receptor binding and gating*” (Biochemical Pharmacology 183:114338, 2021) było wykazanie oddziaływania pomiędzy podjednostkami, obserwowane pomiędzy resztami aromatycznymi α_1 F14 i β_2 F31 u szczytu domeny zewnątrzkomórkowej receptora GABA_A, powyżej miejsca wiązania. Celem badań było ponadto zbadanie funkcji tego oddziaływania w procesach wiązania neuroprzekaźnika i bramkowania kanału jonowego.

Szczegółowe cele projektu:

„Distinct Modulation of Spontaneous and GABA-Evoked Gating by Flurazepam Shapes Cross-Talk Between Agonist-Free and Liganded GABA_A Receptor Activity”

1. Zbadanie wpływu flurazepamu na aktywność spontaniczną receptorów GABA_A typu dzikiego oraz receptorów zmutowanych w pozycji α_1 F64
2. Ocena wpływu flurazepamu na makroskopowe odpowiedzi prądowe przewodzone przez zmutowane receptory w warunkach wysycającego stężenia agonisty
3. Zbadanie wpływu flurazepamu na makroskopowe odpowiedzi prądowe przewodzone przez receptory typu dzikiego wywołane poprzez podanie częściowego agonisty receptorów GABA_A, kwasu piperydino-4-sulfonowego (P4S)
4. Zaproponowanie mechanistycznej interpretacji uzyskanych wyników poprzez zastosowanie modelowania kinetycznego dla makroskopowych odpowiedzi prądowych

„The C loop at the orthosteric binding site is critically involved in GABA_A receptor gating”

1. Zbadanie wpływu mutacji receptora GABA_A w pozycji β_2 F200 na krzywe „odpowiedź-dawka” oraz kinetykę prądów przewodzonych przez te receptory w warunkach wysycenia oraz porównanie uzyskanych efektów z odpowiedziami prądowymi dla receptorów typu dzikiego
2. Weryfikacja hipotezy udziału aminokwasu β_2 F200 w etapie preaktywacji receptora GABA_A poprzez analizę makroskopowych odpowiedzi prądowych przewodzonych przez zmutowane receptory w obecności flurazepamu, w warunkach wysycenia
3. Określenie precyzyjnej funkcji aminokwasu β_2 F200 w bramkowaniu receptora GABA_A poprzez analizę aktywności pojedynczych kanałów jonowych
4. Określenie wpływu zastosowanych mutacji na strukturę badanej pętli C poprzez modelowanie strukturalne metodami *in silico*
5. Ocena i interpretacja obserwowanych efektów przy użyciu modelowania kinetycznego dla makroskopowych odpowiedzi prądowych oraz dla aktywności pojedynczych kanałów jonowych

„Interaction between GABA_A receptor α_1 and β_2 subunits at the N-terminal peripheral regions is crucial for receptor binding and gating”

1. Wykazanie metodami *in silico* powstawania mostka disiarczkowego pomiędzy resztami α_1 F14 i β_2 F31 w warunku substytucji obu tych aminokwasów resztą cysteinową

2. Określenie wpływu dwóch pojedynczych mutacji α_1F14C i β_2F31C oraz podwójnej mutacji $\alpha_1F14C\beta_2F31C$ na krzywe „odpowiedź-dawka” oraz na przebiegi czasowe makroskopowych prądów przewodzonych przez zmutowane receptory $GABA_A$, wywołane podaniem wysycającego stężenia agonisty
3. Zbadanie efektów zerwania mostka disiarczkowego na kinetykę makroskopowych odpowiedzi prądowych uzyskanych dla podwójnego mutantu $\alpha_1F14C\beta_2F31C$ poprzez podanie wysycającego stężenia agonisty oraz ditiotreitolu (DTT) a także sprawdzenie specyficzności obserwowanych efektów poprzez przeprowadzenie analogicznych eksperymentów dla receptorów $GABA_A$ typu dzikiego
4. Zbadanie i porównanie wpływu pojedynczych oraz podwójnej mutacji na rejestrowaną aktywność pojedynczych kanałów jonowych.
5. Zaproponowanie mechanistycznej interpretacji uzyskanych wyników poprzez zastosowanie modelowania kinetycznego makroskopowych odpowiedzi prądowych oraz dla aktywności pojedynczych kanałów jonowych, a także obliczenie metodą „*double-mutant cycle analysis*” zmiany energii swobodnej $\Delta\Delta G$ na podstawie uzyskanych stałych kinetycznych dla zmutowanych receptorów α_1F14C i β_2F31C

MATERIAŁY I METODY

Hodowle komórkowe i ekspresja rekombinowanych receptorów GABA_A

Wszystkie zawarte w rozprawie eksperymenty zostały przeprowadzone na komórkach linii HEK 293, hodowanych w sposób szczegółowo opisany w publikacjach. 48 h przed eksperymentami elektrofizjologicznymi, komórki były poddawane procedurze transfekcji przejściowej przy użyciu komercyjnego odczynnika FuGene (Promega, Madison, USA) lub metodą precypitacji fosforanów wapnia. Wykorzystano adenowirusowy wektor plazmidowy z promotorem pCMV, zawierający cDNA szczura dla poszczególnych podjednostek natywnych i zmutowanych receptora GABA_A oraz dla białka zielonej fluorescencji (EGFP) lub antygenu CD4, dla późniejszej detekcji komórek z ekspresją rekombinowanych receptorów GABA_A.

Pomiary elektrofizjologiczne

W rejestracjach prądów wywołanych podaniem agonisty wykorzystano technikę *patch-clamp*. Do pomiarów makroskopowej aktywności receptorów GABA_A rejestrowanych z całej komórki (konfiguracja „*whole-cell*”) lub z oderwanej łątki błonowej (konfiguracja „*excised patch*”) użyto w przeważającej większości przypadków systemu do ultraszybkiej perfuzji lub w części eksperymentów systemu do szybkiej perfuzji BioLogic (część eksperymentów w pracy „*Distinct Modulation of Spontaneous and GABA-Evoked Gating by Flurazepam Shapes Cross-Talk Between Agonist-Free and Liganded GABA_A Receptor Activity*”). W czasie pomiarów, komórki przebywały w roztworze Ringera, a pipeta pomiarowa wypełniona była roztworem odpowiednim do wprowadzenia do wnętrza komórki. Roztwory zawierające agonistę i/lub modulator podawane były na powierzchnię komórki przez dwukanałową kapilarę z szybkością wymiany roztworów 100-300 μs. Rejestracje prowadzono przy ustalonym napięciu -40 mV. Aktywność pojedynczych kanałów jonowych (ang. „*single channel recordings*”) rejestrowano w konfiguracji pipety pomiarowej w kontakcie z błoną komórkową (konfiguracja „*cell-attached*”). Roztwór agonisty znajdował się w pipecie pomiarowej, a rejestracje prowadzono w sposób ciągłego nagrania przy zadanym napięciu 100 mV. Do akwizycji badanych sygnałów prądowych wykorzystano oprogramowanie Clampex 10.7 firmy Molecular Devices (Sunnyvale, USA).

Analiza rejestrowanych prądów

Uzyskane w pomiarach elektrofizjologicznych dane przeanalizowano w programie Clampfit 10.7 (Molecular Devices) pod kątem wpływu badanych mutacji receptora GABA_A na

kinetykę przebiegu prądowego, wywołanego w odpowiedzi na długie (500 ms) lub krótkie (2 – 15 ms) podanie agonisty i/lub modulatora. Analiza kinetyczna zawierała ocenę długości trwania narostu prądu (ang. „*rise time*”), szybkości poszczególnych składowych makroskopowej desensytyzacji, wyrażanych w postaci stałych kinetycznych: τ_{szybkie} i τ_{wolne} (ang. „ *τ_{fast}* ” i „ *τ_{slow}* ”) poprzez dopasowanie do przebiegów prądowych funkcji eksponencjalnych, wraz z obliczeniem udziału procentowego poszczególnych składowych oraz stacjonarnej wartości amplitudy prądu (ang. „*steady-state-to-peak*”). W przypadkach nagrań o powolnym, nieosiągającym fazy stacjonarnej przebiegu desensytyzacji, stosowano parametry FR (ang. „*fraction remaining*”) opisujące stosunek wartości amplitudy w wybranych punktach czasowych do amplitudy całkowitej, której ubytek nastąpił pod wpływem desensytyzacji, np. FR10 po 10 ms i FR500, po 500 ms. Analiza kinetyki deaktywacji również polegała na dopasowaniu funkcji eksponencjalnych do tej części przebiegów prądowych, a otrzymana średnia wartość stałej kinetycznej $\tau_{\text{deaktywacji}}$ (ang. „*mean τ_{deact}* ”) opisywała szybkość zachodzenia deaktywacji. W eksperymentach służących ocenie wpływu modulatora lub w celu uzyskania krzywej „dawka-odpowieź” mierzona była także maksymalna wartość amplitudy badanego prądu.

Nagrania ciągłe aktywności pojedynczych kanałów jonowych poddane były idealizacji w programie SCAN z pakietu oprogramowania DCProgs (uzyskanego dzięki uprzejmości prof. D. Coulqhouna z University College London). Przetworzone w ten sposób dane z informacją o długości trwania otwarć i zamknięć kanału jonowego wykorzystano do wygenerowania rozkładów dla czasów zamkniętych (ang. „*shut times*”) i czasów otwarć (ang. „*open times*”), na podstawie których przeprowadzono dopasowanie składowych komponent, określanych stałą czasową długości trwania τ i jej udziałem procentowym P% w całym rozkładzie, przy użyciu programu EKDIST (DCProgs).

Modelowanie kinetyczne

Modelowaniu kinetycznemu poddano zarówno nagrania makroskopowych prądów jak i aktywności pojedynczych receptorów GABA_A, w oparciu o najbardziej aktualne schematy modeli kinetycznych opracowanych w Katedrze i Zakładzie Biofizyki i Neurobiologii na przestrzeni ostatnich lat (Brodzki i wsp., 2020; Kisiel i wsp., 2018; Szczot i wsp., 2014). Modelowanie makroskopowe przy użyciu programu ChannelLab 2.0 (Synaptosoft, Decatur, USA) miało charakter trendowy i stanowiło symulacje odpowiednich wartości dla stałych kinetycznych przejść pomiędzy stanami w przypadku receptorów zmutowanych, na bazie modeli kinetycznych uzyskanych wcześniej dla receptorów typu dzikiego. Formalne modelowanie aktywności pojedynczych kanałów jonowych przeprowadzono przy użyciu

oprogramowania HJCFIT (DCProgs), które zostało oparte na metodzie modelowania poprzez najwyższe podobieństwo (ang. „*maximum likelihood method*”) i pozwalało na optymalizację stałych kinetycznych z korektą dla pominiętych zdarzeń z tytułu ograniczonej rozdzielczości pomiarowej.

Zmiany energii swobodnej $\Delta\Delta G$ dla stałych kinetycznych uzyskanych w procesie modelowania kinetycznego aktywności pojedynczych kanałów jonowych dla wybranych zmutowanych receptorów GABA_A, uzyskano wykorzystując schemat obliczeniowy metody „*double-mutant cycle analysis*” (Horovitz, 1996).

Analiza statystyczna

Do analizy istotnych statystycznie różnic pomiędzy badanym parametrem dla receptora zmutowanego względem tego parametru dla receptora typu dzikiego lub dla porównania efektu modulatora względem pomiarów kontrolnych zastosowano test *t* Studenta lub dla danych nie wykazujących rozkładu normalnego, test *U* Manna-Whitneya, przy użyciu programu SigmaPlot 11.0 (Systat Software, San Jose, USA). Wyniki wartości średnich dla badanych parametrów zostały przedstawione jako średnia \pm SEM. Przyjęty poziom istotności wynosił $p < 0.05$.

WYKAZ PUBLIKACJI STANOWIĄCYCH ROZPRAWĘ DOKTORSKĄ

Cykl publikacji

1. Magdalena Jatzak-Śliwa, **Katarzyna Terejko**, Marek Brodzki, Michał A. Michałowski, Marta M. Czyżewska, Joanna M. Nowicka, Anna Andrzejczak, Rakenduvadhana Srinivasan, Jerzy W. Mozrzymas: *Distinct Modulation of Spontaneous and GABA-Evoked Gating by Flurazepam Shapes Cross-Talk Between Agonist-Free and Liganded GABA_A Receptor Activity*. Front Cell Neurosci 12:1–18. (2018)

IF: 3.900

Pkt. MNiSW/KBN: 35.00

2. **Katarzyna Terejko**, Przemysław T. Kaczor, Michał A. Michałowski, Agnieszka Dąbrowska, Jerzy W. Mozrzymas: *The C loop at the orthosteric binding site is critically involved in GABA_A receptor gating*.

Neuropharmacology 166:107903. (2020)

IF: 4.431

Pkt. MNiSW/KBN: 140.00

3. **Katarzyna Terejko**, Michał A. Michałowski, Anna Dominik, Anna Andrzejczak, Jerzy W. Mozrzymas: *Interaction between GABA_A receptor α_1 and β_2 subunits at the N-terminal peripheral regions is crucial for receptor binding and gating*.

Biochem Pharmacol 183:114338. (2021)

IF: 4.960

Pkt. MNiSW/KBN: 100.00

ŁĄCZNY IMPACT FACTOR: 13.291

	Liczba punktów MNiSW/KBN
Do roku 2018	35.00
Do roku 2020	140.00
Do roku 2021	100.00
Razem:	275.00

PUBLIKACJE

1.

„Distinct Modulation of Spontaneous and GABA-Evoked Gating by Flurazepam Shapes Cross-Talk Between Agonist-Free and Liganded GABA_A Receptor Activity”

Magdalena Jaczak-Śliwa, **Katarzyna Terejko**, Marek Brodzki, Michał A. Michałowski,
Marta M. Czyżewska, Joanna M. Nowicka, Anna Andrzejczak, Rakenduvadhana Srinivasan,
Jerzy W. Mozrzymas

Frontiers in Cellular Neuroscience 12 (2018), 1–18.

doi.org/10.3389/fncel.2018.00237



Distinct Modulation of Spontaneous and GABA-Evoked Gating by Flurazepam Shapes Cross-Talk Between Agonist-Free and Liganded GABA_A Receptor Activity

Magdalena Jatczak-Śliwa^{1,2*†}, Katarzyna Terejko^{1†}, Marek Brodzki^{1,2†}, Michał A. Michałowski^{1,2}, Marta M. Czyżewska¹, Joanna M. Nowicka¹, Anna Andrzejczak², Rakenduvadhana Srinivasan² and Jerzy W. Mozrzymas^{1*}

¹ Laboratory of Neuroscience, Department of Biophysics, Wrocław Medical University, Wrocław, Poland, ² Department of Molecular Physiology and Neurobiology, University of Wrocław, Wrocław, Poland

OPEN ACCESS

Edited by:

Andrea Barberis,
Fondazione Istituto Italiano di
Technologia, Italy

Reviewed by:

Marco Beato,
University College London,
United Kingdom
Joseph Henry Steinbach,
Washington University in St. Louis,
United States

*Correspondence:

Magdalena Jatczak-Śliwa
magdalena.jatczak@gmail.com
Jerzy W. Mozrzymas
jerzy.mozrzymas@umed.wroc.pl

[†]These authors have contributed
equally to this work

Received: 25 April 2018

Accepted: 17 July 2018

Published: 28 August 2018

Citation:

Jatczak-Śliwa M, Terejko K,
Brodzki M, Michałowski MA,
Czyżewska MM, Nowicka JM,
Andrzejczak A, Srinivasan R and
Mozrzymas JW (2018) Distinct
Modulation of Spontaneous
and GABA-Evoked Gating by
Flurazepam Shapes Cross-Talk
Between Agonist-Free and Liganded
GABA_A Receptor Activity.
Front. Cell. Neurosci. 12:237.
doi: 10.3389/fncel.2018.00237

GABA_A receptors (GABA_ARs) play a crucial inhibitory role in the CNS. Benzodiazepines (BDZs) are positive modulators of specific subtypes of GABA_ARs, but the underlying mechanism remains obscure. Early studies demonstrated the major impact of BDZs on binding and more recent investigations indicated gating, but it is unclear which transitions are affected. Moreover, the upregulation of GABA_AR spontaneous activity by BDZs indicates their impact on receptor gating but the underlying mechanisms remain unknown. Herein, we investigated the effect of a BDZ (flurazepam) on the spontaneous and GABA-induced activity for wild-type (WT, $\alpha_1\beta_2\gamma_2$) and mutated (at the orthosteric binding site α_1F64) GABA_ARs. Surprisingly, in spite of the localization at the binding site, these mutations increased the spontaneous activity. Flurazepam (FLU) upregulated this activity for mutants and WT receptors to a similar extent by affecting opening/closing transitions. Spontaneous activity affected GABA-evoked currents and is manifested as an overshoot after agonist removal that depended on the modulation by BDZs. We explain the mechanism of this phenomenon as a cross-desensitization of ligand-activated and spontaneously active receptors. Moreover, due to spontaneous activity, FLU-pretreatment and co-application (agonist + FLU) protocols yielded distinct results. We provide also the first evidence that GABA_AR may enter the desensitized state in the absence of GABA in a FLU-dependent manner. Based on our data and model simulations, we propose that FLU affects agonist-induced gating by modifying primarily preactivation and desensitization. We conclude that the mechanisms of modulation of spontaneous and ligand-activated GABA_AR activity concerns gating but distinct transitions are affected in spontaneous and agonist-evoked activity.

Keywords: GABA_A receptor, γ -aminobutyric acid, benzodiazepines, spontaneous activity, preactivation, gating, partial agonist

Abbreviations: ALA, α_1F64A mutant of $\alpha_1\beta_2\gamma_2$ GABA_A receptor; BDZ, benzodiazepine; CYS, α_1F64C mutant of $\alpha_1\beta_2\gamma_2$ GABA_A receptor; FLU, flurazepam, which is a benzodiazepine derivative; FR, fraction of the current that remained after the selected time after the peak; GABA_AR, ionotropic GABAergic receptor, type A; LEU, α_1F64L mutant of $\alpha_1\beta_2\gamma_2$ GABA_A receptor; P4S, piperidine-4-sulfonic acid; PTX, picrotoxin, open GABA_A receptor channel blocker; RT, rise time of currents mediated by GABA_A receptors upon activation; WT, wild-type of $\alpha_1\beta_2\gamma_2$ GABA_A receptor.

INTRODUCTION

GABA (gamma aminobutyric acid) is the major inhibitory neurotransmitter in the brain (Cherubini and Conti, 2001; Fritschy and Brünig, 2003). BDZs are positive modulators of specific subtypes of GABA_ARs (Rudolph and Möhler, 2004), but the mechanism of action of BDZs remains obscure and the controversy is whether BDZs act primarily on the agonist binding step or on gating or on both. In our early studies, we proposed that BDZ receptor agonists affected binding and desensitization (Mozzrymas et al., 2007). Li et al. (2013) reported that BDZs altered the efficacy, and similar conclusions were proposed by Rusch and Forman (2005) and Campo-Soria et al. (2006). More recently, Dixon et al. (2015) proposed that BDZs affected the intermediate conformation, whereas Goldschen-Ohm et al. (2014) concluded that BDZs affected the binding and preactivation (flipping) steps. Thus, although the impact of BDZs on gating transitions is emerging, we decided to investigate which specific transitions are modulated.

Positive modulation of spontaneous activity of WT receptors by BDZs (Campo-Soria et al., 2006) and of mutants favoring spontaneous activity (Downing et al., 2005; Rusch and Forman, 2005; Campo-Soria et al., 2006) indicated an interference with gating. However, the mechanism of the impact of BDZs on spontaneous activity remains unknown. In particular, it is not clear whether BDZs directly activate GABA_ARs or upregulate the spontaneous openings (Downing et al., 2005; Campo-Soria et al., 2006). Moreover, in aforementioned studies, mutations enhancing spontaneous activity were located close to the channel gate, affecting the receptor gating probably at its latest stage, whereas the impact of BDZs could occur earlier. It is possible that mutations located at different sites could result in different molecular scenarios of spontaneous activity. It thus seems interesting to investigate the mutations that are likely to affect the early stages of GABA-induced activation but still result in enhanced spontaneous activity. Considering these premises, we decided to provide a comprehensive description of the effect of BDZ on the spontaneous activity and its impact on GABA-induced currents.

Herein, we address the mechanism of FLU action on GABA_ARs by considering α_1F64 mutants in which gating (primarily preactivation) is affected and by using full and partial (P4S) agonists activating WT receptors. Surprisingly, in spite of their localization at the binding site, these mutations strongly increase spontaneous activity. FLU upregulates the spontaneous activity of both WT receptors and α_1F64 mutants by affecting opening/closing transitions. We provide a mechanistic description of how FLU affects the cross-talk between spontaneous and GABA-induced activity. Based on our data and model simulations, we propose that FLU affects agonist-induced gating by modifying primarily preactivation and desensitization.

MATERIALS AND METHODS

Transfection and Expression of Recombinant GABA_ARs

The experiments were performed on human embryonic kidney (HEK-293) cells cultured as described in Szczot et al. (2014). Twenty-four hours prior to transfection, the cells were replated on poly-d-lysine (1 μ g/ml) coated coverslips (Carl Roth, Karlsruhe, Germany). A standard calcium phosphate precipitation method (Chen and Okayama, 1987) was used to transiently transfect the cells. When stronger expression was needed, FuGENE HD (Promega, Madison, WI, United States) at a 3:1 FuGENE HD:DNA ratio was used. cDNA encoding rat GABA_AR subunits was cloned in a pCMV vector. The $\alpha_1/\beta_2/\gamma_{2L}$ subunits were mixed in the ratio of 1:1:3 (0.5:0.5:1.5 μ g) in the transfected solution, together with 0.5 μ g human cluster of differentiation 4 (CD4) encoding plasmid. This amount of cDNA was used per four coverslips. Recordings in the whole-cell or out-side out configurations were performed 24–48 h after transfection. To successfully detect the transfected cells, Dynabeads CD4 magnetic binding beads were used (Invitrogen, Carlsbad, CA, United States).

Patch Clamp Recordings, Perfusion Systems, and Macroscopic Data Analysis

Currents were low-pass filtered at 10 kHz and recorded at a holding potential of -40 mV using an Axopatch 200B amplifier (Molecular Devices, Sunnyvale, CA, United States) and acquired using a Digidata 1550A acquisition card (Molecular Devices, Sunnyvale, CA, United States). For signal acquisition, pClamp 10.7 software (Molecular Devices, Sunnyvale, CA, United States) was used. Pipettes were pulled from borosilicate glass (OD: 1.5 mm, ID: 1.0 mm; Hilgenberg, Malsfeld, Germany) and filled with an intracellular solution containing (in mM) 137 KCl, 1 CaCl₂, 2 ATP-Mg, 2 MgCl₂, 10 κ -gluconate, 11 EGTA, and 10 HEPES (pH adjusted to 7.2 with KOH). The pipette resistance ranged between 3 and 6 M Ω . Standard Ringer's solution was used as an external saline containing (in mM) 137 NaCl, 5 KCl, 2 CaCl₂, 1 MgCl₂, 10 HEPES, and 20 glucose (pH to 7.2 with NaOH). To avoid osmolarity imbalance, for agonist concentrations > 10 mM, adjustments in reagents concentration were made as described previously by Szczot et al. (2014).

An ultrafast perfusion system using theta-glass capillaries (Hilgenberg, Malsfeld, Germany) mounted on a piezoelectric-driven translator (Physik Instrumente, Karlsruhe, Germany) was used as described in detail by Jonas (1995) and by our group (Mozzrymas et al., 2003, 2007; Szczot et al., 2014). Solutions were supplied simultaneously to the two channels of the theta-glass capillary with a high-precision SP220IZ syringe pump (World Precision Instruments, Inc., Sarasota, FL, United States). The solution exchange time, measured with the open-tip capillary, ranged from 100 to 350 μ s, depending on the size of the theta glass and the flux speed. When such a rapid exchange was not necessary and when more elaborate protocols were

needed (requiring a larger number of channels), a multibarrel rapid solution changer RSC-200 (Bio-Logic Science Instruments, Seyssinet-Pariset, France) was used. Recording on adherent cells showed the highest stability and this recording mode was used for protocols requiring several applications of different solutions (exchange time approximately 20–30 ms), but it was limited to slow signals.

The FLU effect was assessed in terms of the relative values determined in the presence of this drug and in control conditions at saturating [GABA]. The saturating concentration of GABA for WT and mutated $\alpha_1\beta_2\gamma_2$ GABA_AR (at α_1 F64 residue) was previously determined by our group (Szczot et al., 2014) and was established as 100 mM [GABA] for leucine (LEU) and alanine (ALA) mutants, but this concentration was not fully saturating for the cysteine (CYS) mutant (Kisiel et al., 2018). In all experiments testing the impact of FLU, this compound was used at a concentration of 3 μ M. For the majority of recordings, a pretreatment protocol was used in which FLU was present both in the wash solution (Ringer's solution) and the agonist-containing solution. In a part of the experiments, a co-application protocol was used, where FLU was present in the agonist-containing solution but absent in the wash. The two protocols were used to investigate the possible differences in the effect of FLU pretreatment on an agonist-evoked receptor activation (see section "Results"). To study the receptor deactivation time course, two experimental protocols were used: a short pulse of saturating [GABA] whose duration was sufficient to reach the amplitude peak (determined for each mutant separately) and a long (500 ms) agonist application.

The current onset was measured as 10–90% rise time (RT). The kinetics of deactivation was analyzed on normalized traces (amplitude of deactivating current equal to 1) and described in terms of the time constant(s) obtained from either a single exponent: $y(t) = A \cdot \exp(-t/\tau)$ where A is a unitary amplitude and τ is the time constant, or from a sum of two exponential functions: $y(t) = A_{\text{slow}} \cdot \exp(t/\tau_{\text{slow}}) + A_{\text{fast}} \cdot \exp(t/\tau_{\text{fast}})$ where A_{slow} and A_{fast} are the amplitude percentages of slow and fast components, respectively ($A_{\text{slow}} + A_{\text{fast}} = 1$), and τ_{slow} and τ_{fast} are the time constants. In the case of two components, the mean time constant (τ_{mean}) was calculated as $\tau_{\text{mean}} = A_{\text{slow}} \cdot \tau_{\text{slow}} + A_{\text{fast}} \cdot \tau_{\text{fast}}$.

Macroscopic desensitization kinetics was described using exponential fitting (typically two components, denoted as τ_{fast} and τ_{slow}) with a constant value. In the case of currents, for which exponential fitting was problematic (due to, e.g., slow changes), the desensitization onset was quantified as a total amplitude fraction remaining after 10 ms (abbreviated FR10). The extent of desensitization was quantified as a total amplitude fraction remaining after 500 ms (abbreviated FR500).

For the CYS mutant, which exhibited the slowest kinetics, a part of results (current amplitude measurements) was obtained using a Bio-Logic perfusion system using analogous protocols as in the theta-glass experiments. The results of the experiments carried out using these two systems were consistent, and the data were pooled. Experiments in which the extent of spontaneous activity was assessed by applying the open channel blocker picrotoxin (PTX) at a concentration of 100 μ M were carried out using the Bio-Logic perfusion system. The extent of enhancement

of the spontaneous activity by FLU was assessed using the following protocol: first FLU was applied and, after washout, PTX was administered and the extent of amplification was calculated as $(A_{\text{PTX}} + A_{\text{FLU}})/A_{\text{PTX}}$, where A_{PTX} is the amplitude shift after PTX application and A_{FLU} is the amplitude of current appearing upon FLU application (with respect to the baseline in the absence of PTX, **Figures 1A,B**).

All electrophysiological recordings were conducted at room temperature (20–23°C). All chemicals were purchased from Sigma-Aldrich (St. Louis, MO, United States) unless stated otherwise.

Single-Channel Recordings

Single-channel currents were recorded using the patch-clamp technique in the cell-attached mode. Signals were amplified by an Axopatch 200B amplifier (Molecular Devices, Sunnyvale, CA, United States) and digitized by a Digidata 1550B acquisition system (Molecular Devices, Sunnyvale, CA, United States) with a 100 kHz sampling rate. Signals were initially filtered at 10 kHz with a low-pass Bessel filter built-in in the amplifier. The pipette potential was set at 100 mV. Patch pipettes with tip resistance of 6–12 M Ω were pulled from thick-walled, filamented borosilicate glass (OD: 1.5 mm, ID: 0.87 mm; Hilgenberg, Malsfeld, Germany) on a P-1000 horizontal puller (Sutter Instrument, Novato, CA, United States). Pipettes were coated with Sylgard 184 (Dow Corning, Auburn, MI, United States) and fire-polished on a microforge. To minimize the signal noise, the amount of the extracellular solution in the dish (35 mm \varnothing Nunclon, Thermo Fisher, Waltham, MA, United States) was kept at 1 ml, yielding minimal immersion of the recording electrode. For the same reason, only patches with resistance exceeding 10 G Ω were considered suitable for experiments. The extracellular and intrapipette solution consisted of (in mM) 102.7 NaCl, 20 Na-glucuronate, 2 KCl, 2 CaCl₂, 1.2 MgCl₂, 10 HEPES (Roth), 20 TEA-Cl, 14 D-(+)-glucose, and 15 sucrose (Roth), prepared in deionized water. The pH was adjusted to 7.4 with 2M NaOH. Prior to single-channel recordings, control experiments were performed on HEK cells not transfected and those transfected with only CD4 plasmids. In these recordings, we observed very rare, mostly long-lasting openings, but the channels mediating these events had a much lower conductance than $\alpha_1\beta_2\gamma_2$ GABA_A receptors and thereby their interference could be easily eliminated from our analysis.

Analysis of Single-Channel Currents

Recorded signals were additionally filtered off-line (8-pole low-pass Bessel filter) using Clampex 10.7 software (Molecular Devices, Sunnyvale, CA, United States) to achieve a signal-to-noise ratio of at least 15:1. Subsequently, the sampling rate was reduced to maintain a 10:1 sampling-to-filter frequency ratio. To reduce the probability of analyzing the recordings from a multitude of channels, recordings with a high activity and/or ones with visible multiple openings were excluded from further analysis. The idealization of single-channel activity was performed with the SCAN software (DCProgs¹) and idealization

¹<http://www.onemol.org.uk/>

files were processed in EKDIST (DCProgs¹) to create dwell-time distributions, for open and shut events that were then fitted with the sums of exponentials and the respective time constants (τ) and percentages (P) were determined. The DCProgs software package has been kindly given to our group by David Colquhoun (UCL London).

Data and Statistical Analysis

All macroscopic current recordings were analyzed using pClamp 10.7 software (Molecular Devices, Sunnyvale, CA, United States). Only the recordings that did not exceed 20% of signal instability (most often rundown) were qualified for the statistical analysis, which was performed using Excel 2016 (Microsoft, Redmond, WA, United States) and SigmaPlot 11.0 (Systat Software, San Jose, CA, United States). Data comparison was performed using the Student's *t*-test preceded by the Shapiro–Wilk normality test or the Wilcoxon signed-rank test and the Mann–Whitney *U*-test for the data that failed normality assessment. The statistical significance threshold was defined as $p < 0.05$.

Homology Modeling and Ligand Docking

The structural homology model of $\alpha_1\beta_2\gamma_2$ GABA_AR was constructed using a similar approach as that described by Michałowski et al. (2017), but a distinct structural template was selected: a homomeric β_3 GABA_AR crystal structure (Miller and Aricescu, 2014) instead of a glycine receptor (Du et al., 2015). Prior to model construction, the sequence alignment of α_1 , β_2 , γ_2 , and β_3 GABA_AR subunits and sequences of other pentameric ligand gated ion channels (pLGICs) was performed in T-Coffee (Notredame et al., 2000) and refined manually using Jalview (Waterhouse et al., 2009). The MODELLER Python package (Šali and Blundell, 1993) was used to construct 1,000 initial $\alpha_1\beta_2\gamma_2$ GABA_AR structures. Among these, the best ones were selected according to the MODELLER quality estimates DOPE and molpdf and evaluated using RAMPAGE (Lovell et al., 2003). To further improve their quality, an iterative protocol of modeling using the MODELLER's refinement function “loopmodel” was employed. Briefly, the major part of the receptor model was constrained and areas of positions from the Ramachandran outlier region were remodeled until satisfactory quality was achieved. The final model was assessed with the Ramachandran plot evaluation, showing no residues in the outlier region (97.8 and 2.2% in favored and allowed regions, respectively). The ligands investigated in the present study were docked to the obtained homology model. The structures of GABA, P4S, and FLU were taken from the Zinc database (Irwin et al., 2012) and initially inserted into their respective binding sites according to the binding position of benzamidine in the experimental homomeric β_3 GABA_AR crystal structure (Miller and Aricescu, 2014). The final binding positions and the binding energy were obtained by the AutoDock Vina (Trott and Olson, 2010) flexible fit docking method. Each ligand was docked several times and the best binding position was selected according to the energy level and the properties of amino acids building the binding site. Upon docking, the

free energy of binding (ΔG , [kcal/mol]) was estimated for each ligand. Analysis of the results and visualizations were performed using VMD (Humphrey et al., 1996) and Python scripts.

Kinetic Scheme Modeling

Spontaneous activity was described using the kinetic scheme proposed by Kisiel et al. (2018), but to describe the modulation by FLU, an additional binding step for this modulator was added and the remaining rate constants were reassessed. To estimate the FLU binding/unbinding rates, ligand docking was used and the dissociation constant (K_D) was calculated using Eq. 1 (ΔG : binding energy, R : gas constant, T : temperature) as follows.

$$K_D = e^{\frac{\Delta G}{RT}} \quad (1)$$

$$K_D = \frac{k_{\text{off}}}{k_{\text{on}}} \quad (2)$$

Having established the ratio of the unbinding and binding rates (Eq. 2, $k_{\text{on/off}}$: binding/unbinding rates), the absolute values of these rate constants were optimized to reproduce the experimentally observed RT and deactivation kinetics upon FLU application (Figure 9A). The remaining rates were estimated according to single-channel open time distributions. In addition, to reproduce the kinetics of responses to exogenous FLU applications and overshoot, the selected rates were altered, but the resultant mean open times remained preserved. To describe GABA and P4S-evoked activity of the mutated receptor and its modulation by FLU, the kinetic scheme of the flipped Jones–Westbrook model from Szczot et al. (2014) was employed. It needs to be underlined that this model was optimized to fit the current responses recorded in the excised patch outside-out configuration, whereas in the present study we have collected data in the whole-cell mode because these recordings were more stable and had larger amplitudes and this was advantageous especially when recording currents mediated by mutants and/or evoked by the partial agonist. However, due to the slower solution exchange in the whole-cell configuration, the current onset, which was the fastest response characteristic, was slower than that measured in the outside-out patches. Nevertheless, all the effects of FLU on current responses (including the acceleration of current onset) observed on the excised patches were well-reproduced in the whole-cell recordings. In this situation, formal fits to the rising phase of current traces measured in the whole-cell configuration would lead to the misinterpretation of the slower current onset (than in excised patches) as slower binding and/or gating features underlying onset kinetics. Considering these premises, we employed the binding rate constants estimated in our previous study (Szczot et al., 2014) as control conditions and modified the rate constants to reproduce the relative impact of FLU on GABA_ARs. To reproduce both fast and slow components of macroscopic desensitization, it was necessary to incorporate an additional slow desensitizing state (Figure 8C, A₂D' state). To describe the changes in kinetics of mutated receptors and in their modulation by FLU, the rate constants were adjusted to best reproduce the trends observed experimentally (mainly:

amplitude, RT change trend, FR10, FR500, and/or desensitization and deactivation time constants). Adding the second desensitized state led to the construction of a more extensive model in which we had to consider a possibility that multiple sets of transition rates would result in similar simulated traces. Thus, to reduce the degrees of freedom, according to preliminary simulations and data from literature, some of the rates were fixed. The β and α rates were fixed, because these rates were not affected by CYS and LEU mutations (Szczoł et al., 2014) at saturating [GABA]. Moreover, WT receptor modulation by FLU at saturation is relatively weak; hence, we did not expect any significant impact of FLU on A₂O-associated rates. On the other hand, the preactivation rates (δ , γ), highly influenced by mutations, were varied to obtain the optimal fit. In addition, in all receptors, FLU changed the amplitude and accelerated the onset kinetics. This effect could be only reproduced by the changes in flipping rates, but not A₂O-associated rates. Iterative simulations were performed using custom Python scripts and ChanneLab 2.0 (Synaptosoft, Decatur, GA, United States) and the parameters describing the simulated current time course were calculated in pClamp 10.7 software (Molecular Devices, Sunnyvale, CA, United States).

RESULTS

Flurazepam Affects Spontaneous Activity of WT Receptors and α_1 F64 Mutants

It has been reported that various types of GABA_ARs, including $\alpha_1\beta_2\gamma_2$, show spontaneous activity that can be enhanced by BDZs (Mortensen et al., 2003), but the underlying mechanism remains unknown. Interestingly, for GABA-evoked currents, Gielen et al. (2012) and Dixon et al. (2015) suggested the impact of BDZs on the preactivation, but our recent report indicated that spontaneous openings do not require the preactivation step (Kisiel et al., 2018). To explore this problem, we compared the BDZ sensitivity of spontaneous activity mediated by WT receptors and by α_1 F64 mutants in which the preactivation step is impaired (Szczoł et al., 2014; Kisiel et al., 2018). As expected, the WT receptor showed a low spontaneous activity revealed by 100 μ M PTX (Figures 1A,C), but the mutations at the α_1 F64 residue strongly increased it (Figures 1B,C). There was no statistically significant differences in the extent of potentiation by FLU on WT receptors and all considered mutants (LEU, ALA, CYS, Figure 1D). The onset of currents observed after FLU application and mediated by WT receptors was very slow (1.63 ± 0.15 s, $n = 22$) and for the α_1 F64 mutants it was slightly (but significantly) faster (1.09 ± 0.07 s, $n = 16$ for LEU; 1.12 ± 0.08 s, $n = 17$ for ALA; and 1.26 ± 0.01 s, $n = 35$ for CYS, data not shown). These currents had an extremely slow deactivation after FLU removal (Figures 1A,B,E) that we found to be correlated with FLU binding energetics (see section “Model Simulations”). When studying the spontaneous activity, a precaution should be taken to rule out trace contaminations by GABA. We have thus additionally tested applications of low GABA concentration (1–100 nM, with and without FLU present in the bath). As shown in Figures 1Fa,G, currents

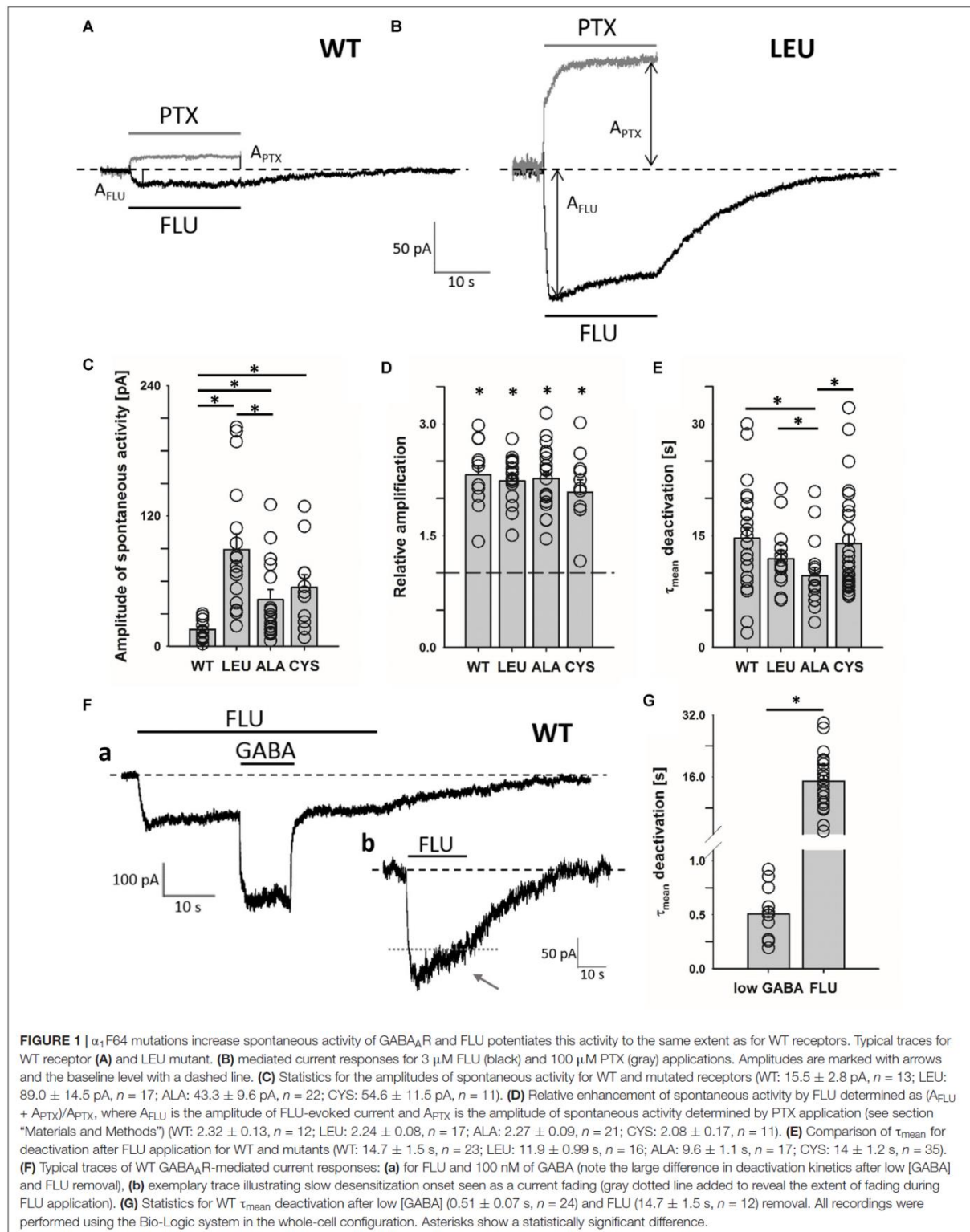
following FLU application and responses to 100 nM GABA had deactivation kinetics differing by nearly two orders of magnitude (Figure 1G, similar proportions were observed when GABA was applied alone, data not shown). Thus, if there was any trace contamination from GABA (wash, FLU- and GABA-containing solutions were prepared with the same Ringer's saline), then a rapid component would be expected also after FLU removal, but that was not observed. It is worth noting that in the case of prolonged exposure to FLU, an initial current onset is followed by a weak but clear fading, indicating the desensitization of the unbound receptor (Figure 1Fb, arrow).

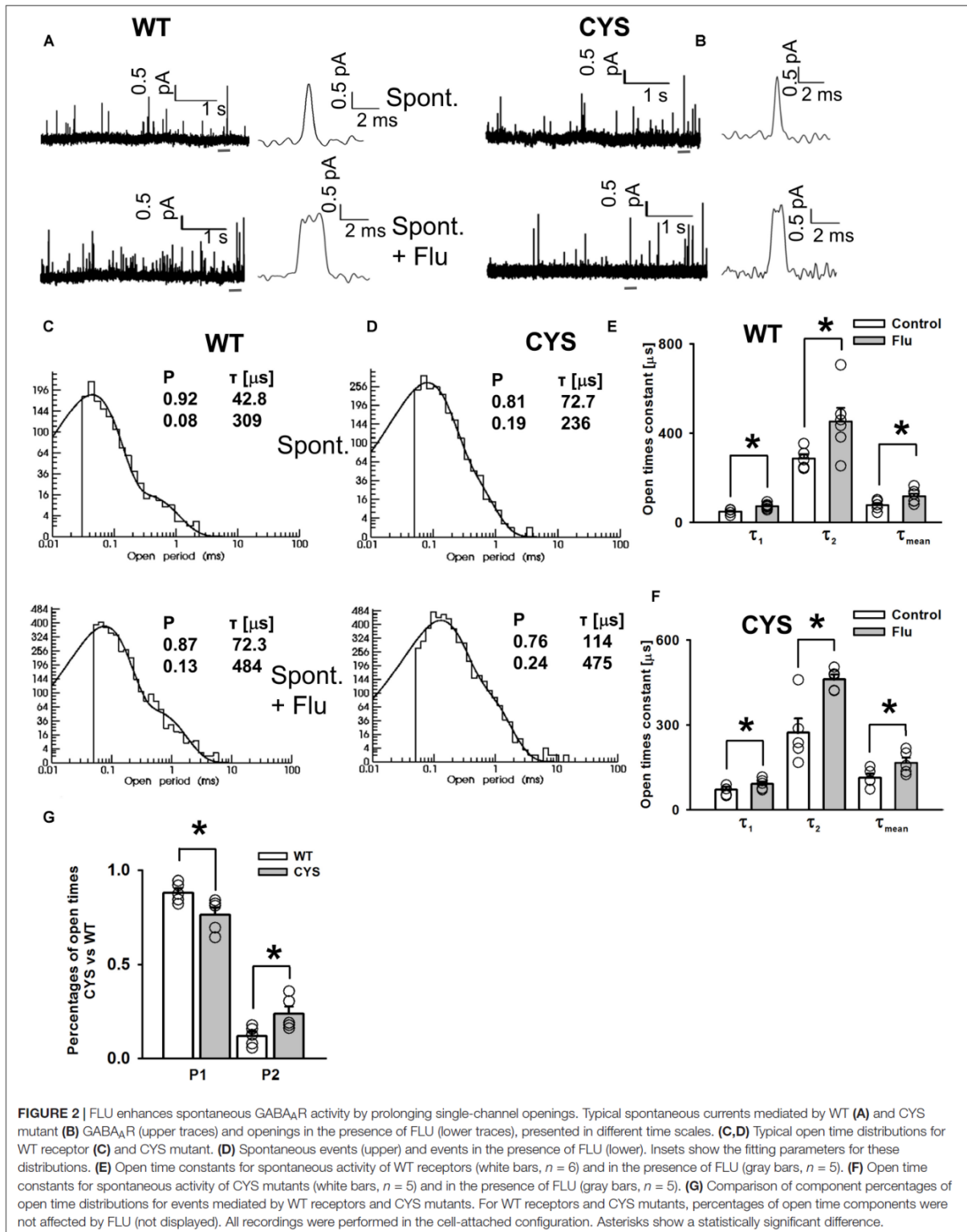
Flurazepam Affects Open Times of Spontaneous Openings

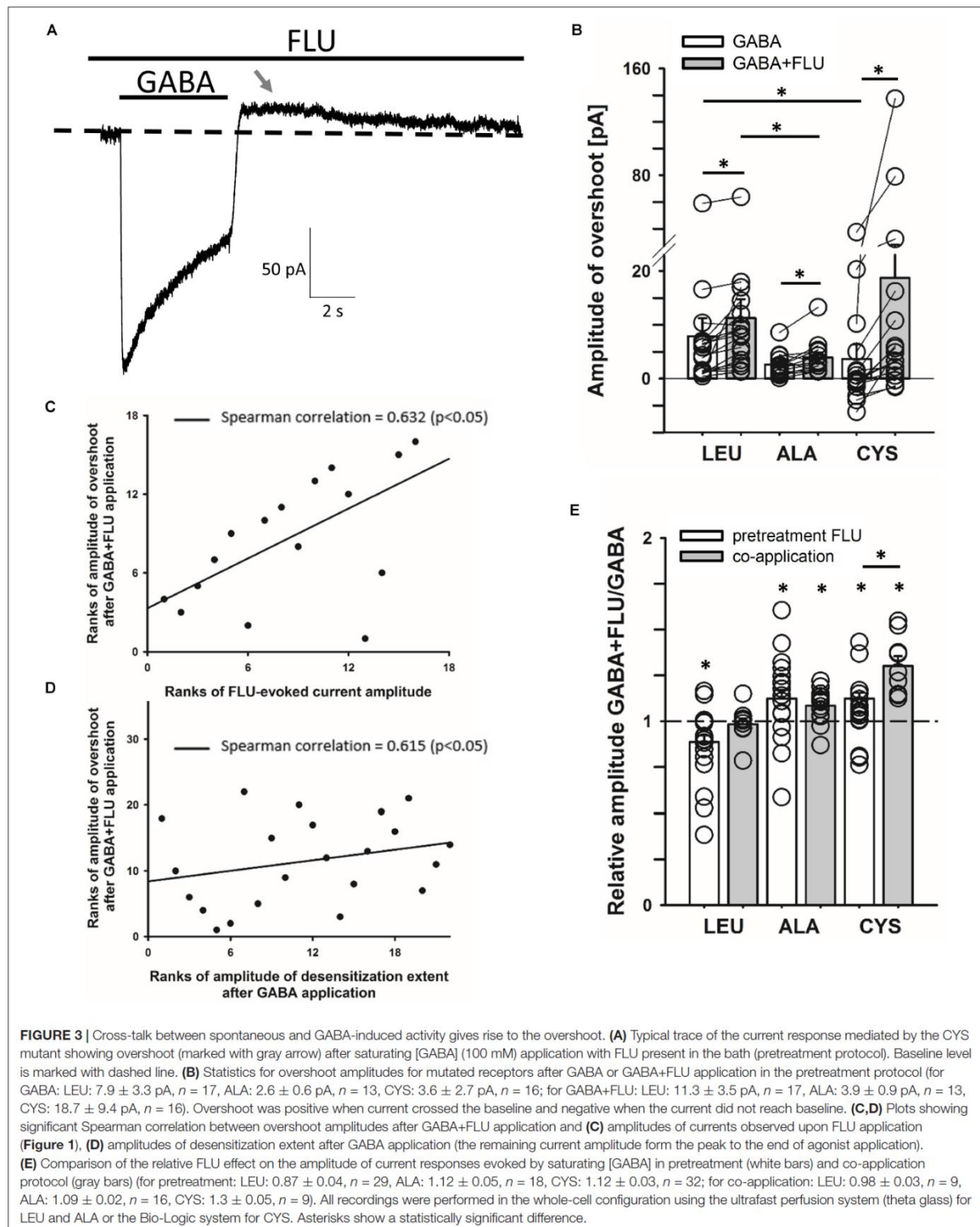
To further explore the modulation of spontaneous events by FLU, we conducted single-channel recordings as described by Kisiel et al. (2018; see section “Materials and Methods”). Considering the similarity in the FLU effect on WT receptors and mutants, we limited these recordings to the WT and the CYS mutant (Figures 2A,B), which is most distinct from the native receptor (Kisiel et al., 2018). Open time distributions for WT and CYS receptors had two components with time constants that did not differ between these receptor types, but for CYS mutants the percentage of the slower component was larger (Figures 2C,D,G). Interestingly, FLU produced a similar effect on the activity of the WT and CYS mutants by significantly increasing both time constants (Figures 2C–F) and thereby the mean open time (Figures 2E,F). The analysis of closed times did not reveal any major difference but it was problematic as spontaneous activity did not show bursts (formally the number of openings per burst was invariably 1) (Kisiel et al., 2018), excluding any assessment of the number of channels in the patch.

Cross-Talk of Spontaneous and GABA-Evoked Activity

We asked whether the modulation of spontaneous activity by FLU might affect the GABA-elicited activity. When BDZs are tested, cells are typically pretreated with these drugs prior to the application of agonist and the “baseline” is commonly interpreted as the “no activity” reference which, because of spontaneous activity, is problematic. In Figure 3A, a typical response to saturating [GABA], in the presence of FLU, mediated by the CYS mutants (pretreatment protocol) is shown. It is evident that after GABA removal, deactivation is followed by an overshoot (arrow in Figure 3A). Although in the case of WT receptors, the spontaneous activity was weak (Figure 1C), in cells with strong expression, the overshoot could be also seen (data not shown), indicating a common mechanism. As we discuss it in Section “Model Simulations,” this phenomenon reflects a cross-desensitization of spontaneous and ligand-activated receptors. The following evidence indicates the involvement of spontaneous activity and its modulation by FLU in the overshoot phenomenon. The enhancement of spontaneous activity by FLU







is associated with an increased overshoot (Figure 3B). This relationship is further supported by a significant correlation between the amplitudes of the overshoot and the amplitudes of currents observed upon the application of FLU (Figure 3C). Moreover, in the case of the CYS mutant, we observed a clear correlation between GABA-induced macroscopic desensitization and the amplitude of the overshoot (Figure 3D). Considering thus a potential impact of spontaneous activity on GABA-evoked responses, we compared the amplitudes of currents evoked by saturating [GABA] using the pretreatment and co-application protocols. As is shown in Figure 3E, the relative current amplitude measured using the co-application protocol was different from that upon FLU pretreatment.

Impact of FLU on GABA-Evoked Responses Mediated by α_1 F64 Mutants

The impact of FLU on current responses mediated by saturating [GABA] was described by us for the $\alpha_1\beta_2\gamma_2$ receptors in our report (Mercik et al., 2007). Briefly, FLU slightly but significantly reduced the current amplitude; macroscopic desensitization was not affected and deactivation showed a slight and not significant prolongation. Similar effects were observed for cultured hippocampal neurons (Mozzrymas et al., 2007), which express primarily the $\alpha_1\beta_2\gamma_2$ receptors. Considering that α_1 F64 mutations strongly affect the receptor gating (particularly flipping/preactivation), we next investigated the impact of FLU on currents elicited by saturating [GABA] and mediated by these mutants. In contrast to WT receptors, current responses elicited by 100 mM GABA for CYS mutants were significantly potentiated by FLU in the pretreatment protocol (Figures 3E, 4A,B) and this effect was significantly larger when co-applying FLU with GABA (Figure 3E). In the case of the ALA mutant, the effect of FLU was weaker but potentiation in both pretreatment and co-application protocols was significant (Figures 3E, 4B). On the contrary, for the LEU mutant, we found that FLU slightly decreased the current amplitude in the pretreatment protocol but did not affect it when co-applied with GABA (Figures 3E, 4B). A similarity in the FLU effect on WT receptors and LEU mutants is consistent with our finding that this mutant showed the closest resemblance to the WT receptors among those considered in Szczot et al. (2014) and in the present study.

The observation that FLU exerted a qualitatively different effect on the current amplitudes for WT receptors and mutants (CYS and ALA) indicates a difference in receptor gating and we thus extended our analysis to the time course of these responses. Whereas FLU had no effect on the onset kinetics in the case of WT receptors (Mercik et al., 2007), a significant shortening of the current RT was observed for all considered α_1 F64 mutants (Figures 4C,D). Moreover, FLU affected the macroscopic desensitization primarily by accelerating its rapid component (Figures 4E,Fa, absolute values for desensitization and deactivation time course parameters in control conditions are disclosed in the Figure legend) for LEU and ALA mutants but not for CYS, for which it was assessed as the FR10 parameter that remained unaffected (Figures 4E,Fb). An increase in the FR500 parameter for LEU and ALA (but not CYS) mutants indicated the

impact of FLU on the extent of desensitization (Figures 4G,H). The mean time constant for deactivation (τ_{mean}) for currents elicited by short GABA pulses was not significantly affected by FLU in all mutants, but in the case of LEU, the fast component was accelerated together with a change in percentages for time constants (Figures 4Ia,b). In the case of deactivation measured after a prolonged application (500 ms) of saturating [GABA], no effect of FLU was found for all considered mutants (Figure 4Ic).

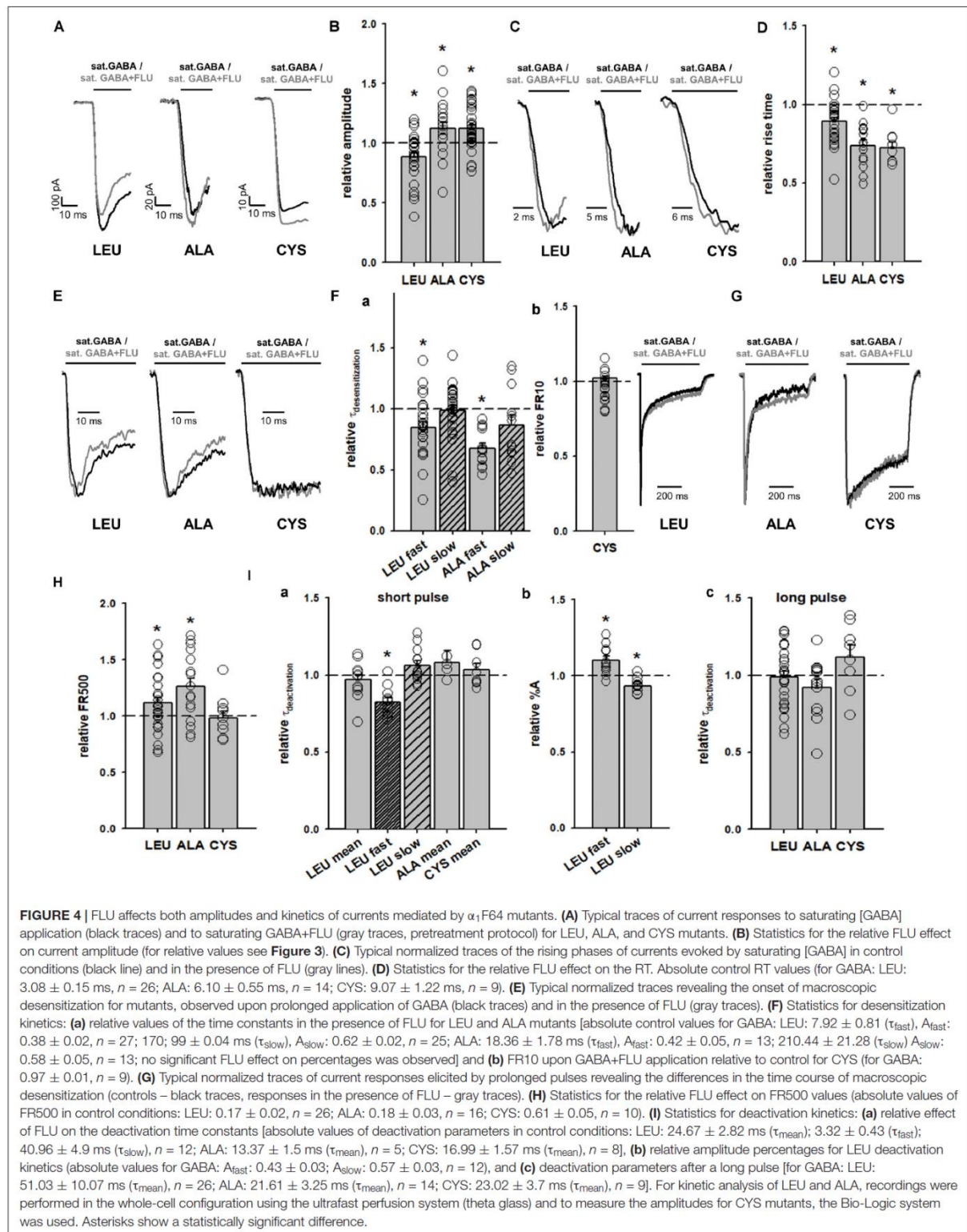
Impact of Flurazepam on Currents Evoked by a Partial Agonist P4S

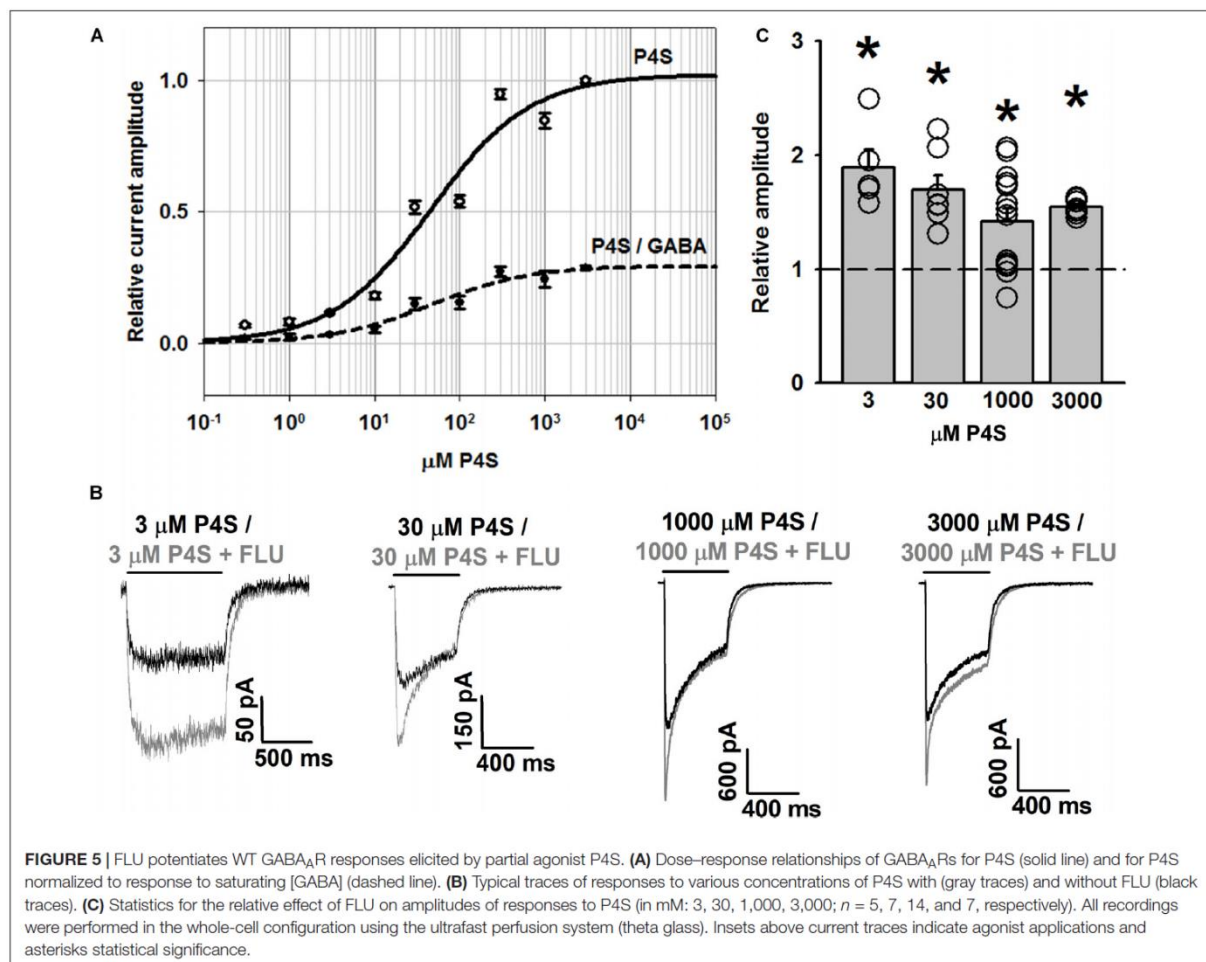
To further address the effect of FLU on GABA_AR gating, we have analyzed its impact on responses elicited by a partial agonist P4S. As expected, the dose-response obtained for P4S showed saturation at current values considerably lower than for GABA but the values of EC50 did not show any major difference (EC50 = 46 μ M for P4S, Figure 5A, compared to 40 μ M for GABA determined by Brodzki et al., 2016). Notably, in contrast to our observations for GABA (Mercik et al., 2007), responses to saturating concentrations of P4S were clearly potentiated by FLU for the entire range of concentrations used (Figures 5A-C).

Importantly, whereas FLU only slightly affected the time course of responses evoked by saturating [GABA] (Mercik et al., 2007), the kinetics of currents elicited by saturating [P4S] was clearly altered (Figures 5B, 6A). The most apparent effect of FLU on P4S-evoked responses was the enhancement of the macroscopic desensitization (Figures 5B, 6A). For responses to 30 μ M P4S, FR10 was close to 1 (minimal desensitization) and was unaffected by FLU (data not shown). Likewise, at low [P4S] (3 μ M), FR500 was not affected but at 30 μ M and higher concentrations, a strong increase in the extent of macroscopic desensitization (FR500) was observed (Figures 6A,B). For responses evoked by saturating (1 mM) P4S, the exponential fit was possible and revealed that FLU robustly increased in the rate and extent of macroscopic desensitization (accelerated τ_{fAst} and decreased FR500, Figures 6B-D). Notably, the desensitization onset for P4S-evoked currents was much slower (even in the presence of FLU) than that for saturating [GABA] (Mercik et al., 2007).

As we have previously shown (Szczot et al., 2014), the onset kinetics for currents evoked by saturating [P4S] was much slower than that of the responses elicited by 10 mM GABA. However, whereas for saturating [GABA] FLU had no effect on RT (Mercik et al., 2007), we show here that this compound clearly accelerated it for responses evoked by P4S (30 μ M–3 mM) including saturation (Figures 6E,F).

For short and long P4S pulses, deactivation kinetics was much faster than for GABA-evoked currents (for 1 mM P4S, short pulse: $\tau_{\text{mean}} = 20.59 \pm 3.83$ ms, $n = 7$, long pulse $\tau_{\text{mean}} = 54.44 \pm 6.23$ ms, $n = 14$; for GABA: $\tau_{\text{mean}} = 52.29 \pm 24.77$ ms, long pulse $\tau_{\text{mean}} = 232.69 \pm 33.51$ ms; $p < 0.05$ for τ_{mean} comparison for short and long pulses). When applying a short pulse of 1 mM P4S, FLU prolonged the deactivation kinetics (for FLU: $\tau_{\text{mean}} = 24.35 \pm 2.84$ ms, $n = 7$, $p < 0.05$, Figure 6G) and a qualitatively analogous effect was observed after





a long (500 ms) pulse of P4S at various concentrations (Figures 6H,I).

Taking altogether, we reveal that the FLU effects on currents evoked by P4S are by far more pronounced than in the case of GABA. Moreover, at a qualitative level, the FLU effects on currents evoked by P4S show similarity to those observed for currents mediated by the $\alpha 1F64$ mutants.

Model Simulations

To obtain further insight into the mechanisms whereby FLU modulates the spontaneous and ligand-induced GABA_AR activity, model simulations were investigated. First, we asked whether very slow deactivation of spontaneous currents upon FLU application (Figure 1) is associated with ligand binding. To address this issue, the dissociation constant for this compound was assessed using homology modeling and docking studies, and the binding properties for GABA and P4S were also determined. The binding modes for considered compounds are presented in Figures 7A–C with estimated binding energies and disassociation constants, disclosed in the legend. Notably, the

lowest disassociation constant value was for FLU, indicating a slow unbinding and deactivation kinetics.

Spontaneous activity was modeled using the same kinetic scheme as proposed by Kisiel et al. (2018); Figure 8A. To model the FLU modulation of spontaneous activity, an additional state (RM, receptor with bound modulator) was introduced (Figure 8B) and the values of the rate constants were assessed as described in Section “Materials and Methods.” The effects of FLU modulation in both WT and CYS mutants were modeled by the decrease in α_m , α'_M , and d_m , which are the rates determining the mean open times of the respective open states (Figure 2E). In addition to fully mimicking the FLU effects observed in macroscopic recordings, β_M was increased (Figures 8A,B, simulation in Figure 9A).

The fact that the overshoot was particularly prominent in the case of mutants (Figure 3B) suggests the involvement of spontaneous events. To further explore this issue, simulations were considered using the model proposed by (Szczot et al., 2014; Figure 8C) connected with the branch describing the spontaneous activity (Figure 8A). These simulations reproduced

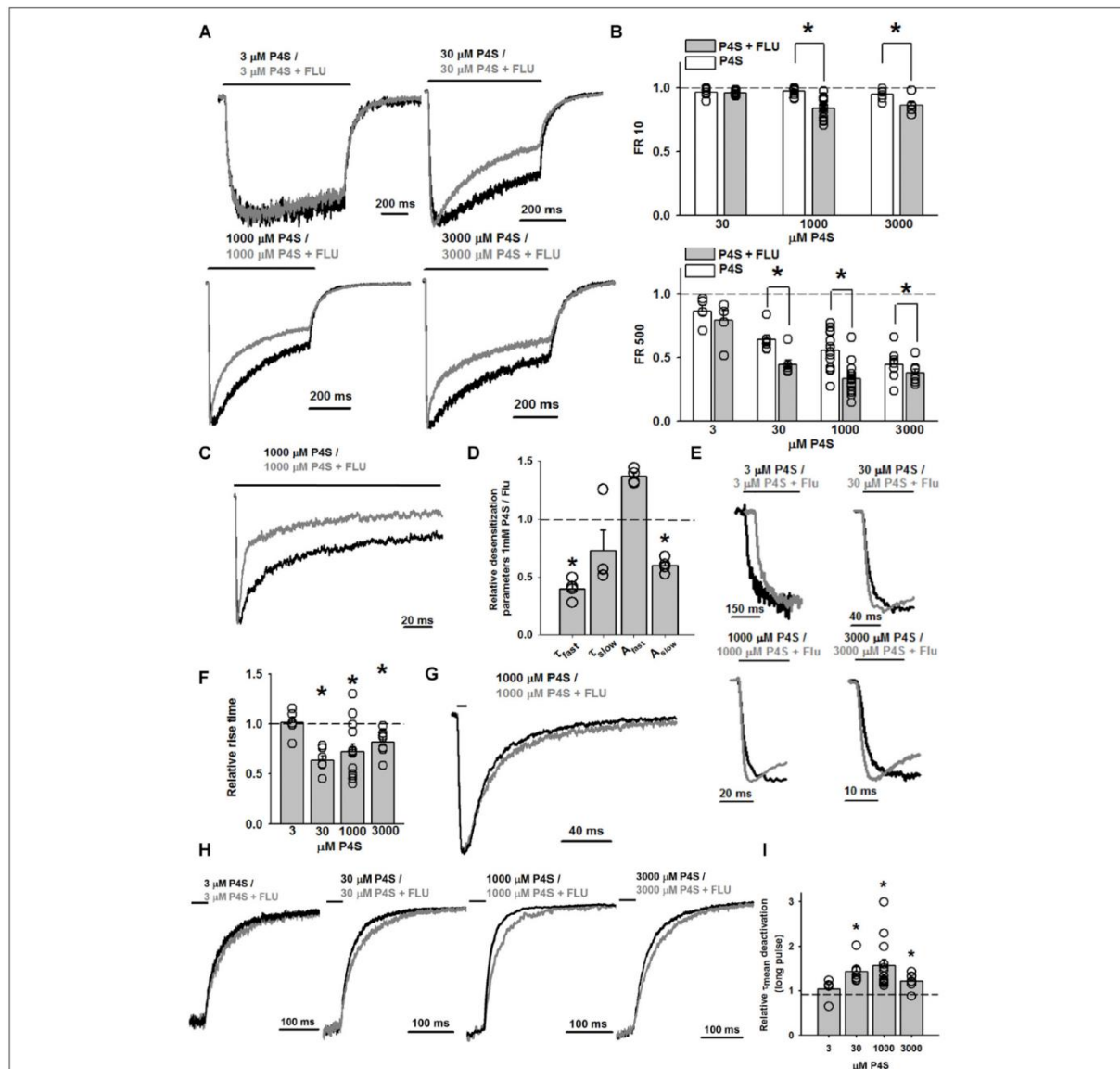
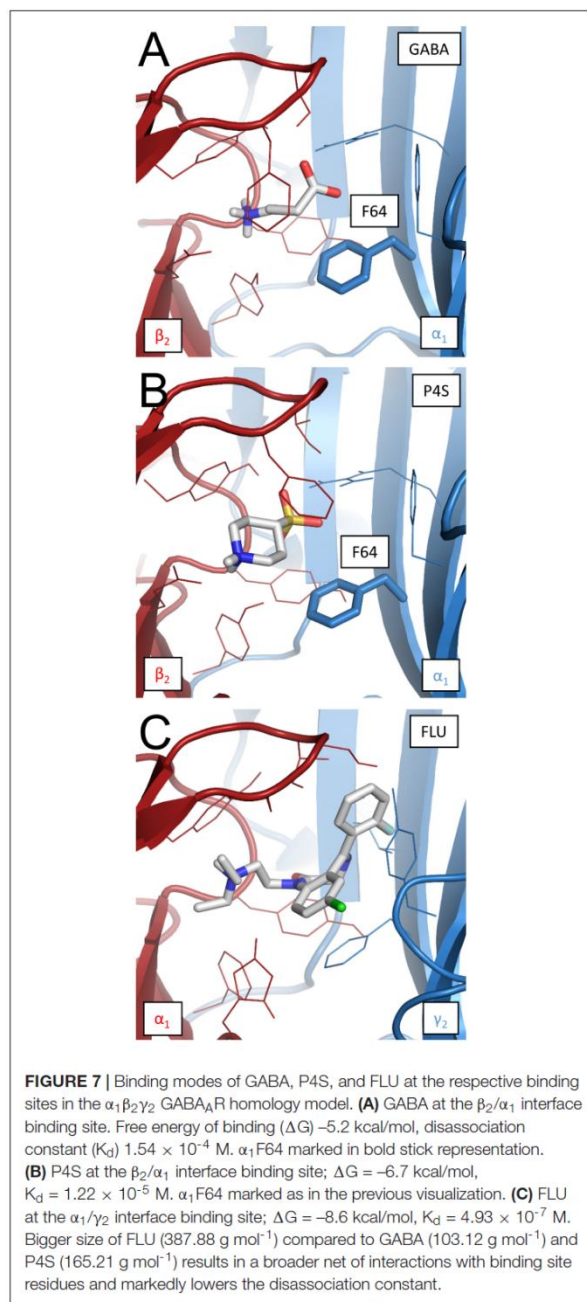


FIGURE 6 | FLU markedly affects the kinetic profile of WT GABA_AR-mediated currents evoked by partial agonist P4S. **(A)** Typical normalized traces of current responses to various concentrations of P4S, mediated by WT GABA_AR in control conditions (black traces) and in the presence of FLU (gray traces). **(B)** Bar charts illustrating the statistics of the FLU effect on FR10 and FR500 parameters for responses evoked by P4S (in mM: 3, 30, 1,000, 3,000; *n* = 5, 7, 14, and 7, respectively). **(C)** Typical normalized traces recorded from outside-out patches containing WT GABA_ARs responding to 1 mM P4S alone (black trace) and in the presence of FLU (gray trace). **(D)** Relative macroscopic desensitization time course parameters for recordings from outside-out patches. Absolute values for control (1 mM P4S: τ_{fast} : 4.14 ± 0.69 ms; τ_{slow} : 197.07 ± 22.32 ms; A_{fast} : 0.52 ± 0.02; A_{slow} : 0.48 ± 0.02; *n* = 4) **(E)** Close-up, normalized traces of currents evoked by various concentrations of P4S alone (black traces) and in the presence of FLU (gray traces) with emphasis on the effect of FLU on the current onset. **(F)** Statistics for the relative FLU effect on the RT measured at various P4S concentrations. Absolute values of RT for control (3 μM: 71.98 ± 4.72 ms, *n* = 5; 30 μM: 20.35 ± 2.07 ms, *n* = 7; 1 mM: 6.79 ± 0.60 ms, *n* = 14; 3 mM: 5.89 ± 0.55 ms, *n* = 7). **(G)** Typical normalized traces of current responses to 1 mM P4S alone (black trace) and in the presence of FLU (gray trace). Note a slowdown of deactivation in the presence of FLU. **(H)** Close-up, normalized traces of currents evoked by various concentrations of P4S alone (black traces) and in the presence of FLU (gray traces) with emphasis on the effect of FLU on the current deactivation after prolonged agonist pulse. **(I)** Relative effect of FLU on deactivation time constants for responses to various concentrations of P4S, measured after prolonged agonist pulse. Absolute values of τ_{mean} for control (3 μM: 77.15 ± 5.32 ms, *n* = 5; 30 μM: 60.23 ± 5.39 ms, *n* = 7; 1 mM: 54.44 ± 6.23 ms, *n* = 14; 3 mM: 78.11 ± 7.59 ms, *n* = 7). All recordings were performed in the whole-cell configuration using the ultrafast perfusion system (theta glass). Insets above current traces indicate agonist applications and asterisks statistical significance.

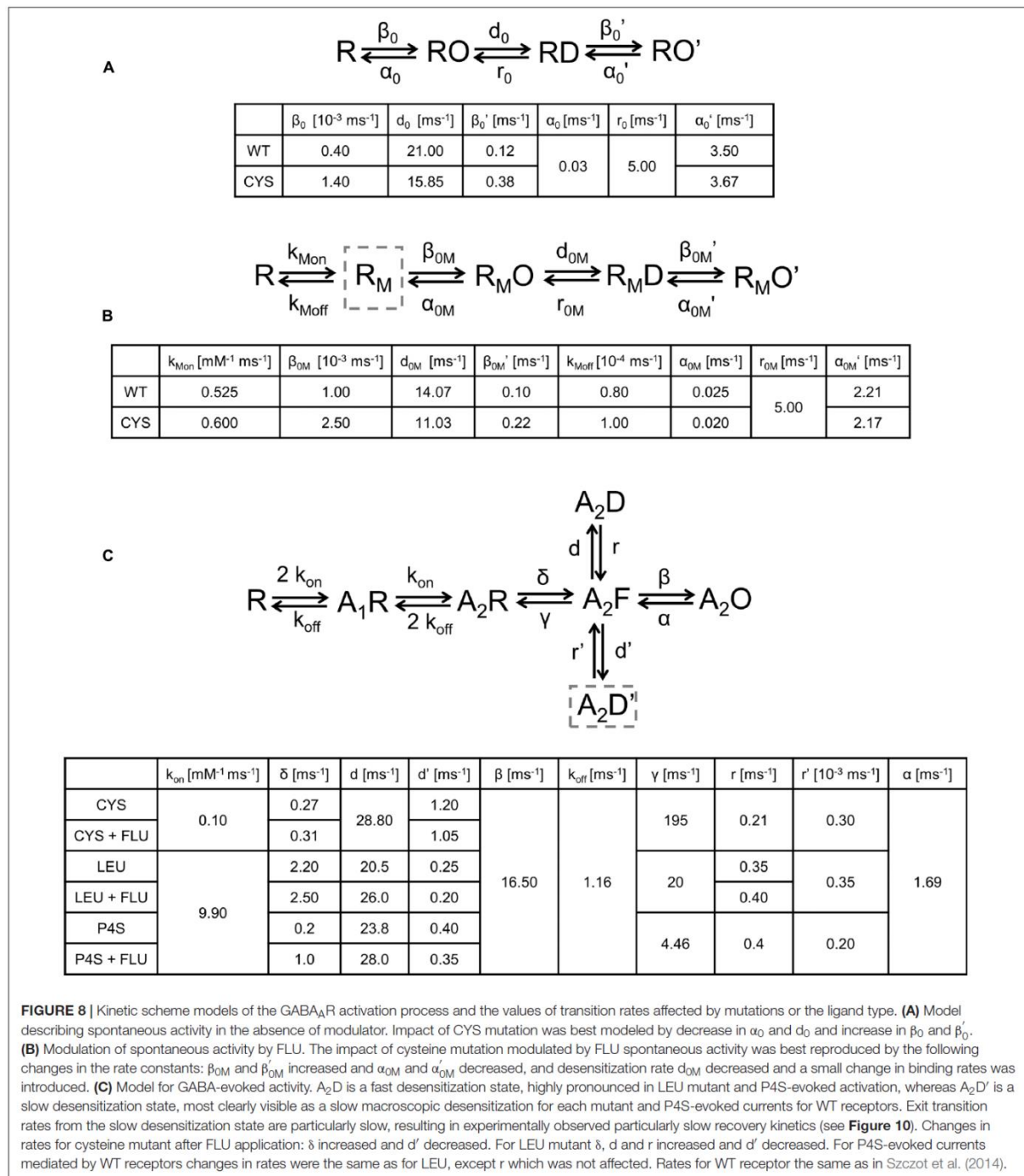


the dependence of the overshoot on the spontaneous activity (**Figure 9B**) and provided a mechanistic explanation for this phenomenon. The agonist pulse desensitizes the majority of receptors and thereby reduces the pool of spontaneously active channels and therefore, after agonist removal, the current exceeds the “baseline” (overshoot) and then slowly returns to the level prior to the agonist pulse, reflecting resensitization.

In several studies, the description of desensitization was limited to the fast component, in the range of a few milliseconds, claiming that this component is the most relevant to the time scale of synaptic events (e.g., Jones and Westbrook, 1995; Mozrzymas et al., 1999; Barberis et al., 2000). However, in the present study, the considered mutants show a prominent slow desensitization. We made an attempt to include this component in our modeling by adding additional desensitized transition, originating from the flipped state (**Figure 8C**). This transition allowed to fairly reproduce the slow component for the desensitization rate d' considerably slower than d and a particularly slow resensitization rate r' (**Figure 8C**). However, such values of d' and r' would predict a remarkably slow recovery. To provide experimental support for this prediction, we have performed recordings for LEU mutants in which a prolonged saturating GABA pulse, inducing macroscopic slow desensitization, is followed by a variable washout interval and a brief test pulse revealing the extent of recovery (**Figure 10**). As shown in **Figure 10**, these experiments confirm a very slow recovery predicted by the model.

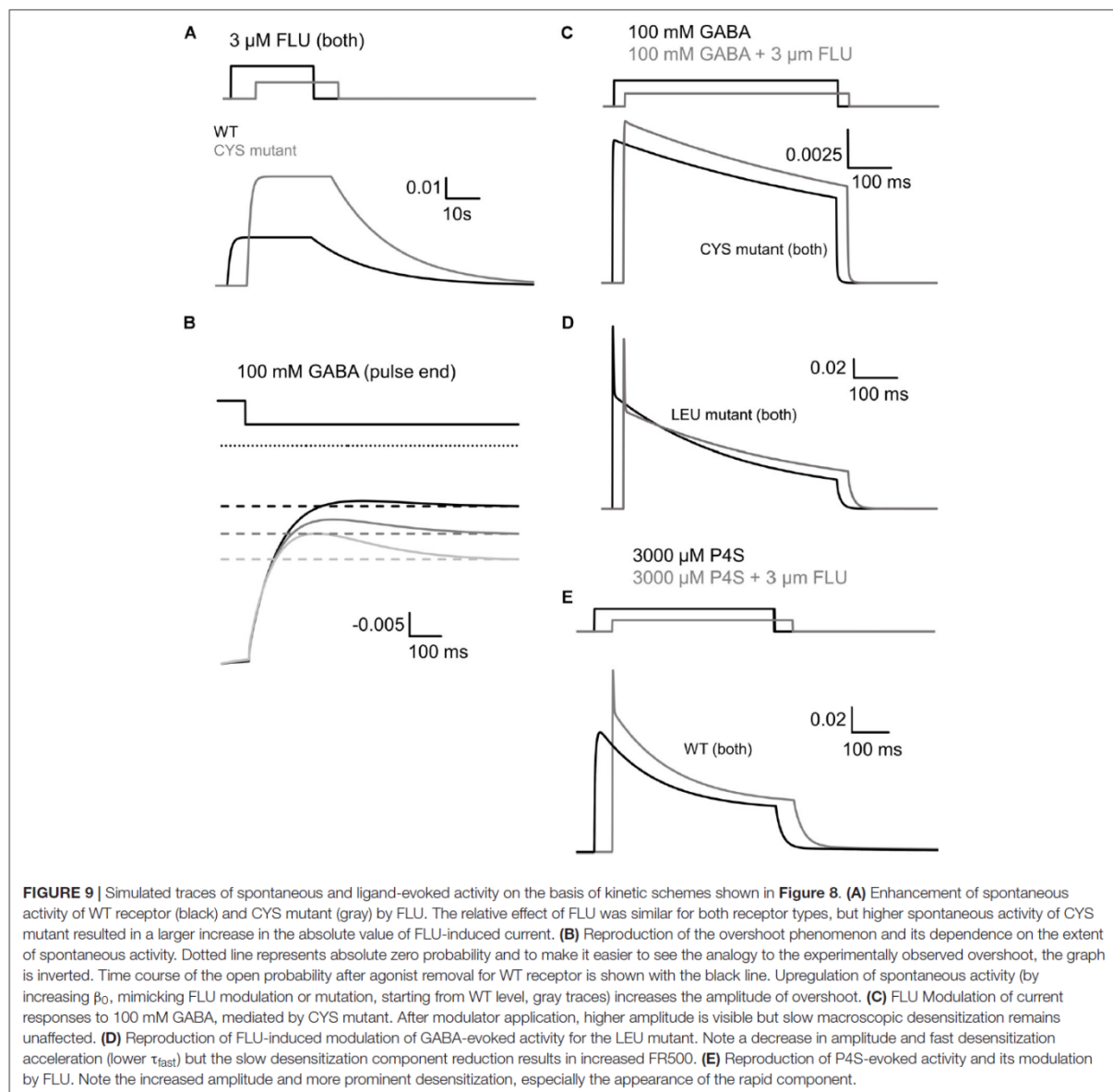
Thus, to describe FLU effects on GABA-evoked currents mediated by mutants, the model with fast and slow desensitization states was considered (**Figure 8C**) that allowed to reproduce a very slow macroscopic desensitization for the CYS mutant due to mainly a slow desensitization transition, although a prominent overshoot for this mutant argues for a contribution from the fast component that is not manifested as a rapid fading due to extremely slow flipping (Szczot et al., 2014). In the case of the LEU mutant, a combination of slow and fast desensitization was necessary to reproduce our observations. Notably, the slow flipping rate in mutants (Szczot et al., 2014; Kisiel et al., 2018) made it possible to clearly observe the effect of upregulating these rate constants by FLU as a trend of changes toward the WT phenotype. The increased amplitude for the CYS mutant (**Figures 4A,B**) was modeled by increasing the flipping (δ) rate that also mimicked the acceleration of the current onset (**Figures 4C,D**, simulated response in **Figure 9C**). To maintain the correct value of FR500, d' was decreased. The LEU mutant showed mixed effects of FLU action: fast desensitization was enhanced, whereas FR500 increased (**Figures 4F,H**), requiring an increase of d and r , and a decrease of d' , further confirming the need to include the two desensitization states. To reproduce a decreased amplitude and an accelerated RT for the LEU mutant (**Figures 4A–D**), the increase in d was not sufficient and, especially to correctly mimic the RT acceleration, an increase in δ (as for the CYS mutant) was needed (see simulated response in **Figure 9D**).

The activation of WT GABA_AR by a partial agonist P4S is expected to occur with a reduced flipping rate with respect to GABA (Gielen et al., 2012; Szczot et al., 2014). Our major observation was that FLU tended to change the P4S-evoked currents toward the kinetic phenotype observed for GABA-evoked responses: most evidently, FLU accelerated the onset and macroscopic desensitization and increased the amplitude (**Figures 5, 6**). These effects could be fairly reproduced by increasing δ but to maintain the correct FR500 value, an increased d' , similar to the LEU mutant, was required (**Figure 9E**).



Note that in contrast to the α_1F64 mutants, in the case of WT receptors, the FLU effect on currents evoked by saturating GABA was weak (Lavoie and Twyman, 1996; Mercik et al., 2007). To clarify this issue, we have run additional series of simulations

for WT receptors activated by saturating GABA. We found that the flipping rate in these receptors is so fast that its further increase by FLU is not effective and the entry into the open states is counterbalanced by the entry into the rapidly desensitizing

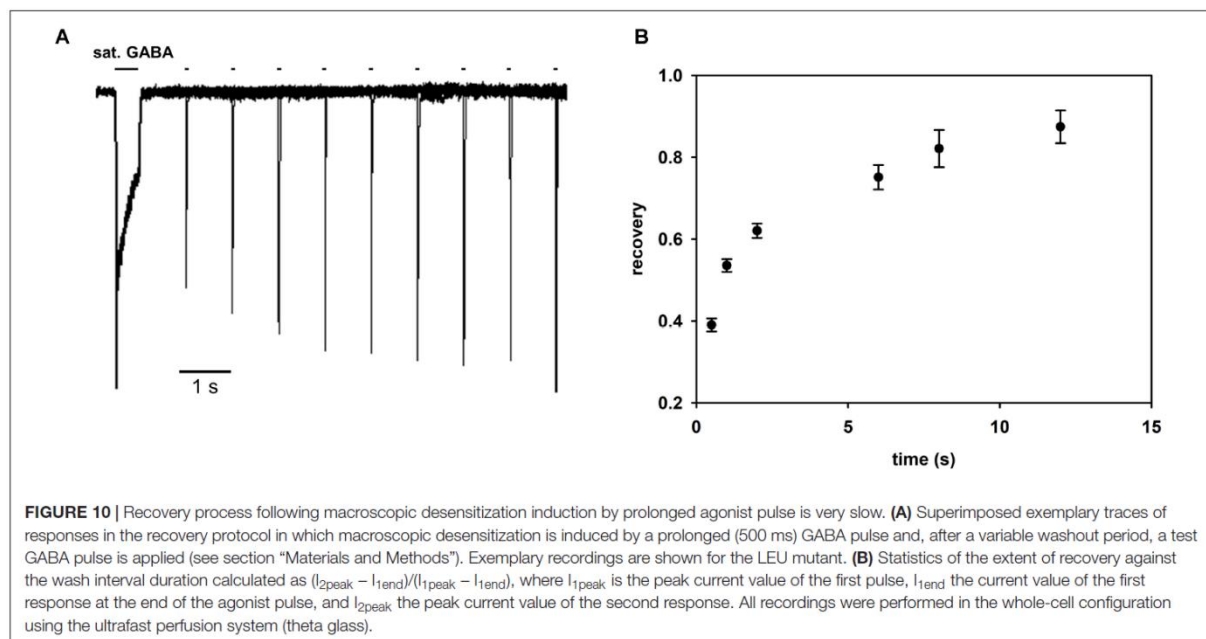


state, giving rise eventually to the decrease in current. Thus, a prominent impact of increased flipping on current kinetics in the case of mutants and P4S-evoked currents for WT receptors was possible because it was much slower than in the case of WT receptors.

DISCUSSION

In the present study, we present the first, to our knowledge, thorough analysis of a mechanism whereby a BDZ FLU affects the spontaneous activity of GABA_AR. Our macroscopic and

single-channel analyses indicate that FLU affects the opening/closing transitions, thereby reinforcing the notion that the BDZs affect the receptor gating. Moreover, upon prolonged exposure to FLU, the receptors undergo a slow macroscopic desensitization (**Figure 1Fb**) that demonstrates, for the first time, that the GABA_AR may enter the desensitized state in the absence of the orthosteric agonist and this process may depend on BDZs. However, the percentage of unliganded desensitized GABA_ARs remains unknown. Our homology modeling indicated that a particularly slow deactivation kinetics after FLU removal (**Figure 1**) could result from a markedly slower unbinding rate for FLU compared



to GABA or P4S. In addition, our data, obtained using the pretreatment and co-application protocols, provide a methodological hint that the spontaneous activity, especially in the presence of BDZs, may affect the readout of GABA-evoked responses.

Considering that the spontaneous activity represents a form of receptor gating, it might be surprising that the mutations located at the binding site (i.e., distantly from the gate) strongly affect it. However, the mutations at the binding site affecting spontaneous activity have been already described, e.g., the mutation at the β_2 E155 residue (Newell et al., 2004) or at the 102 residue in the ρ_1 homomers (Torres and Weiss, 2002). It seems thus that the molecular structure of GABA_AR macromolecule assures an efficient communication between distant localizations. Moreover, it is not surprising that the modulation of spontaneous activity by FLU for WT receptors and mutants was similar, as the kinetic features of this activity for these receptors are analogous (Kisiel et al., 2018).

Considering the impact of FLU on spontaneous GABA_AR activity, two possible mechanisms could be considered: a direct activation by FLU or a modulatory effect on existing events. Our interpretation is leaning toward the second possibility for the following reasons. (i) There are two open time components in control conditions and in the presence of FLU also there were two components but with significantly different time constants (Figure 2). If FLU activated some extra openings, then we would expect some extra component(s) in the open time distributions (besides those found in the control recordings) that were actually not found. The fact that in the presence of FLU we see two components with different time constants provides an argument for a modulatory mechanism. (ii) The activation of

extra events by FLU would be expected to increase the overall frequency of events while the open time components of control spontaneous activity should be preserved in the presence of this BDZ. As we already pointed out, this prediction is not observed, but in reference to the frequency issue we saw a trend toward an increase in the presence of FLU, although it did not reach significance due to the large data scatter. We believe that this trend to increase the frequency in the presence of FLU is likely to represent a lower percentage of undetected events due to a prolongation of the open times. Undoubtedly, there is a percentage of extremely short events that are at the border line of our resolution. Prolongation of openings by FLU increases the chances of detection of these short openings, giving rise to apparently a larger frequency of events with distinct open time distribution than in control conditions. On the other hand, we cannot exclude some modulatory effect of FLU on the opening rates (β) of spontaneous events.

Interestingly, the cross-talk between the spontaneous and GABA-evoked activity, manifested by the overshoot, is sensitive to the modulation of spontaneous openings by FLU. A similar overshoot phenomenon was reported previously by Wagner et al. (2005) for GABA_AR containing the ϵ subunit. It seems interesting to extend the analysis of cross-talk between spontaneous and GABA-evoked activity to other receptor types, including those contributing to both tonic and phasic inhibition (like, e.g., GABA_ARs containing $\alpha 5$ subunit; Caraiscos et al., 2004; Zarnowska et al., 2009) or those mediating tonic currents. Our major conclusion regarding the mechanism of GABA_AR modulation by FLU is that this compound enhances the flipping and desensitization rates pointing thus to a “mixed” effect.

Our proposal that FLU upregulates the flipping rate is based on the experiments on α_1 F64 mutants and on the activation of the WT receptor by a partial agonist P4S. Indeed, in our model simulations for these two sets of experiments, most FLU effects could be mimicked by the increased flipping rate, which altered the current kinetics toward the WT receptor phenotype. On the other hand, the impact of FLU on currents mediated by α_1 F64 mutants and on P4S-evoked responses of WT receptors showed some differences (Figures 4–6). This could result from the different values of flipping rates in α_1 F64 mutants and WT receptors activated by P4S but also because, as shown in our recent report (Kisiel et al., 2018), the mutation at the α_1 F64 residue alters not only flipping but also other gating transitions. Moreover, although there is an emerging agreement that partial agonists differ from full ones primarily by the flipping transitions (Lape et al., 2008), it cannot be taken for granted that other rate constants are equal for P4S and GABA. Notably, besides a prominent effect of FLU on the flipping rate, our analysis indicates a clear effect on desensitization. It needs to be emphasized that a diversity of the effects of the BDZ on gating is manifested here additionally by the fact that FLU affects opening/closing for spontaneous events whereas flipping and desensitization are affected for GABA-evoked activation. It seems thus that FLU may exert a mixed effect on the receptor gating, requiring further studies using different agonists and different mutations.

Taking altogether, we demonstrate that FLU affects the gating properties of the $\alpha_1\beta_2\gamma_2$ GABA_AR, but this modulation is characterized by a distinct mechanism in the case of spontaneous and GABA-evoked activity. Moreover, our analysis of spontaneous and agonist-evoked activity provides further evidence that the phenomenon of flipping requires an interaction with the agonist and the desensitization process may take place

in the absence of the orthosteric ligand. This study extends our knowledge on the mechanism of action of BDZs in the context of the structure–function relationship of GABA_ARs, offering new perspectives in designing these drugs for clinical use.

DATA AVAILABILITY

Datasets are available on request. Please contact corresponding authors.

AUTHOR CONTRIBUTIONS

MJ-Ś designed and performed the experiments, analyzed the data, and wrote the paper. KT performed the experiments, analyzed the data, and wrote the paper. MB participated in carrying out the experiments, analyzing the data, and writing the paper. MM performed homology modeling, ligand docking, kinetic simulations, and wrote the paper. MC performed the experiments and analyzed the data. JN and AA contributed to some experiments and performed a preliminary analysis. RS performed a part of single-channel experiments. JM conceived and supervised the project, designed the research, participated in data analysis and model simulations, wrote most parts of the paper and edited the final version of the manuscript, and procured financial support.

FUNDING

This work was supported by the Polish National Science Centre (Grants numbers DEC-2013/11/B/NZ3/00983 and DEC-2015/18/A/NZ1/00395).

REFERENCES

- Barberis, A., Cherubini, E., and Mozrzymas, J. W. (2000). Zinc inhibits miniature GABAergic currents by allosteric modulation of GABA_A receptor gating. *J. Neurosci.* 20, 8618–8627. doi: 10.1523/JNEUROSCI.20-23-08618.2000
- Brodzki, M., Rutkowski, R., Jatczak, M., Kisiel, M., Czyżewska, M. M., and Mozrzymas, J. W. (2016). Comparison of kinetic and pharmacological profiles of recombinant $\alpha_1\gamma_2$ L and $\alpha_1\beta_2\gamma_2$ L GABA_A receptors - A clue to the role of intersubunit interactions. *Eur. J. Pharmacol.* 784, 81–89. doi: 10.1016/j.ejphar.2016.05.015
- Campo-Soria, C., Chang, Y., and Weiss, D. S. (2006). Mechanism of action of benzodiazepines on GABA_A receptors. *Br. J. Pharmacol.* 148, 984–990. doi: 10.1038/sj.bjp.0706796
- Caraiscos, V. B., Elliott, E. M., You-Ten, K. E., Cheng, V. Y., Belelli, D., Newell, J. G., et al. (2004). Tonic inhibition in mouse hippocampal CA1 pyramidal neurons is mediated by alpha5 subunit-containing gamma-aminobutyric acid type A receptors. *Proc. Natl. Acad. Sci. U.S.A.* 101, 3662–3667. doi: 10.1073/pnas.0307231101
- Chen, C., and Okayama, H. (1987). High-efficiency transformation of mammalian cells by plasmid DNA. *Mol. Cell. Biol.* 7, 2745–2752. doi: 10.1128/MCB.7.8.2745
- Cherubini, E., and Conti, F. (2001). Generating diversity at GABAergic synapses. *Trends Neurosci.* 24, 155–162. doi: 10.1016/S0166-2236(00)01724-0
- Dixon, C. L., Harrison, N. L., Lynch, J. W., and Keramidis, A. (2015). Zolpidem and eszopiclone prime $\alpha_1\beta_2\gamma_2$ GABA_A receptors for longer duration of activity. *Br. J. Pharmacol.* 172, 3522–3536. doi: 10.1111/bph.13142
- Downing, S. S., Lee, Y. T., Farb, D. H., and Gibbs, T. T. (2005). Benzodiazepine modulation of partial agonist efficacy and spontaneously active GABA_A receptors supports an allosteric model of modulation. *Br. J. Pharmacol.* 145, 894–906. doi: 10.1038/sj.bjp.0706251
- Du, J., Lü, W., Wu, S., Cheng, Y., and Gouaux, E. (2015). Glycine receptor mechanism elucidated by electron cryo-microscopy. *Nature* 526, 224–229. doi: 10.1038/nature14853
- Fritschy, J.-M., and Brüning, I. (2003). Formation and plasticity of GABAergic synapses: physiological mechanisms and pathophysiological implications. *Pharmacol. Ther.* 98, 299–323. doi: 10.1016/S0163-7258(03)00037-8
- Gielen, M. C., Lumb, M. J., and Smart, T. G. (2012). Benzodiazepines modulate GABA_A receptors by regulating the preactivation step after GABA binding. *J. Neurosci.* 32, 5707–5715. doi: 10.1523/JNEUROSCI.5663-11.2012
- Goldschen-Ohm, M. P., Haroldson, A., Jones, M. V., and Pearce, R. A. (2014). A nonequilibrium binary elements-based kinetic model for benzodiazepine regulation of GABA_A receptors. *J. Gen. Physiol.* 144, 27–39. doi: 10.1085/jgp.201411183
- Humphrey, W., Dalke, A., and Schulten, K. (1996). VMD: visual molecular dynamics. *J. Mol. Graph.* 14, 33–38. doi: 10.1016/0263-7855(96)00018-5
- Irwin, J. J., Sterling, T., Mysinger, M. M., Bolstad, E. S., and Coleman, R. G. (2012). ZINC: a free tool to discover chemistry for biology. *J. Chem. Inf. Model.* 52, 1757–1768. doi: 10.1021/ci3001277
- Jonas, P. (1995). “Fast application of agonists to isolated membrane patches,” in *Single-Channel Recording*, eds B. Sakmann and E. Neher (Boston, MA: Springer), 231–243.

- Jones, M. V., and Westbrook, G. L. (1995). Desensitized states prolong GABA_A channel responses to brief agonist pulses. *Neuron* 15, 181–191. doi: 10.1016/0896-6273(95)90075-6
- Kisiel, M., Jatczak, M., Brodzki, M., and Mozrzymas, J. W. (2018). Spontaneous activity, singly bound states and the impact of alpha1Phe64 mutation on GABA_AR gating in the novel kinetic model based on the single-channel recordings. *Neuropharmacology* 131, 453–474. doi: 10.1016/j.neuropharm.2017.11.030
- Lape, R., Colquhoun, D., and Sivilotti, L. G. (2008). On the nature of partial agonism in the nicotinic receptor superfamily. *Nature* 454, 722–727. doi: 10.1038/nature07139
- Lavoie, A. M., and Twyman, R. E. (1996). Direct evidence for diazepam modulation of GABA_A receptor microscopic affinity. *Neuropharmacology* 35, 1383–1392. doi: 10.1016/S0028-3908(96)00077-9
- Li, P., Eaton, M. M., Steinbach, J. H., and Akk, G. (2013). The benzodiazepine diazepam potentiates responses of $\alpha 1\beta 2\gamma 2L$ γ -aminobutyric acid type A receptors activated by either γ -aminobutyric acid or allosteric agonists. *Anesthesiology* 118, 1417–1425. doi: 10.1097/ALN.0b013e318289bcd3
- Lovell, S. C., Davis, I. W., Arendall, W. B., De Bakker, P. I. W., Word, J. M., Prisant, M. G., et al. (2003). Structure validation by Calpha geometry: phi,psi and Cbeta deviation. *Proteins* 50, 437–450. doi: 10.1002/prot.10286
- Mercik, K., Piast, M., and Mozrzymas, J. W. (2007). Benzodiazepine receptor agonists affect both binding and gating of recombinant alpha1beta2gamma2 gamma-aminobutyric acid-A receptors. *Neuroreport* 18, 781–785. doi: 10.1097/WNR.0b013e3280c1e2fb
- Michalowski, M. A., Kraszewski, S., and Mozrzymas, J. W. (2017). Binding site opening by loop C shift and chloride ion-pore interaction in the GABA A receptor model. *Phys. Chem. Chem. Phys.* 19, 13664–13678. doi: 10.1039/c7cp00582b
- Miller, P. S., and Aricescu, A. R. (2014). Crystal structure of a human GABA A receptor. *Nature* 512, 270. doi: 10.1038/nature13293
- Mortensen, M., Wafford, K. A., Wingrove, P., and Ebert, B. (2003). Pharmacology of GABA_A receptors exhibiting different levels of spontaneous activity. *Eur. J. Pharmacol.* 476, 17–24. doi: 10.1016/S0014-2999(03)02125-3
- Mozrzymas, J. W., Barberis, A., Mercik, K., and Zarnowska, E. D. (2003). Binding sites, singly bound states, and conformation coupling shape GABA-evoked currents. *J. Neurophysiol.* 89, 871–883. doi: 10.1152/jn.00951.2002
- Mozrzymas, J. W., Barberis, A., Michalak, K., and Cherubini, E. (1999). Chlorpromazine inhibits miniature GABAergic currents by reducing the binding and by increasing the unbinding rate of GABA_A Receptors. *J. Neurosci.* 19, 2474–2488. doi: 10.1523/JNEUROSCI.19-07-02474.1999
- Mozrzymas, J. W., Wojtowicz, T., Piast, M., Lebida, K., Wyrembek, P., and Mercik, K. (2007). GABA transient sets the susceptibility of mIPSCs to modulation by benzodiazepine receptor agonists in rat hippocampal neurons. *J. Physiol.* 585, 29–46. doi: 10.1113/jphysiol.2007.143602
- Newell, J. G., McDevitt, R. A., and Czajkowski, C. (2004). Mutation of glutamate 155 of the GABA_A receptor beta2 subunit produces a spontaneously open channel: a trigger for channel activation. *J. Neurosci.* 24, 11226–11235. doi: 10.1523/JNEUROSCI.3746-04.2004
- Notredame, C., Higgins, D. G., and Heringa, J. (2000). T-coffee: a novel method for fast and accurate multiple sequence alignment. *J. Mol. Biol.* 302, 205–217. doi: 10.1006/jmbi.2000.4042
- Rudolph, U., and Möhler, H. (2004). Analysis of GABA_A receptor function and dissection of the pharmacology of benzodiazepines and general anesthetics through mouse genetics. *Annu. Rev. Pharmacol. Toxicol.* 44, 475–498. doi: 10.1146/annurev.pharmtox.44.101802.121429
- Rusch, D., and Forman, S. A. (2005). Classic benzodiazepines modulate the open-close equilibrium in alpha1beta2gamma2L gamma-aminobutyric acid type A receptors. *Anesthesiology* 102, 783–792. doi: 10.1097/0000542-200504000-00014
- Šali, A., and Blundell, T. L. (1993). Comparative protein modelling by satisfaction of spatial restraints. *J. Mol. Biol.* 234, 779–815. doi: 10.1006/jmbi.1993.1626
- Szczot, M., Kisiel, M., Czyzewska, M. M., and Mozrzymas, J. W. (2014). alpha1F64 Residue at GABA(A) receptor binding site is involved in gating by influencing the receptor flipping transitions. *J. Neurosci.* 34, 3193–3209. doi: 10.1523/JNEUROSCI.2533-13.2014
- Torres, V. I., and Weiss, D. S. (2002). Identification of a tyrosine in the agonist binding site of the homomeric rho1 gamma-aminobutyric acid (GABA) receptor that, when mutated, produces spontaneous opening. *J. Biol. Chem.* 277, 43741–43748. doi: 10.1074/jbc.M202007200
- Trott, O., and Olson, A. J. (2010). AutoDock Vina: improving the speed and accuracy of docking with a new scoring function, efficient optimization, and multithreading. *J. Comput. Chem.* 31, 455–461. doi: 10.1002/jcc.21334
- Wagner, D. A., Goldschen-Ohm, M. P., Hales, T. G., and Jones, M. V. (2005). Kinetics and spontaneous open probability conferred by the epsilon subunit of the GABA_A receptor. *J. Neurosci.* 25, 10462–10468. doi: 10.1523/JNEUROSCI.1658-05.2005
- Waterhouse, A. M., Procter, J. B., Martin, D. M. A., Clamp, M., and Barton, G. J. (2009). Jalview Version 2—a multiple sequence alignment editor and analysis workbench. *Bioinformatics* 25, 1189–1191. doi: 10.1093/bioinformatics/btp033
- Zarnowska, E. D., Keist, R., Rudolph, U., and Pearce, R. A. (2009). GABA_A receptor alpha5 subunits contribute to GABA_A slow synaptic inhibition in mouse hippocampus. *J. Neurophysiol.* 101, 1179–1191. doi: 10.1152/jn.91203.2008

Conflict of Interest Statement: The authors declare that the research was conducted in the absence of any commercial or financial relationships that could be construed as a potential conflict of interest.

The handling Editor declared a past co-authorship with one of the authors, JM.

Copyright © 2018 Jatczak-Śliwa, Terejko, Brodzki, Michalowski, Czyzewska, Nowicka, Andrzejczak, Srinivasan and Mozrzymas. This is an open-access article distributed under the terms of the Creative Commons Attribution License (CC BY). The use, distribution or reproduction in other forums is permitted, provided the original author(s) and the copyright owner(s) are credited and that the original publication in this journal is cited, in accordance with accepted academic practice. No use, distribution or reproduction is permitted which does not comply with these terms.

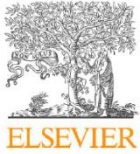
2.

„The C loop at the orthosteric binding site is critically involved in GABA_A receptor gating”

Katarzyna Terejko, Przemysław T. Kaczor, Michał A. Michałowski, Agnieszka Dąbrowska,
Jerzy W. Mozrzymas

Neuropharmacology 166 (2020), 107903.

doi.org/10.1016/j.neuropharm.2019.107903



The C loop at the orthosteric binding site is critically involved in GABA_A receptor gating



Katarzyna Terejko^{a,*}, Przemysław T. Kaczor^{a,1}, Michał A. Michałowski^{a,b,1},
Agnieszka Dąbrowska^a, Jerzy W. Mozrzyński^{a,D,**}

^aLaboratory of Neuroscience, Department of Biophysics, Wrocław Medical University, ul. Chałubińskiego 3A, 50-368, Wrocław, Poland

^bDepartment of Molecular Physiology and Neurobiology, University of Wrocław, ul. Sienkiewicza 21, 50-335, Wrocław, Poland

HIGHLIGHTS

- Macroscopic and single-channel analysis revealed the effects of a C loop mutation.
- The C loop controls receptor gating, including preactivation, desensitization, and opening.
- The C loop mutation alters flurazepam sensitivity by affecting the preactivation transition.
- The C loop mutation distorts its structure, displacing the tip from the binding site.
- The C loop is critically involved in the binding and gating of GABA_ARs.

ARTICLE INFO

Keywords:

Pentameric receptors
Structure-function
Single-channel
Current responses
Kinetic modeling

ABSTRACT

GABA_A receptors (GABA_ARs) play a crucial role in mammalian adult brain inhibition. The dysfunction of GABAergic drive is related to such disorders as epilepsy, schizophrenia, and depression. Substantial progress has recently been made in describing the static structure of GABA_ARs, but the molecular mechanisms that underlie the activation process remain elusive. The C loop of the GABA_AR structure shows the largest movement upon ligand binding to the orthosteric binding site, a phenomenon that is referred to as “capping.” The C loop is known to be involved in agonist binding, but its role in the gating of Cys-loop receptors is still debated. Herein, we investigated this issue by analyzing the impact of a β₂F200 residue mutation of the C loop on gating properties of α₁β₂γ₂ GABA_ARs. Extensive analyses and the modeling of current responses to saturating agonist application demonstrated that this mutation strongly affected preactivation, opening, closing and desensitization, i.e. all considered gating steps. Single-channel analysis revealed that the β₂F200 mutation slowed all shut time components, and open times were shortened. Model fitting of these single-channel data further confirmed that the β₂F200 mutation strongly affected all of the gating characteristics. We also found that this mutation altered receptor sensitivity to the benzodiazepine flurazepam, which was attributable to a change in preactivation kinetics. *In silico* analysis indicated that the β₂F200 mutation resulted in distortion of the C loop structure, causing the movement of its tip from the binding site. Altogether, we provide the first evidence that C loop critically controls GABA_AR gating.

1. Introduction

γ-Aminobutyric acid type A receptors (GABA_ARs) are pentameric ligand-gated ion channels (pLGICs) that are permeable to anions and mediate inhibition in the adult brain (Farrant and Nusser, 2005; Mody and Pearce, 2004). GABA_A receptors are also a member of the Cys-loop

receptor family together with nicotinic acetylcholine receptors (nAChRs), glycine receptors (GlyRs), and 5-hydroxytryptamine type 3 receptors (5-HT₃Rs; Cederholm et al., 2009; Miller and Smart, 2010; Thompson et al., 2010). The balance between inhibition and excitation is critical for proper functioning of the central nervous system. The dysfunction of GABAergic drive may lead to epilepsy, anxiety disorders,

* Corresponding author.

** Corresponding author. Laboratory of Neuroscience, Department of Biophysics, Wrocław Medical University, ul. Chałubińskiego 3A, 50-368, Wrocław, Poland.
E-mail addresses: kat.terejko@gmail.com (K. Terejko), jerzy.mozrzymski@umed.wroc.pl (J.W. Mozrzyński).

¹ These authors contributed equally.

<https://doi.org/10.1016/j.neuropharm.2019.107903>

Received 26 April 2019; Received in revised form 15 November 2019; Accepted 2 December 2019

Available online 03 December 2019

0028-3908/© 2020 The Authors. Published by Elsevier Ltd. This is an open access article under the CC BY license (<http://creativecommons.org/licenses/by/4.0/>).

Non-standard abbreviations used in paper			
5-HT ₃ R	5-hydroxytryptamine type 3 receptor	F200Y	β_2 F200Y mutant of $\alpha_1\beta_2\gamma_2$ GABA _A receptor
LBS	ligand binding site	GABA _A R	γ -aminobutyric acid receptor type A
BDZ	benzodiazepine	nAChR	nicotinic acetylcholine receptor
FLU	flurazepam (benzodiazepine derivative)	GlyR	glycine receptor
CD4	cluster of differentiation 4 (surface glycoprotein in T-cells, monocytes, macrophages and dendritic cells)	pCMV	adenoviral vector (plasmid) with the promoter for cytomegalovirus
ECD	extracellular domain	pLGIC	pentameric ligand-gated ion channel
EGFP	enhanced green fluorescent protein	RT	rise time of currents mediated by GABA _A receptors upon activation
F200	β_2 F200 in $\alpha_1\beta_2\gamma_2$ GABA _A receptor or its homologues in pLGICs	TMD	transmembrane domain
F200C	β_2 F200C mutant of $\alpha_1\beta_2\gamma_2$ GABA _A receptor	WT	wildtype of $\alpha_1\beta_2\gamma_2$ GABA _A receptor
F200I	β_2 F200I mutant of $\alpha_1\beta_2\gamma_2$ GABA _A receptor	Y205	β_2 Y205 in $\alpha_1\beta_2\gamma_2$ GABA _A receptor or its homologues in pLGICs

autism, depression, and schizophrenia (Brickley and Mody, 2012; Gafford et al., 2012; Rudolph and Möhler, 2006). GABA_A receptor-mediated inhibition is a target of many clinically relevant pharmacological modulators, including benzodiazepines and anesthetics, among others (Rudolph and Möhler, 2004; Sieghart and Savić, 2018; Sigel and Steinmann, 2012). The pLGICs activation process is based on the coupling of ligand binding to the extracellular binding site with opening of the channel gate that is located in the transmembrane domain (Cederholm et al., 2009; Miller and Smart, 2010). Abundant data on the structure of GABA_ARs has recently emerged (Laverty et al., 2019; Masiulis et al., 2019; Miller et al., 2018; Phulera et al., 2018; Zhu et al., 2018). Since the ligand binding site (LBS) and channel gate are particularly distant (approximately 40–50 Å; Miller and Smart, 2010; Unwin, 2005), the transduction of the activation signal down to the receptor gate is expected to be very complex, and the underlying molecular mechanisms remain elusive. Two LBSs of GABA_ARs are localized at the interface of the principal $\beta(+)$ subunit and complementary $\alpha(-)$ subunit (Smith and Olsen, 1995). Ligand binding is stabilized by cation- π interactions of aromatic residues that create an “aromatic box” that surrounds the binding pocket in the LBS (Padgett et al., 2007), which is a structure that is highly conserved among the Cys-loop receptor family (Nys et al., 2013; Zhong et al., 1998). Structurally, three peptide loops (A-C loops) of the principal subunit form the LBS whereas three β -sheets (D-F loops) contribute from the complementary one (Nemecz et al., 2016; Thompson et al., 2010). Previous cysteine substitution studies (Venkatachalan and Czajkowski, 2008; Wagner and Czajkowski, 2001) and molecular dynamics investigations (Cheng et al., 2006; Michałowski et al., 2017) indicated that the C loop undergoes the most substantial movement upon ligand binding as it moves from its default, open position toward the binding pocket, effectively closing it, a phenomenon referred to as “capping.” One issue that is related to the role of the C loop is whether it is involved locally, affecting primarily the binding process, or whether it additionally exerts a long-range effect to shape receptor gating. The influence of the C loop on the affinity and efficacy of GABA_ARs was suggested by Wagner and Czajkowski (2001). Importantly, after description of the flipping (preactivation) process in a seminal study by Lape et al. (2008), Mukhtasimova et al. (2009) performed a single-channel analysis of AChRs and proposed that C loop “capping” initiated the flipping transition, thus affecting receptor gating. Molecular dynamics studies by Cheng et al. (2006) revealed that the C-loop closure of α_7 nAChRs was associated with a sequence of structural changes that resulted in pore widening, indicating a C loop-dependent gating mechanism. However, the findings of Purohit and Auerbach (2013) did not support the idea of direct energy transfer from the LBS to the receptor gate via the C loop in the nAChRs, restricting the role of this loop in these receptors to the binding process. Pless and Lynch (2009) studied GlyRs and did not find direct evidence that movement of the C loop shapes receptor efficacy, but they did not exclude the possibility that movement of the C loop might affect receptor

gating features by altering interactions between the bound agonist and the D and E loops. Considering these divergent results for different Cys-loop receptors, the precise role of the C loop in binding and gating remains elusive and, in particular, in the case of GABA_ARs, it still awaits thorough investigations. Our recent studies at the macroscopic and single-channel levels shed new light on GABA_AR gating by underscoring flipping (preactivation) transitions (Kisiel et al., 2018; Szczot et al., 2014). Taking advantage of this background, we analyzed high-resolution macroscopic (non-stationary) and single-channel (stationary) recordings for various mutants of the β_2 F200 residue that, together with *in silico* docking and structural considerations, clearly indicated that this mutation affects both binding and gating transitions. Qualitative changes in the modulatory effect of the benzodiazepine flurazepam (FLU) on mutants relative to the wildtype (WT) receptor provided further evidence of the impact of the mutation on the preactivation transition. Altogether, we showed that the C loop is critically involved in both the binding and gating of GABA_ARs.

2. Materials and methods

2.1. Cell culture and expression of recombinant GABA_A receptors

All of the experiments were performed with the human embryonic kidney 293 (HEK293) cell line (European Collection of Authenticated Cell Culture). The cells were cultured in Dulbecco's Modified Eagle's Medium with 10% fetal bovine serum and 1% penicillin/streptomycin (Thermo Fisher Scientific) in a humidified atmosphere with 5% CO₂ at 37 °C. The cells were replated on poly-D-lysine (1 µg/ml)-coated coverslips (Carl Roth) 24 h before transfection. The cells were transiently transfected using FuGENE HD (Promega) at a 3:1 FuGENE HD:DNA ratio with an adenoviral vector (plasmid) with the promoter for cytomegalovirus (pCMV) that contained cDNA of GABA_AR subunits. The $\alpha_1/\beta_2/\gamma_2$ subunits were mixed in a 1:1:3 ratio (0.5:0.5:1.5 µg) in transfection solution, together with 0.5 µg human cluster of differentiation 4 (CD4) or enhanced green fluorescent protein (EGFP)-encoding plasmid. This subunit ratio was maintained for WT and mutated receptors because mutation of the β_2 subunit did not cause weaker receptor expression. Immediately before the experiments, Dynabeads CD4 magnetic binding beads (Invitrogen) were used for the recognition of successfully transfected cells (in the case of co-transfection with CD4). When EGFP was co-transfected, cells were visualized with a fluorescence illuminator (470 nm wavelength, CoolLED, Andover, UK) that was mounted on a modular inverted microscope (Leica DMI8, Wetzlar, Germany).

2.2. Electrophysiological recordings

Recordings were performed 24–48 h after transfection. All of the electrophysiological data were recorded using the patch-clamp

technique. Currents were low-pass-filtered at 10 kHz and recorded at a holding potential of -40 mV using an Axopatch 200B amplifier (Molecular Devices) and acquired using a Digidata 1550A acquisition card (Molecular Devices). For signal acquisition, pClamp 10.7 software (Molecular Devices) was used. Pipettes were pulled from borosilicate glass (outer diameter, 1.5 mm; inner diameter, 1.0 mm; Hilgenberg) using a P-97 horizontal puller (Sutter Instruments) and filled with intracellular solution that contained 137 mM KCl, 1 mM CaCl_2 , 2 mM ATP-Mg, 2 mM MgCl_2 , 10 mM K-gluconate, 11 mM EGTA, and 10 mM HEPES, with the pH adjusted to 7.2 with KOH. The pipette resistance ranged from 3 to 5 M Ω . Standard Ringer's solution was used as the external saline, which contained 137 mM NaCl, 5 mM KCl, 2 mM CaCl_2 , 1 mM MgCl_2 , 10 mM HEPES, and 20 mM glucose, with the pH adjusted to 7.2 with NaOH. The osmolarity of solutions that contained > 10 mM of agonist was adjusted with glucose up to ~ 320 mOsm as described previously (Szczot et al., 2014). The solutions were supplied using an ultrafast perfusion system. Theta-glass capillaries (Hilgenberg) were mounted on a piezoelectric-driven translator (Physik Instrumente) as described in detail previously by Jonas (1995) and our group (Mozzrymas et al., 2003a, 2003b, 2007; Szczot et al., 2014). The solutions were simultaneously supplied to the two channels of the theta-glass by a high-precision SP220IZ syringe pump (World Precision Instruments). The open tip solution exchange time ranged from 150 to 250 μ s, depending on the size of the theta-glass and speed of flux.

Single-channel recordings and analyses that were applied herein are described in more detail in our recent paper (Kisiel et al., 2018). Recordings were performed in the cell-attached configuration at a pipette potential of 100 mV using an Axopatch 200B amplifier (Molecular Devices). The signals were first filtered at 10 kHz with a low-pass Bessel filter (mounted on the amplifier) and digitized at 100 kHz using a Digidata 1550B acquisition card and Clampex 10.7 software (Molecular Devices). Pipettes were prepared from thick-wall (outer diameter, 1.5 mm; inner diameter, 0.87 mm), filamented borosilicate glass (Hilgenberg) using a P-1000 horizontal puller (Sutter Instruments), and their resistance (with intrapipette Ringer's solution) was in the range of 5–12 M Ω . The pipettes were coated with Sylgard (Dow Corning) to reduce noise and fire-polished. Extracellular (and intrapipette) saline differed from the saline solution that was used for the macroscopic current recordings and consisted of 102.7 mM NaCl, 20 mM Na-gluconate, 2 mM KCl, 2 mM CaCl_2 , 1.2 mM MgCl_2 , 10 mM HEPES (Carl Roth), 20 mM TEA-Cl, 14 mM D-(+)-glucose, and 15 mM sucrose (Carl Roth), dissolved in deionized water with the pH adjusted to 7.4 by 2 M NaOH. In the experiments in which a high GABA concentration (100 mM) was applied, a low-chloride solution was used instead to maintain osmolarity of ~ 320 mOsm: 70 mM NaCl, 10 mM Na-gluconate, 2 mM KCl, 2 mM CaCl_2 , 1.2 mM MgCl_2 , 10 mM HEPES (Carl Roth), 20 mM TEA-Cl, and 14 mM D-(+)-glucose. To reduce noise, the level of the extracellular solution was kept at a minimal possible level (1 ml in the 35 mm diameter recording dish; Nunc), and traces were selected for further analysis if the patches had a seal resistance > 10 G Ω . All of the electrophysiological recordings were conducted at room temperature (20–23 °C). All of the chemicals were purchased from Sigma-Aldrich Merck unless stated otherwise.

3. Theory/calculation

3.1. Experimental design and analysis of macroscopic currents

Dose-response relationships for mutated receptors were obtained from currents that were evoked by a wide range of non-saturating [GABA] concentrations relative to responses that were elicited by saturating [GABA] concentrations on the same cell and fitted using the Hill equation:

$$EC = \frac{1}{1 + \left(\frac{EC_{50}}{[GABA]}\right)^{n_h}}$$

where EC_{50} is half-maximal concentration, and n_h is the Hill coefficient.

The saturating concentration of GABA was assessed for each mutant individually. For dose-response relationships, recordings were performed in both whole-cell (lifted cell mode) and excised-patch configurations. The effect of the benzodiazepine FLU was assessed at 3 μ M, and this drug was present in the wash (pretreatment) and in the solution that contained saturating [GABA]. Kinetic analysis was performed exclusively for currents that were recorded in the excised-patch configuration. Two application protocols were used: long (500 ms) and short (1.5–3 ms). The current onset was assessed as the 10–90% rise time (RT). The macroscopic deactivation time course (current kinetics after agonist removal) was fitted with either a single exponential or a sum of two exponential components according to the following equation:

$$I(t) = \sum_{n=1}^f A_n e^{-t/\tau_n}$$

where A_n is the amplitude of the n -th component, and τ_n is the respective time constant. The mean time constant (τ_{deact}) for $f = 2$ was calculated as the following:

$$\tau_{deact} = \%A_1 \tau_1 + \%A_2 \tau_2$$

where $\%A_n$ is the percentage of the respective component ($\%A_1 + \%A_2 = 1$). Deactivation kinetics were determined for both short applications (to minimize macroscopic desensitization) and after long (500 ms) applications when deactivation was observed after macroscopic desensitization onset.

The rapid macroscopic desensitization component was assessed by fitting the exponential function with a constant coefficient:

$$I(t) = Ae^{-t/\tau_{desens}} + C$$

where A is the fast desensitization amplitude, τ_{desens} is the time constant, and C is the constant value that represents the stationary non-desensitizing current. To precisely describe the kinetics of the rapid desensitization component, the time window for fitting that ranged from 7 to 15 ms from the current peak was set for each fitting. The proper choice of the fitting range allowed to avoid the interference from slower desensitization components that typically have a time constant of roughly 100 ms (Jatczak-Sliwa et al., 2018; Jones and Westbrook, 1995; Szczot et al., 2014). The steady state-to-peak parameter (ss/peak) was used to describe the extent of fast desensitization (low ss/peak – large extent of desensitization), calculated as the following:

$$ss/peak = \frac{C}{A_{max}}$$

where C is the aforementioned constant value, and A_{max} is the peak amplitude.

Data presentation and the statistical analysis were performed using SigmaPlot 11.0 software (Systat Software) and Excel 2016 software (Microsoft). Data were analyzed in terms of distribution normality using the Shapiro-Wilk test and outlier identification using Grubb's test. Significant differences between WT (control group) and each of the β_2 F200 mutants were tested independently using Student's t -test or the Mann-Whitney U test (when data did not pass the normality test). The use of this simple test was justified by the fact that all of the results were based on comparisons between only two groups at a time. Similarly, in the case of pharmacological considerations (Fig. 4), in which test and control recordings were performed on the same cell, the paired test was used, but only two groups were compared at a time. Values of $p < 0.05$ were considered statistically significant.

3.2. Homology modeling and ligand docking

The sequence alignment of α_1 , β_2 , and γ_2 GABA_AR subunits and other pLGICs was performed in T-Coffee (Di Tommaso et al., 2011) and refined manually using Jalview (Waterhouse et al., 2009). Three “base WT” homology models of the $\alpha_1\beta_2\gamma_2$ GABA_AR ECD were used in the present study. The first model was based on a homomeric β_3 GABA_AR structure (Miller and Aricescu, 2014), similar to Jatzcak-Sliwa et al. (2018). The other two models were based on A and B conformations of $\alpha_1\beta_2\gamma_2$ GABA_AR that were described by Zhu et al. (2018). In the case of these latter two models (Zhu et al., 2018), only the missing residues were introduced because these templates depicted the same assembly type as the one that was investigated in the present study. The MODELLER Python package (Šali and Blundell, 1993) was used to construct these models using *automodel* class. In the next step, mutations (F200C, F200I, and F200Y) were introduced to each “base WT” model, and 20 new models of each type were constructed. From these 20 models, the best model was selected by best molpdf score, assessed by the MODELLER package. Thus, three “base WT” and three “base F200C,” “base F200I,” and “base F200Y” models of $\alpha_1\beta_2\gamma_2$ GABA_AR were obtained. The GABA molecule was initially positioned in both LBSs of each model according to its position in the structures from Zhu et al. (2018). The final binding positions and binding energy were determined by the AutoDock Vina (Trott and Olson, 2009) stiff and flexible fit docking methods. In the stiff method, only the GABA molecule was able to move within the LBS, whereas the local macromolecule’s structure was kept immobilized. In the flexible method, both GABA and the functional groups of residues that formed the site were mobile (with a fixed backbone). Because there were three “base” models for each receptor type (WT and mutants) and because GABA was docked to both LBSs, the total number of six binding modes was assessed for each receptor type for both the stiff and flexible methods. C loop modeling was also performed using the MODELLER package. The same models (“base”) as those that were used for docking were rebuilt with the *loopmodel* class with constrained positions of all atoms, with the exception of residues that formed the C loop tip. A total of 100 new models for each “base” model were created (resulting in 300 “loop WT,” “loop F200C,” “loop F200I,” and “loop F200Y” models). DOPE energy scores of residues that formed the C loop were calculated using MODELLER evaluation functions, and all of the models were evaluated visually to exclude incorrect ones (e.g., having overlapping loops). Analysis of the results and visualizations were performed using VMD (Humphrey et al., 1996) and Python scripts.

3.3. Simulations and kinetic modeling of macroscopic currents

The kinetic modeling of macroscopic currents was performed using ChannelLab 2.0 software (Synaptosoft). No formal fitting to experimental traces was performed. An extensive trend analysis based on several scenarios for the values of the rate constants was instead considered. The final model rate constants were selected according to the best reproduction of experimentally observed current response parameters: RT, ss/peak ratio, τ_{desens} (long pulse), and τ_{deact} (short pulse). Additionally, the rates were selected to reproduce the EC₅₀ value and amplitude increase in the presence of FLU (for the F200C mutant). Information from docking studies (i.e., the assessment of binding affinity) and single-channel analysis (e.g., shortening of open times; see below) was also considered. The best reproduction of the experimental results was achieved for τ_{desens} (long pulse), ss/peak, and EC₅₀. Slightly lower accuracy was achieved for reproduction of the RT and deactivation time constant, τ_{deact} , in the case of quickly deactivating mutants. However, the relative changes relative to WT were properly reproduced. Lower accuracy in reproducing these current features could result from the limited speed of our application system. The kinetic modeling of macroscopic currents was performed for the F200C mutant only because this receptor presented the largest differences compared

with WT.

3.4. Single-channel analysis

Single-channel kinetic analysis and modeling were performed using SCAN, EKDIST, and HJCFIT software (DCprogs pack), which was kindly provided to our group by David Colquhoun. Similar to the macroscopic current analysis, the single-channel experiments were assumed to be performed at saturating [GABA] concentrations. For the F200C mutant, 100 mM GABA saturation was incomplete by a small margin. This problem is discussed further in Section 5.2. Traces that contained at least 10000 events were considered for the analysis. Signals were stored as Axon Binary File (.abf) files and filtered to obtain a signal-to-noise ratio of at least 15. The final cutoff frequency (*fc*) was calculated as the following:

$$1 / fc = 1 / fa + 1 / fd$$

where *fa* is the analog filter frequency (typically 10 kHz), and *fd* is the digital frequency (offline filtering with 8-pole low-pass Bessel filter by pClamp software). The sampling frequency, *fs*, was reduced to $fs = 10 \cdot fc$. Recordings that showed multilevel openings were excluded from the analysis. The recordings revealed different modes of activity (Kisiel et al., 2018; Lema and Auerbach, 2006) that clearly differed in open probability. In the present study, only the predominant activity mode was included in the analysis. The criteria that were used to select this predominant mode are described in detail in Kisiel et al., 2018. Only clusters were included in our analysis, which were extracted visually and exported individually to separate files. Recordings that were selected in this way were then idealized by a time-course fitting procedure and saved with SCAN software as *.scn files and then used to generate distributions (with EKDIST) of shut and open time periods and fit them with the sum of exponentials (in figures; P% = relative areas, τ = time constants). Time resolution was identified separately for each recording within the range of 40–80 μ s for open and shut times, and these values were then used in the model simulations. As explained in our recent study (Kisiel et al., 2018), the longest shut time components were not considered informative because of their low percentage and high variability and because they could be affected by the activity of more than one channel in the patch. Thus, although each time shut times distributions for WT receptors were fitted with four exponentials, the statistics is presented for three fastest components. To define bursts, critical time (*tcrit*) was determined, based on the analysis of the shut times distributions, which typically consisted of four components for WT and F200Y receptors and three components for F200C and F200I mutations. Bursts were then defined by *tcrit*, calculated by EKDIST software, using Jackson’s criterion (Jackson et al., 1983) that was applied to the third and fourth components of the shut times distributions for WT and F200Y or for the second and third components of the shut times distributions for F200I and F200C mutations. Bursts that were detected using this method consisted of several events. For this reason, even if at least 10000 events were present in the analyzed trace, they were typically not sufficiently numerous to build a burst duration distribution that could be reliably fitted. Instead, the mean burst duration was calculated as the arithmetic mean.

Kinetic modeling based on single-channel data (stored in *.scn files) was performed using HJCFIT software (DCWinprogs, provided by David Colquhoun), which is based on the maximum likelihood method that enabled optimization of the rate constants in the model. To verify the model predictions, dwell times distributions that were generated by the model (at experimental and 0 μ s resolutions) were confronted with those that were obtained experimentally. For recordings that were performed for WT receptors, we compared the present results (Tables 1 and 2) with our previous data (Kisiel et al., 2018) and found that they were very consistent. For the mutants, we considered that the modeling was consistent if the distribution parameters that were obtained from

the model fitting (P and τ ; Tables 1 and 2) reproduced significant changes between the same parameters in the experimental distributions when comparing WT and specific mutants (see Section 4.7).

4. Results

4.1. Sequence analysis of C loop in pLGICs and choice of mutations

The C loop connects β -strands 9 and 10 and is a structural motif that is well conserved in each member of the pLGIC family. In the β_2 subunit of the GABA_AR, the C loop starts at position F200 and ends at Y205. The latter residue is well conserved in pLGICs (Fig. 1). In our hands, GABA_ARs with mutations at this position were non-functional. Although F200 is less conserved than Y205, it is conserved in all β , τ , and δ GABA_AR subunits (which form the principal side of the LBS). Interestingly, in all α - and γ -type subunits that do not form the principal side of the LBS, phenylalanine is replaced by other residues (Fig. 1), indicating its role in ligand binding. A similar scheme is observed in nAChRs (tyrosine at a position that is homologous to F200 in principal subunits and a non-aromatic residue in complementary subunits), GLIC, ELIC, and GlyRs (aromatic residue at a position that is homologous to F200; Fig. 1). Considering these observations, the following scheme emerges. Phenylalanine or tyrosine starts or ends the C loop in pLGIC subunits, forming the principal side of the LBS. This indicates the key involvement of F200- and Y205-homologous residues in the activation of pLGICs. In the present study, we examined the role of an F200 residue mutation in $\alpha_1\beta_2\gamma_2$ GABA_ARs. The following mutations were selected: β_2 F200C (F200C) because this mutation is expected to induce substantial disturbances in the structure of the C loop, β_2 F200I (F200I) to validate the effect of aromatic ring removal and thus modification of

the “aromatic box” structure of the LBS, and β_2 F200Y (F200Y) to examine the effects of a slight modification of LBS architecture by the addition of a hydroxyl group while maintaining the aromatic group.

4.2. Impact of β_2 F200 mutation on macroscopic GABAergic currents

To assess the impact of mutations at the β_2 F200 residue on receptor responsiveness to GABA, dose-response relationships were determined (Fig. 2a). As expected, Cys and Ile substitutions resulted in a substantial rightward shift of the dose-response relationship that was in qualitative agreement with previous reports (Tran et al., 2011; Wagner and Czajkowski, 2001). Note that the dashed line in Fig. 2a shows the dose-response relationship function for WT receptors that was recently determined by our group under the same experimental conditions (Brodzki et al., 2016). Interestingly, in the case of the F200Y mutant, the dose-response function was shifted in the opposite direction relative

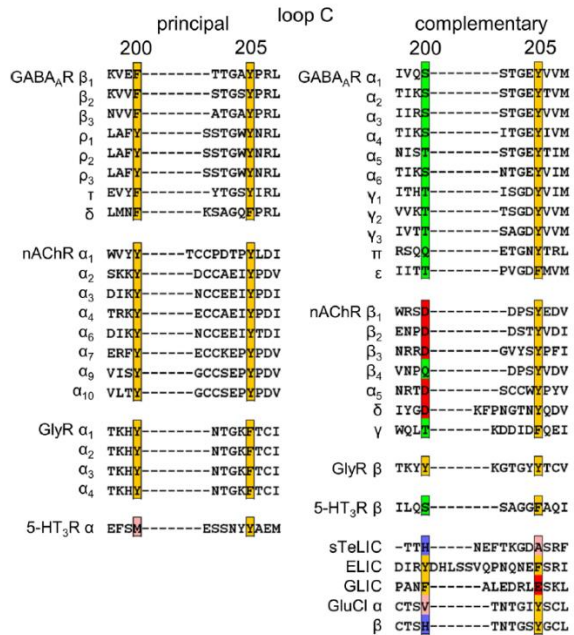


Fig. 1. Conservation of aromatic residues at the C loop tip in pLGICs. Subunits that form homomeric assemblies or principal sides of the LBSs in heteromeric assemblies are shown on the left. The right shows subunits that make complementary sides of the binding sites or of bacterial and nematode channels. The aromatic (yellow) character of F200 homologues is well conserved in the C loop at the principal side (left), whereas at the complementary side, F200 is replaced by a variety of residues. The aromatic character of Y205 is highly conserved and does not depend on the subunit type.

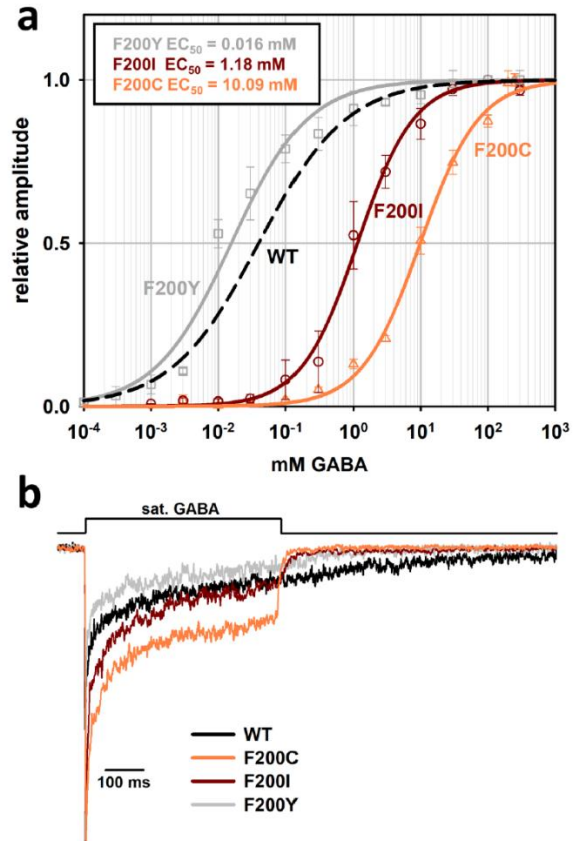


Fig. 2. Mutations of β_2 F200 residue affect the dose-response relationship and kinetics of currents that are evoked by saturating [GABA] concentrations. (a) Dose-response relationships normalized to maximum current amplitudes that were evoked by saturating [GABA] (F200Y: 10 mM; F200I: 30 mM; F200C: 200 mM) and fitted with the Hill equation. The dose-response curve for WT (black dashed line) was recently assessed by our group (Brodzki et al., 2016): $EC_{50} = 0.04$; Hill coefficient $n_h = 0.67$. EC_{50} values for respective mutants are shown in the inset. Hill coefficient for F200Y (gray squares): $n_h = 0.76$. Hill coefficient for F200I (dark red circles): $n_h = 1.04$. Hill coefficient for F200C (orange triangles): $n_h = 0.99$. (b) Examples of typical normalized responses to 500 ms application of a saturating [GABA] concentration for each mutant and for WT. Note the marked differences in the current time course between WT and the mutants, indicating marked alterations of receptor gating.

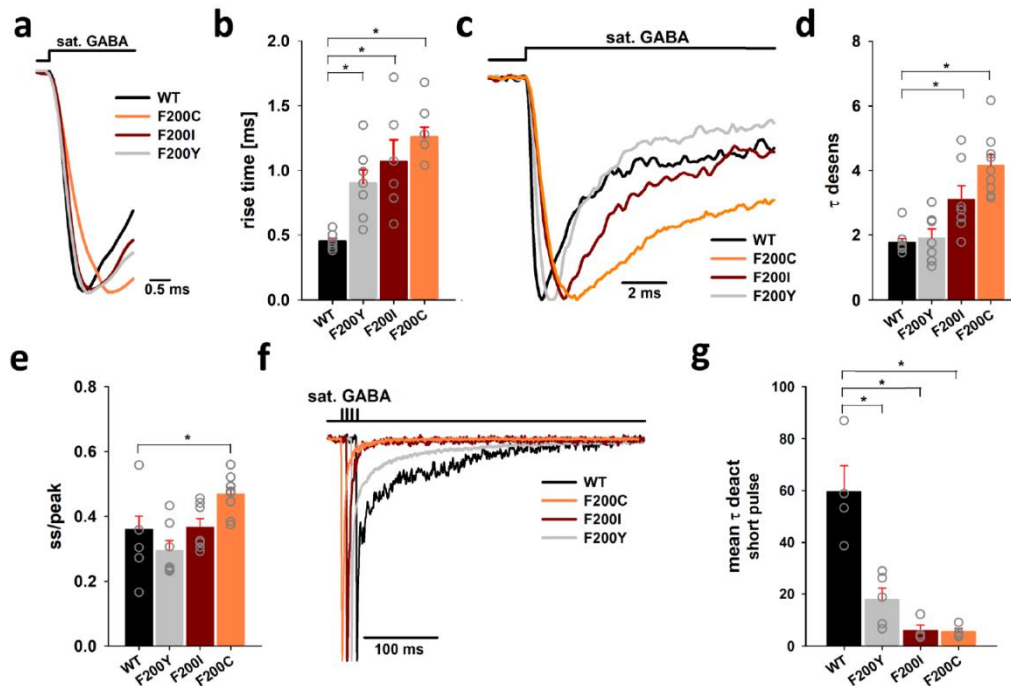


Fig. 3. Mutation of the β_2 F200 residue affects the kinetics of macroscopic currents that are elicited by saturating [GABA] concentrations, indicating changes in gating properties of the receptor. (a) Normalized traces of WT (black) and the F200Y (gray), F200I (dark red), and F200C (orange) mutants, showing that the mutations slowed onset kinetics of current responses. The inset above the traces represents agonist application. (b) Statistics for mean values of rise time for WT and the mutants. Note that the rise time significantly slowed relative to WT for all of the mutants. (c) Normalized typical traces that show fast macroscopic desensitization for WT (black) and the F200Y (gray), F200I (dark red), and F200C (orange) mutants that were elicited by prolonged agonist application. (d) Statistics for macroscopic fast desensitization time constant (τ_{desens}) for WT and β_2 F200 mutants. (e) Statistics for the steady state-to-peak ratio. (f) Normalized typical traces of currents that were evoked by short application of a saturating [GABA] concentration, showing changes in deactivation kinetics between WT (black) and the F200Y (gray), F200I (dark red), and F200C (orange) mutants. For display purposes, the traces were slightly time shifted. (g) Statistics for deactivation kinetics (mean deactivation time constant) for currents that were elicited by a short pulse. Asterisks indicate a statistically significant difference between each mutant compared with WT.

to WT, although the extent of this shift was markedly less than with F200I and F200C.

As shown in the example traces in Fig. 2b, distinct mutations of the β_2 F200 residue profoundly affected the time course of currents that were elicited by saturating GABA concentrations, clearly indicating that this mutation may strongly affect receptor gating. Therefore, we investigated this issue by performing a detailed analysis of the current time course using different protocols. To ensure the highest fidelity of these recordings and analysis, they were performed exclusively in the outside-out configuration at which the fastest agonist exchange speed could be achieved. In the analysis that is presented below, all of the comparisons were performed relative to the values that were obtained for WT receptors. Mutation of the β_2 F200 residue clearly slowed the current onset, with the strongest effect for the cysteine mutant (WT: 0.45 ± 0.02 ms, $n = 8$; F200Y: 0.9 ± 0.1 ms, $n = 7$, $p < 0.001$; F200I: 1.07 ± 0.17 ms, $n = 6$, $p < 0.001$; F200C: 1.26 ± 0.08 ms, $n = 8$, $p < 0.001$; Fig. 3a and b). Next, we analyzed the rapid component of macroscopic desensitization and found that the mutation slowed the time constant, τ_{desens} (Fig. 3c and d). Again, the strongest effect was observed for F200C (WT: 1.77 ± 0.12 ms, $n = 7$; F200Y: 1.91 ± 0.28 ms, $n = 7$, $p > 0.05$; F200I: 3.1 ± 0.43 ms, $n = 7$, $p = 0.008$; F200C: 4.17 ± 0.32 ms, $n = 9$, $p < 0.001$). However, no difference in τ_{desens} was found between WT and the tyrosine mutant. Moreover, for the cysteine mutant, the extent of desensitization was markedly reduced (i.e., the ss/peak significantly increased; Fig. 3e), whereas no effect was found for F200I or F200Y (WT: 0.36 ± 0.04 ,

$n = 9$; F200Y: 0.29 ± 0.03 , $n = 7$, $p > 0.05$; F200I: 0.37 ± 0.03 , $n = 7$, $p > 0.05$; F200C: 0.47 ± 0.02 , $n = 9$, $p = 0.042$; Fig. 3e). The time course of current responses to the short application of a high GABA concentration is believed to qualitatively mirror kinetic features of synaptic currents (Jones and Westbrook, 1995). Therefore, we examined currents that were elicited by 1.5–3 ms applications of saturating GABA. As shown in Fig. 3f and g, β_2 F200 mutations affected deactivation kinetics, and this effect was particularly strong for the F200C and F200I mutants, indicated by the mean deactivation time constant, τ_{deact} (WT: 59.43 ± 10.1 ms, $n = 4$; F200Y: 17.84 ± 4.52 ms, $n = 5$, $p = 0.005$; F200I: 5.96 ± 2.13 ms, $n = 4$, $p = 0.002$; F200C: 5.56 ± 1.23 ms, $n = 4$, $p = 0.002$; Fig. 3f and g).

4.3. β_2 F200 mutation affects receptor sensitivity to flurazepam

Recent studies provided extensive evidence that benzodiazepines upregulate GABA_AR activity by affecting receptor gating (Downing et al., 2005; Gielen et al., 2012; Mercik et al., 2007). This modulatory effect was previously ascribed primarily to an enhancement of binding (Krampfl et al., 1998; Lavoie and Twyman, 1996). The observation that benzodiazepines enhance the amplitudes of WT receptor-mediated responses to saturating partial agonists or currents that are elicited by saturating full agonists mediated by mutants, indicated that the major modulatory mechanism of benzodiazepines involves upregulation of the flipping (preactivation) transition. For instance, in our recent study (Jatczak-Śliwa et al., 2018), such a FLU-induced higher amplitude of

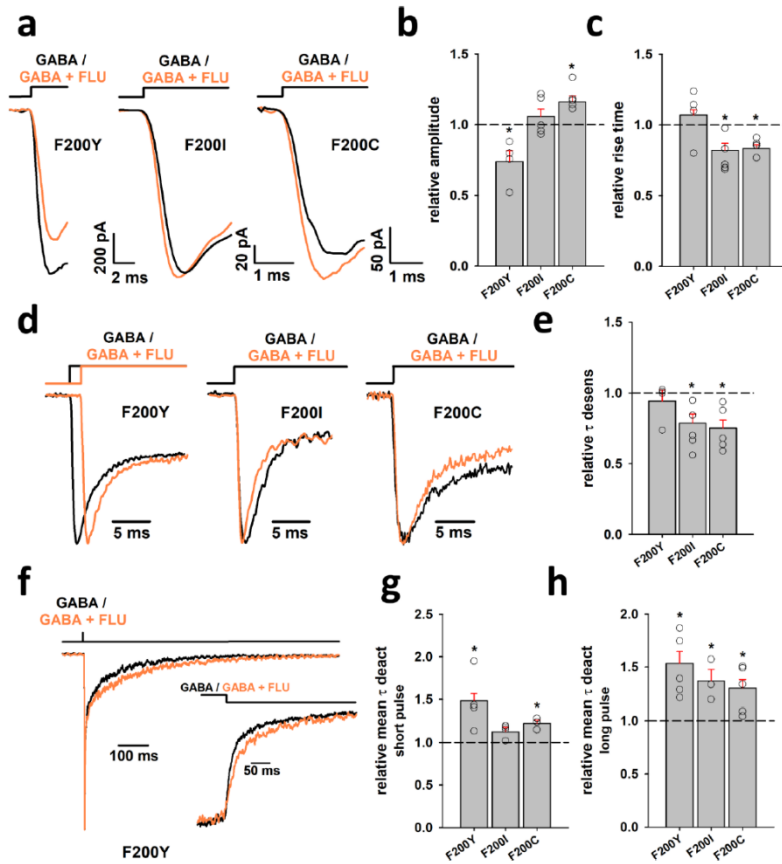


Fig. 4. Flurazepam exerts diverse modulatory effects on current responses to saturating [GABA] that are mediated by β_2 F200 mutants. (a) Typical superimposed traces of currents evoked by saturating [GABA] concentrations (black traces) and saturating [GABA] concentrations in the presence of flurazepam (FLU) (orange traces). Note that FLU differentially affected the current amplitude, decreasing it for the F200Y mutant and increasing it for the F200C mutant. Onset was accelerated by FLU for the F200I and F200C mutants. (b) Statistics for the relative amplitude values (GABA + FLU normalized to GABA). (c) Statistics for relative rise time values. (d) Typical normalized and superimposed traces of currents that were evoked by prolonged agonist applications, revealing the diverse impact of FLU (orange traces) on fast macroscopic desensitization in the mutants relative to control conditions (black traces). For display purposes, for the F200Y mutant, the control trace and the trace that was recorded in the presence of FLU were shifted as they overlapped. (e) Statistics for relative desensitization time constant (τ_{desens}) values for the mutants. (f) Typical normalized traces of currents that were evoked by brief agonist applications of [GABA] (black traces) and [GABA] + FLU (orange traces) for the F200Y mutant. The inset shows typical normalized superimposed traces of deactivation kinetics after a long (500 ms) pulse for this mutant. (g) Corresponding statistics for relative mean deactivation time constant (τ_{deact}) values after a short pulse for the mutants. (h) Statistics for relative mean τ_{deact} after a long pulse. Asterisks indicate a statistically significant difference between [GABA] + FLU and the control.

GABA-evoked responses provided key evidence that mutation of the α_1 F64 residue primarily affected the flipping (preactivation) transition. Thus, we tested the sensitivity of the β_2 F200 mutants to FLU, expecting that such sensitivity would reflect the impact of the mutations on receptor gating. Notably, among the mutants that were studied, F200Y exhibited a kinetic phenotype that was most similar to WT (Fig. 3), and the effect of FLU was comparable to WT (relative amplitude: 0.73 ± 0.07 , $n = 4$, $p = 0.018$, comparison between amplitudes with and without FLU; Fig. 4a and b). This was comparable to the effect of FLU on WT that was described by Mercik et al. (2007) and Mozrzymas et al. (2007). The F200C mutant had the most pronounced alterations of kinetic features, and the effect of FLU on amplitude was inverted

relative to WT (relative amplitude: 1.16 ± 0.04 , $n = 6$, $p = 0.023$; Fig. 4a and b). The F200I mutant exhibited an intermediate effect of FLU (relative amplitude: 1.06 ± 0.05 , $n = 7$, $p > 0.05$; Fig. 4a and b). To further explore the impact of FLU on the mutants, we analyzed the way in which FLU affects the time course of current responses to saturating [GABA]. For the F200I and F200C mutants, FLU significantly accelerated the onset kinetics, whereas it did not change for the F200Y mutant (relative values for F200Y: 1.07 ± 0.03 , $n = 4$, $p > 0.05$; relative values for F200I: 0.81 ± 0.05 , $n = 6$, $p = 0.027$; relative values for F200C: 0.83 ± 0.02 , $n = 6$, $p = 0.008$; Fig. 4a, c). Macroscopic desensitization was significantly accelerated by FLU for F200C and F200I. For F200Y, however, this effect was negligible (relative

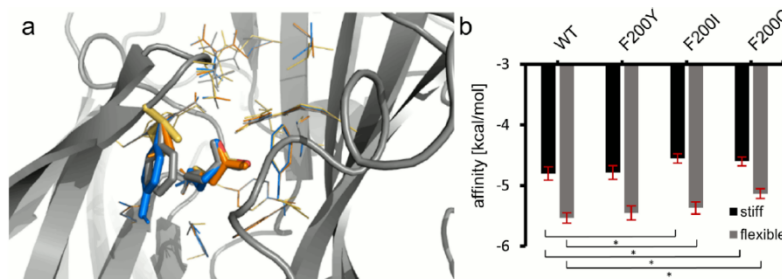


Fig. 5. Docking modeling indicates that the affinity for GABA is reduced for the F200I and F200C mutants but not for the F200Y mutant. (a) Best binding modes (determined by the flexible docking method) of the GABA molecule in WT and mutated receptor models based on the structure from Zhu et al. (2018). WT model (gray). F200Y mutant (blue). F200I (yellow). F200C (orange). For the mutants, only the GABA molecule and residues that formed the binding site are presented. The β_2 F200 residue, respective mutants, and GABA molecule are shown in bold stick representation. (b) Average affinities of GABA binding that were determined using the stiff and flexible docking methods. Note a significant reduction of affinity for the F200I and F200C mutants, which was mainly attributable to disturbances of low-energy "aromatic box" interactions that are conserved in the F200Y mutant. Asterisks indicate a statistically significant difference between groups (indicated by bars).

reduction of affinity for the F200I and F200C mutants, which was mainly attributable to disturbances of low-energy "aromatic box" interactions that are conserved in the F200Y mutant. Asterisks indicate a statistically significant difference between groups (indicated by bars).

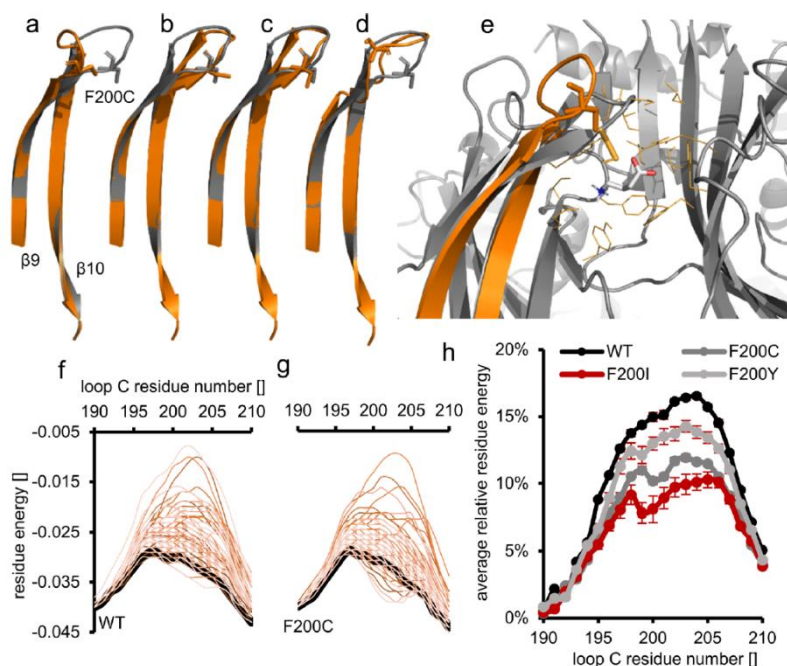


Fig. 6. Numerical analysis of C loop folds suggests that F200C and F200I mutations induce changes in C loop structure. (a–d) Example alternative C loop folds of the F200C mutant. In each picture, the “base” F200C mutant homology model that was based on the GABA_AR structure from Zhu et al. (2018) is shown in gray (DOPE energy score = -0.713). Alternative folds of the C loop are shown in orange (backbone not constrained by experimental WT structure): (a) outward fold (-0.704), (b) inward fold and cysteine functional group twist (-0.708), (c) similar to b, but the cysteine orientation is conserved (-0.717), and (d) more pronounced disturbance in the structure but with less favorable energy (-0.667). (e) Same fold as in a but aligned to the F200C mutant binding mode from the docking studies. Note that the C loop tip is moved away from the LBS center, which could impair ligand binding and possibly gating transitions. (f, g) Example energy profiles of C loop residues for alternative folds. (f) Energy of WT models: WT “base” model (based on GABA_AR structure from Zhu et al., 2018) (thick black line) and energies of subsequent models with unconstrained C loop structure (thin orange lines). (g) Same as f but for the F200C mutant. Note that in contrast to WT (f), the F200C mutant (g) has more alternative folds with energy that is similar or lower relative to the “base” model. (h) Average energies of C loop alternative folds for each mutant and WT relative to their “base” models. Each mutant showed more energetically favorable alternative folds than WT, but their number was the smallest for F200Y among the mutants.

τ_{desens} for F200Y: 0.94 ± 0.07 , $n = 4$, $p > 0.05$; relative τ_{desens} for F200I: 0.78 ± 0.06 , $n = 7$, $p = 0.024$; relative τ_{desens} for F200C: 0.75 ± 0.05 , $n = 6$, $p = 0.023$; Fig. 4d and e). Flurazepam had no significant effect on the extent of desensitization (relative ss/peak for F200Y: 0.95 ± 0.02 , $n = 4$; relative ss/peak for F200I: 0.95 ± 0.05 , $n = 7$; relative ss/peak for F200C: 0.92 ± 0.04 , $n = 6$, $p > 0.05$, data not shown). Finally, the effect of FLU on deactivation kinetics was examined for currents that were mediated by the mutants. When applying a short (1.5–3 ms) GABA pulse, we observed a trend toward a FLU-induced slowing of deactivation kinetics that was statistically significant for F200Y and F200C (relative τ_{deact} for F200Y: 1.48 ± 0.08 , $n = 4$, $p = 0.018$; relative τ_{deact} for F200I: 1.12 ± 0.04 , $n = 4$, $p > 0.05$; relative τ_{deact} for F200C: 1.22 ± 0.04 , $n = 3$, $p = 0.02$). Moreover, FLU significantly prolonged the deactivation time course that was observed after long (500 ms) GABA application (relative τ_{deact} for F200Y: 1.53 ± 0.11 , $n = 6$, $p = 0.031$; relative τ_{deact} for F200I: 1.36 ± 0.1 , $n = 3$, $p < 0.001$; relative τ_{deact} for F200C: 1.3 ± 0.08 , $n = 6$, $p = 0.003$; Fig. 4f–h).

4.4. Interactions between C loop and GABA molecule and impact of mutations on receptor structure

To provide further insights into the molecular mechanisms whereby the mutations affected receptor kinetics, including the dose-response relationship, GABA docking to structural models was investigated. The selected binding modes are presented in Fig. 5a, and their affinities are presented in Fig. 5b. Independent of the method used (i.e., stiff or flexible), each mutation led to a decrease in binding affinity, with the exception of F200Y, in which the difference relative to WT did not reach significance (Fig. 5b). The similar affinities for WT and the F200Y mutant was unsurprising because conservation of the aromatic ring in F200Y was expected to largely maintain the network of cation- π interactions with a ligand molecule (Fig. 5a). However, for the F200Y mutant, a leftward shift of the dose-response relationship was observed

(Fig. 2a), which unlikely results from an increase in affinity. Moreover, as indicated by Colquhoun (1998), alterations of gating could also result in a shift of the dose-response relationship. As we present below, modeling of the experimental data indicated that for the tyrosine mutant, a lower EC_{50} might be attributable to an increase in the flipping gating rate. In contrast to F200Y, GABA docking for F200C and F200I predicted significantly lower binding affinity compared with WT, which is compatible with the rightward shift of the dose-response relationships for these mutants (Fig. 2a). Additionally, deactivation was strongly accelerated for these mutants, which could reflect less efficient ligand binding compared with WT. However, an additional consideration in these docking studies was that the backbone conformation of the receptor was kept immobile and was the same as in the experimental structural template that was used to build the WT and mutant models. Thus, this type of docking approach would be unable to reveal possible effects of mutations on general structure of the C loop, which is known to be highly mobile. To address the issue of structural changes in the ligand-free C loop that were induced by the mutations, an additional approach was applied. In contrast to docking, the C loop tip was allowed to fold freely according to the most favorable energy. Example alternative structures of the F200C mutant C loop are presented in Fig. 6a–d. Fig. 6e further presents visualization in the context of the LBS. The thick black line in Fig. 6f and g represents the energy profile for the part of the protein at the LBS that contains the C loop region (residues 190–210) in the reference structure. In the case of WT and the mutants, most of the alternative C loop folds (thin orange lines in Fig. 6f and g) had higher energy than in the case of backbone preservation from the structural template (thick black line in Fig. 6f and g). For WT (Fig. 6f), almost none of the models had more favorable energies than the reference structure, and similar results were obtained for the tyrosine mutant. In contrast, a fraction of the alternative fold models of F200C (Fig. 6g) and F200I exhibited energies that were more favorable than the reference backbone fold. This means that these mutations may favor structural changes in this loop relative to the template.

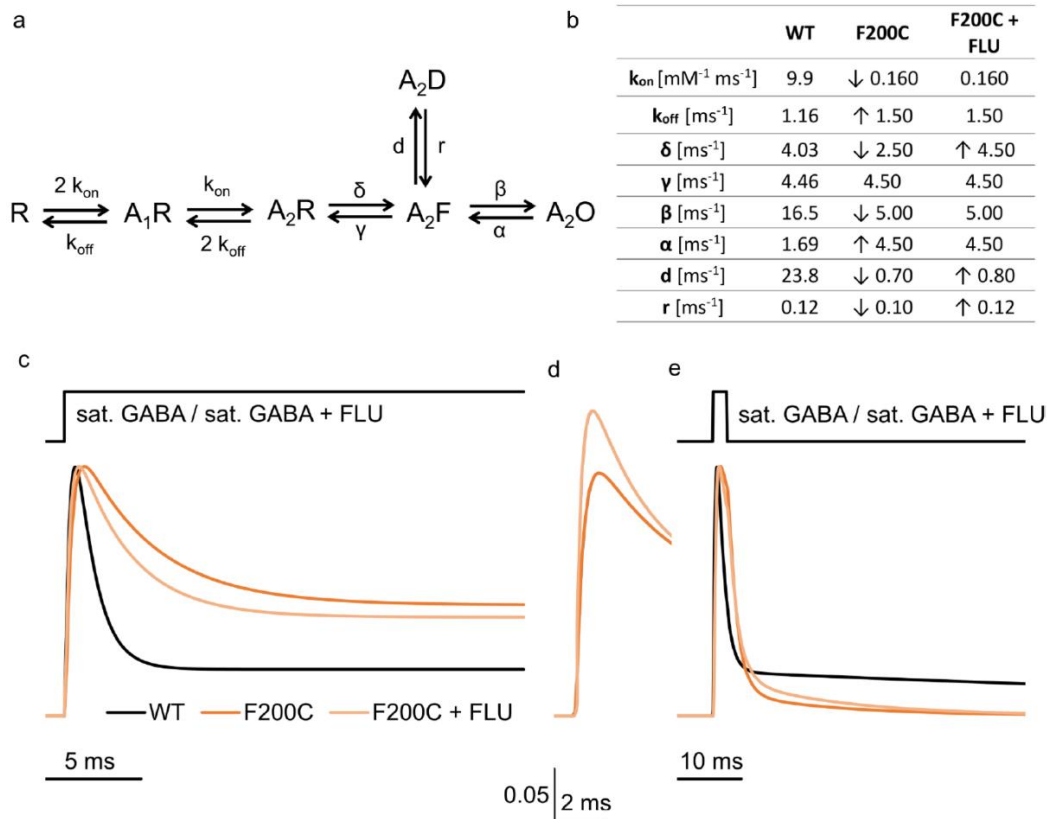


Fig. 7. Model simulations of macroscopic currents reveal that the F200C mutation affects both ligand binding and gating of the receptor. (a) Kinetic model topology (“flipped Jones-Westbrook model”) from Szczot et al. (2014) that was used to model macroscopic currents for WT and the F200C mutant. (b) Rate constants for WT receptors and the F200C and F200C mutants in the presence of FLU. The F200C mutation strongly impaired binding by reducing the k_{on} rate and increasing the unbinding rate (k_{off}). Gating transitions were also affected: transition into flipped state (δ), opening/closing (β and α), and desensitization (d and r). The effect of FLU for the F200C mutation (see Fig. 4) was best reproduced by an increase in the flip rate (δ) up to the level of WT and by increasing desensitization rates. (c–e) Simulated current responses. (c) Normalized response to a long pulse of a saturating GABA concentration. Notice prolonged current onset, slower desensitization, and a higher ss/peak ratio for the F200C mutant and their “rescue” toward the levels of WT after FLU treatment. (d) The same responses as in c but not normalized, showing the reproduction of the effect of FLU on current amplitude. (e) Response to short GABA application under control conditions (black) and in the presence of FLU (gray). Notice a markedly slower deactivation time course for WT and the prolongation of deactivation by FLU for the F200C mutant.

Furthermore, in most cases, this alternative fold reflected C loop tip movement away from the LBS, but some folds also exhibited inward C loop movement (Fig. 6a–d). In both cases, this would lead to a reduction of binding affinities below those that were estimated in the docking studies.

Altogether, the results of the structural modeling of WT receptors and the mutants (Fig. 6h) indicated that both the binding mode and C loop structure of F200Y were most similar to WT. The F200C and F200I mutants may exhibit disruptions of C loop conformation that could explain the increase in EC_{50} values and changes in current response kinetics. Importantly, the F200I mutant exhibited a smaller decrease in binding affinity than F200C, which appears to be compatible with a 10-fold lower EC_{50} value in the case of F200I.

4.5. Model simulations for macroscopic currents

To provide a mechanistic interpretation of the profound kinetic changes that were observed in our macroscopic recordings and that were induced by the β_2 F200 residue mutation, model fitting was considered. The F200Y mutation resulted in a phenotype that was similar to WT, but the F200I and F200C mutations clearly altered receptor

kinetics, and the impact of the F200C mutation was considerably larger. We thus conducted model fitting for the cysteine mutant. We used the framework of the model that is presented in Fig. 7a, which was previously considered by our group in our recent report (Szczot et al., 2014). Notably, this model is markedly simplified with regard to the one that was used for single-channel modeling (Model 1, Fig. 10a) because it contains only one open state and one desensitized state. As reported by Colquhoun and Lape (2012), the modeling of macroscopic currents is much more vulnerable to overparametrization than the single-channel analysis. Indeed, in our macroscopic modeling that was based on extended models that were used in single-channel modeling, making a unique interpretation was difficult in terms of the reliable optimization of rate constants. We thus considered a minimum requirement model, in which each gating feature is represented by one branch of the model.

The rate constants of the model were selected to best reproduce the effect of the F200C mutation. For this mutant, a very strong rightward shift of the dose-response function was observed (Fig. 2a). Although a shift of the dose-response relationship can principally occur because of a change in affinity or gating (especially efficacy; Colquhoun, 1998), strong modification of the binding properties was required to reproduce

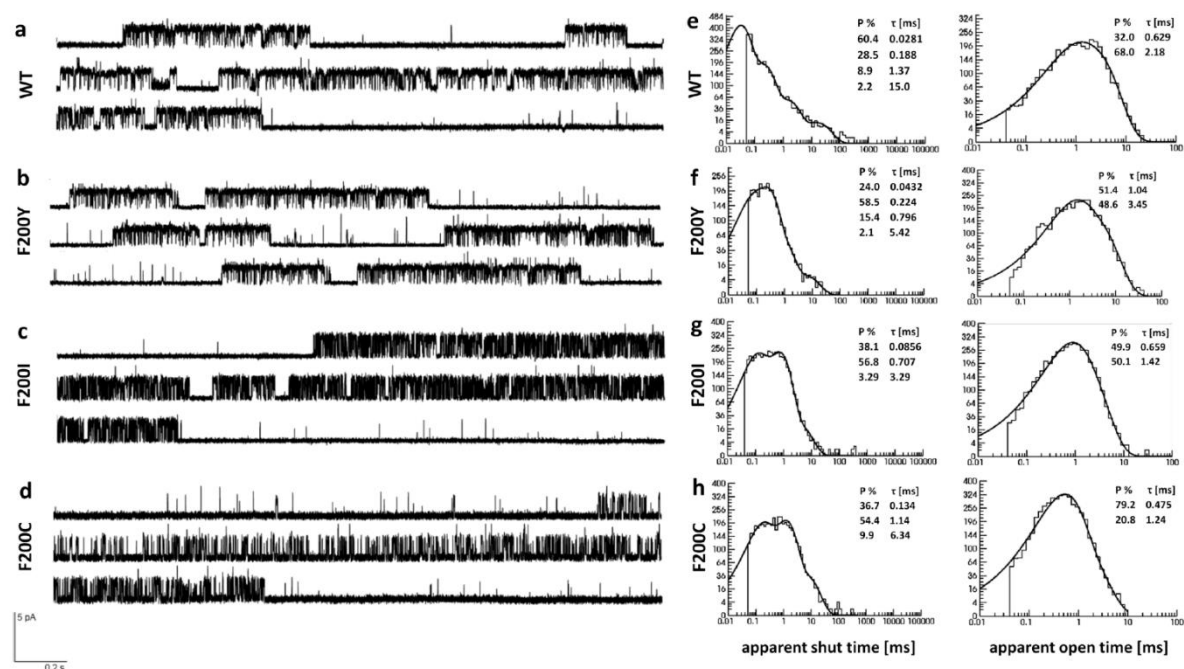


Fig. 8. Single-channel analysis reveals that β_2 F200 mutations alter both shut and open dwell times distributions relative to WT receptors. (a–d) Typical single-channel activity with prominent clusters that were recorded from WT (a), F200Y (b), F200I (c), and F200C (d). (e–h) Typical dwell times distributions for single-channel recordings for WT receptors and mutants (indicated on the left). The left column shows typical shut times distributions with fitted probability density functions. The inset shows the parameters. The right column shows analogous information for open times distributions (also see Tables 1 and 2 for statistics).

both the dose-response relationship shift and modifications of the time course of macroscopic currents that were evoked by non-saturating [GABA] and mediated by the mutant. This was unsurprising because this mutation involves a key residue at the orthosteric LBS. As described above, the extent of impact of the mutation on receptor binding properties was assessed using docking and C loop structure modeling. Both of these aspects were involved in weakening of the LBS. The major difficulty in model fitting was that each current kinetic feature (e.g., current onset or macroscopic desensitization) may depend on all of the rate constants in the kinetic model (Colquhoun, 1998; Mozrzymas et al., 2003). To reproduce the effect of the F200C mutation on current onset kinetics, a reduction of flipping and desensitization rates was required. A decrease in the flipping rate, δ , was also needed (together with the weakening of binding characteristics) to reproduce a robust increase in the EC_{50} value for the F200C mutant. Another key observation was a marked slowing of macroscopic desensitization (Fig. 3c and d). This effect could be fairly reproduced by reducing the desensitization rate, d , which was also compatible with the reduction of the current onset rate. Additionally, a reduction of the d rate constant enabled us to reproduce rapid deactivation kinetics in the case of the F200C mutant. Slower macroscopic desensitization could be alternatively reproduced by a decrease in the closing rate, α . However, this scenario would predict slow deactivation for currents that are mediated by the mutant, in contrast to our experimental observations. Most importantly, it would contradict the single-channel data that consistently revealed a shortening of open time (Table 2) and hence the increase in α rates. Simulated responses for WT and F200C are presented in Fig. 7c–e, together with tables of the respective rate constants (Fig. 7b).

Another line of evidence that was useful for deciphering the mechanism of action of the F200C mutation on receptor gating was the effect of FLU which, in contrast to WT receptors, increased the amplitudes of current responses that were mediated by the F200C mutant

(Fig. 4a and b). Importantly, as suggested by the aforementioned kinetic modeling, this mutation markedly reduced the flipping rate, δ , and its upregulation was necessary to reproduce the FLU-induced increase in current amplitude. Importantly, the reduction of this rate constant by the mutation was a prerequisite to reproduce the observed effect of FLU on amplitude for the F200C mutant. As discussed in our recent paper (Jatczak-Śliwa et al., 2018), the flipping rate, δ , for WT receptors is so fast that its further acceleration by FLU does not increase the open probability. Thus, the lack of the FLU-induced increase in the amplitude of current responses that are mediated by the F200I mutant (i.e., no effect on amplitude) and F200Y mutant (i.e., lower amplitude) is interpreted as a consequence of a weaker effect of these mutations on the flipping rate and, hence, closer similarity to the phenotype that is observed for WT receptors. The effect of FLU on the flipping rate, δ , was crucial for reproducing kinetic changes that were induced by this compound (Fig. 4); therefore, other gating rate constants had to be modified. To reproduce the effect of FLU on macroscopic desensitization (Fig. 4d, e), d and r had to be increased to values that were closer to WT receptors (see Fig. 7b for transition rates and Fig. 7c–e for simulated responses). The upregulation of desensitization by FLU is consistent with our previous study of a different mutant (α_1 F64, Jatczak-Śliwa et al., 2018). Moreover, under conditions of a rapid flipping rate, δ , an increase in the desensitization rate, d , led to a reduction of the current amplitude that was consistently described previously and also in the present study for the F200Y mutant. Altogether, our macroscopic analysis indicated that the F200C mutation dramatically affected binding and altered all of the considered gating features, including preactivation, opening/closing, and desensitization.

4.6. Impact of β_2 F200 mutation on single-channel activity

Single-channel recordings were performed in the cell-attached

Table 1
Shut times distributions for WT and β_2 F200 mutations. P_1 , percentages; τ_1 , time constant that describes distributions of apparent shut times for cluster activity for WT and β_2 F200 mutants. Values in brackets were obtained from simulations with Model 1 (WT, F200Y) and Model 2 (F200I, F200C) (shown in Fig. 10a and b), with experimental resolution and renormalization of percentages (P) from $\tau = 0$ to infinity, with area sum = 1 (normal brackets) and correction for missed events [square brackets]. Data were obtained from at least four patches. Values of parameters that reached a significant difference relative to WT are marked in bold and with an asterisk (*).

Shut time	P_1	τ_1 [ms]	P_2	τ_2 [ms]	P_3	τ_3 [ms]	P_4	τ_4 [ms]	T_{sum} [ms]
WT	66.36 ± 1.71 (53.20 ± 2.54) [54.61 ± 2.49]	0.03 ± 0.002 (0.07 ± 0.02) [0.07 ± 0.02]	24.84 ± 1.86 (31.54 ± 2.54) [32.63 ± 2.03]	0.22 ± 0.01 (0.29 ± 0.04) [0.29 ± 0.04]	7.04 ± 1.04 (8.96 ± 2.51) [8.59 ± 1.43]	1.19 ± 0.18 (1.32 ± 0.27) [1.32 ± 0.27]	1.68 ± 0.45 (4.32 ± 0.78) [4.17 ± 0.76]	11.45 ± 3.21 (6.44 ± 1.57) [6.43 ± 1.57]	0.30 ± 0.45 (0.52 ± 0.11) [0.50 ± 0.11]
F200Y	28.45 ± 6.96* (25.64 ± 1.82)* [28.29 ± 1.36]*	0.05 ± 0.01* (0.05 ± 0.01) [0.05 ± 0.01]	47.63 ± 7.71* (50.99 ± 3.86)* [50.16 ± 3.63]*	0.21 ± 0.03 (0.23 ± 0.02) [0.22 ± 0.02]	21.40 ± 4.10* (21.31 ± 2.73)* [19.63 ± 2.58]*	0.75 ± 0.22 (0.80 ± 0.15) [0.79 ± 0.15]	2.55 ± 1.10 (2.06 ± 0.31)* [1.92 ± 0.27]*	4.63 ± 1.33 (15.70 ± 0.05)* [15.68 ± 0.04]*	0.36 ± 0.05 (0.61 ± 0.02) [0.57 ± 0.02]
F200I	41.43 ± 2.65* (36.36 ± 2.38)* [37.52 ± 2.40]*	0.10 ± 0.01* (0.11 ± 0.01)* [0.11 ± 0.01]*	54.12 ± 2.75* (51.95 ± 2.82)* [51.20 ± 2.72]*	0.78 ± 0.04* (0.66 ± 0.05)* [0.64 ± 0.05]*	4.43 ± 0.40 (11.20 ± 1.46) [11.28 ± 2.59]	5.28 ± 0.58* (3.63 ± 0.66)* [3.62 ± 0.66]*	-	-	0.72 ± 0.06 (0.79 ± 0.05)* [0.70 ± 0.05]
F200C	33.50 ± 1.29* (30.78 ± 1.14)* [33.79 ± 1.50]*	0.11 ± 0.01* (0.12 ± 0.03)* [0.11 ± 0.03]	55.08 ± 3.95* (40.26 ± 8.04) [39.87 ± 7.81]	1.25 ± 0.09* (0.80 ± 0.10)* [0.78 ± 0.09]*	11.64 ± 3.62 (28.97 ± 7.48)* [26.33 ± 6.68]*	5.48 ± 0.21* (4.35 ± 1.31)* [4.27 ± 1.33]*	-	-	1.37 ± 0.20* (1.34 ± 0.13)* [1.21 ± 0.11]*

configuration using GABA concentrations that sought to saturate the receptors. For WT, F200Y, and F200I receptors, 10 and 30 mM GABA, respectively, were clearly sufficient to ensure saturation. However, as shown by the macroscopic recordings, a GABA concentration of 100 mM missed saturation for F200C by a small margin (12%). Short-lasting macroscopic recordings could be performed under conditions of a very high [GABA] concentration (even 200 mM, which reached saturation), but long-lasting single-channel recordings showed greater instability that resulted in a progressive increase in noise, much faster patch loss, and alterations of single-channel activity (e.g., a random drift in contributions from various modes). Thus, under these conditions, we were unable to reach an appropriate number of transitions (~10000), which reduced the reliability of our analysis. We decided to complete single-channel recordings at 10 mM (WT) and 100 mM (F200C mutant). In Section 5.2 below, we argue that a minor offset from saturation for the F200C mutant was unlikely to significantly affect our conclusions.

Both WT receptors and all of the considered β_2 F200 mutants presented clear cluster activity that could be easily identified visually for the dominant mode of activity (Fig. 8), and the analysis was limited to clusters of the dominant mode (in WT and β_2 F200 mutants) as described previously (Kisiel et al., 2018). Although activity of the mutants took the form of clusters (similar to WT), their single-channel activity presented marked differences from WT (Fig. 8). The analysis of the open and shut times distributions indeed confirmed a profound impact of the mutations on receptor kinetics. As explained in Section 3.4, for the F200C mutants, the three shortest shut time components could be reliably described; therefore, comparisons with WT were made for the three shortest components. As shown in the example distributions in Fig. 8 and Table 1, the cysteine mutation resulted in a several-fold slowdown of all three shut time constants, and the percentage of the fastest component was reduced in the F200C mutant by nearly half (Table 1). The weighted average of shut times was 0.3 ms ± 0.06 ms for WT ($n = 5$) and 1.37 ± 0.2 ms for F200C ($n = 5$; $p < 0.001$), thus confirming a profound change that was induced by this mutation. The F200C mutation also strongly affected receptor opening (Fig. 8). Indeed, both time constants were shortened relative to WT by at least half (Table 2), and the weighted average of open times was 1.9 ± 0.17 ms for WT and 0.63 ± 0.08 ms for F200C ($n = 5$; $p < 0.001$). For the F200I mutant, both the shut and open times distributions were also strongly altered relative to WT, but the differences were smaller than for the F200C mutant (Tables 1 and 2). Again, all three of the considered shut time constants significantly slowed, and the weighted average of shut times was 0.69 ± 0.06 ms ($n = 6$; $p = 0.004$; Table 1). In the case of open times for the F200I mutant, both time constants were shortened relative to WT, and the weighted average of open times was 0.98 ± 0.08 ms ($n = 6$; $p < 0.001$), which was significantly shorter than in WT. Both the F200C and F200I mutations decreased Popen (Fig. 9a), but changes in the burst length reached statistical significance only for F200C (18.31 ± 3.09 ms, $n = 5$, $p = 0.013$; Fig. 9b) compared with WT (73.86 ± 17.26 ms, $n = 5$; burst length for F200I: 41.94 ± 6.62 ms, $n = 6$, $p = 0.096$). Thus, the F200I mutation produced a kinetic phenotype that was between WT and F200C, which is compatible with the macroscopic recordings (Figs. 2 and 3). The F200Y mutation resulted in a phenotype that was very similar to WT (Figs. 8 and 10). Surprisingly, the distribution of shut and open times revealed significant changes in their percentages (Tables 1 and 2). However, for the F200Y mutant, the weighted average for shut times (0.36 ± 0.05 ms) and open times (1.78 ± 0.13 ms, $n = 4$) was not significantly different from WT ($p = 0.47$ and $p = 0.42$, respectively).

Table 2

Open times distributions for WT and β_2 F200 mutations. P, percentages; τ , time constant that describes distributions of apparent opens time for cluster activity for WT and β_2 F200 mutants. Values in brackets were obtained from simulations with Model 1 (WT, F200Y) and Model 2 (F00I, F200C) (shown in Fig. 10a and b), with experimental resolution (normal brackets) and correction for missed events [square brackets]. Data were obtained from at least four patches. Values of parameters that reached a significant difference relative to WT are marked in **bold** and with an asterisk (*).

Open time	P ₁	τ_1 [ms]	P ₂	τ_2 [ms]	T _{open} [ms]
WT	38.20 ± 10.13 (46.95 ± 10.23) [61.76 ± 9.09]	0.75 ± 0.20 (0.90 ± 0.18) [0.76 ± 0.15]	71.90 ± 0.98 (53.05 ± 10.23) [38.24 ± 9.09]	2.67 ± 0.2 (2.39 ± 0.23) [2.10 ± 0.28]	1.98 ± 0.17 (1.69 ± 0.13) [1.24 ± 0.11]
F200Y	53.43 ± 7.34* (54.66 ± 3.95) [72.11 ± 0.07]	0.94 ± 0.20 (0.95 ± 0.12) [0.74 ± 0.07]	46.58 ± 7.34* (45.33 ± 3.95) [27.89 ± 5.26]	2.70 ± 0.23 (2.71 ± 0.37) [2.37 ± 0.29]	1.78 ± 0.13 (1.77 ± 0.21) [1.22 ± 0.12]
F200I	44.65 ± 7.83 (59.74 ± 6.82) [67.93 ± 6.40]	0.53 ± 0.09 (0.65 ± 0.09) [0.62 ± 0.07]	55.35 ± 7.83 (40.26 ± 6.82) [32.07 ± 6.40]	1.31 ± 0.10* (1.27 ± 0.17)* [1.28 ± 0.13]*	0.98 ± 0.08* (0.93 ± 0.07)* [0.82 ± 0.06]*
F200C	67.32 ± 7.82* (60.41 ± 12.96) [68.29 ± 12.05]	0.43 ± 0.06 (0.41 ± 0.06)* [0.37 ± 0.05]*	32.67 ± 7.82* (39.59 ± 12.96) [31.71 ± 12.05]	1.07 ± 0.08* (1.13 ± 0.07)* [1.03 ± 0.05]*	0.63 ± 0.08* (0.73 ± 0.13)* [0.59 ± 0.06]*

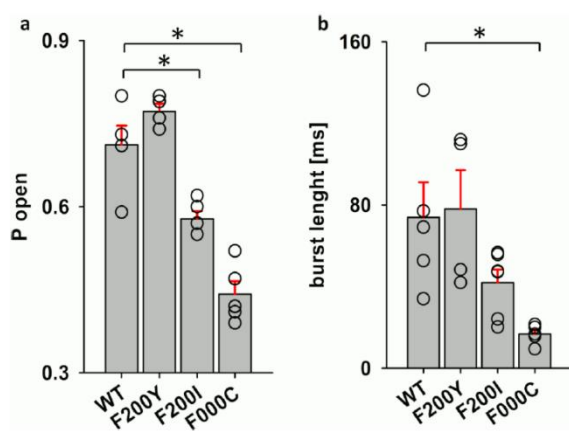


Fig. 9. β_2 F200 mutations affect burst length and open probability (Popen). (a) Statistics for burst length for WT and β_2 F200 mutations. (b) Statistics for open probability for WT and the mutants. Note a dramatic burst shortening and decrease in Popen for the F200C mutant. Asterisks indicate statistical significance.

4.7. Single-channel modeling

Model simulations were performed under the assumption of saturation, implying that the binding steps in the models were omitted. For WT receptors, the model with two open and two desensitized states (Kisiel et al., 2018) was considered (Model 1, Fig. 10a). However, for the β_2 F200 mutants, only one desensitized state was needed (Model 2, Fig. 10b). Attempts to fit the data with the model with two desensitized states resulted in a reduction of fit reliability because one of the desensitized states had very low occupancy. The fitting of WT receptor single-channel activity (at 10 mM) yielded rate constants (Table 3) that were very similar to those in our previous study (Kisiel et al., 2018).

Profound differences between distributions that were generated for WT receptors and the mutants (Fig. 8, Tables 1 and 2) provided the first indication that receptor gating was strongly affected by the F200I and F200C mutations. Indeed, our model fitting confirmed this. Opening and closing for the F200C mutant showed that flipping (preactivation) and desensitization rate constants were significantly affected, with a trend toward an increase in the unflipping rate, γ , and a decrease in d_2 , but these changes did not reach statistical significance (Table 3). Interestingly, the F200C mutation affected all aspects of receptor gating. An analogous effect was found for the F200I mutant, with the exception of the rate constant, α_2 , but the differences between the respective rate

constants compared with WT were less than for F200C (Table 3), thus reproducing our observations that were based on fitting parameters for shut and open times distributions (Tables 1 and 2). In contrast to the F200I and F200C mutations, the F200Y mutation resulted in a prominent increase in both rate constants, γ and δ , but the equilibrium constant, γ/δ , for F200Y (1.61) was slightly higher compared with WT (1.51).

5. Discussion

5.1. Fundamental role of the C loop in the GABA_A receptor activation process

The major finding of the present study was that mutation of the key aromatic residue of the C loop, F200, at the principal β_2 subunit gave rise to dramatic impairments in binding and also caused profound alterations of receptor gating properties. A weakening of binding is unsurprising because this residue is a key constituent of the “aromatic box” at the LBS. Our *in silico* docking studies clearly indicated that the F200C mutation decreased the affinity of the orthosteric LBS. Standard docking (with a fixed backbone) alone was insufficient to reproduce the extent of the reduction of binding affinity that was needed to reproduce the experimental data. However, modeling the impact of this mutation on the C loop structure provided further evidence of such a robust decrease in binding affinity. Docking indicated a lower impact of the F200I mutation on affinity than for F200C (Fig. 5b), but the effects of both mutations on the structure of the C loop were similar. Both F200C and F200I are proposed to cause deformation of the C loop backbone by changing the position of its tip, thus impairing the ability of the receptor to “catch” the ligand (Fig. 6e). Moreover, after ligand binding and C loop stabilization, the docking studies predicted that the interactions between the agonist and the receptor structure were more effective for the F200I mutant than for the F200C mutant, which was consistent with a lower EC₅₀ value for the F200I mutant. A major role for the C loop in defining the affinity of Cys-loop receptors was previously proposed by other authors (Pless and Lynch, 2009; Purohit and Auerbach, 2013; Wagner and Czajkowski, 2001). Our most novel and surprising finding was the pronounced impact of the β_2 F200 mutation on gating properties of the GABA_AR. Importantly, this mutation affected all aspects of receptor gating, including flipping (preactivation), efficacy (opening and closing), and desensitization. These changes in gating properties have been consistently supported by several lines of evidence: (i) robust alterations of the time course of currents that are elicited by saturating [GABA] (Figs. 2 and 3) and (ii) dramatic changes in single-channel features, reflected by the fact that nearly all open and shut time constants in distributions of shut and open dwell times were altered by this mutation. All of the time constants in the shut times distributions showed a few-fold increase compared with WT (Table 1).

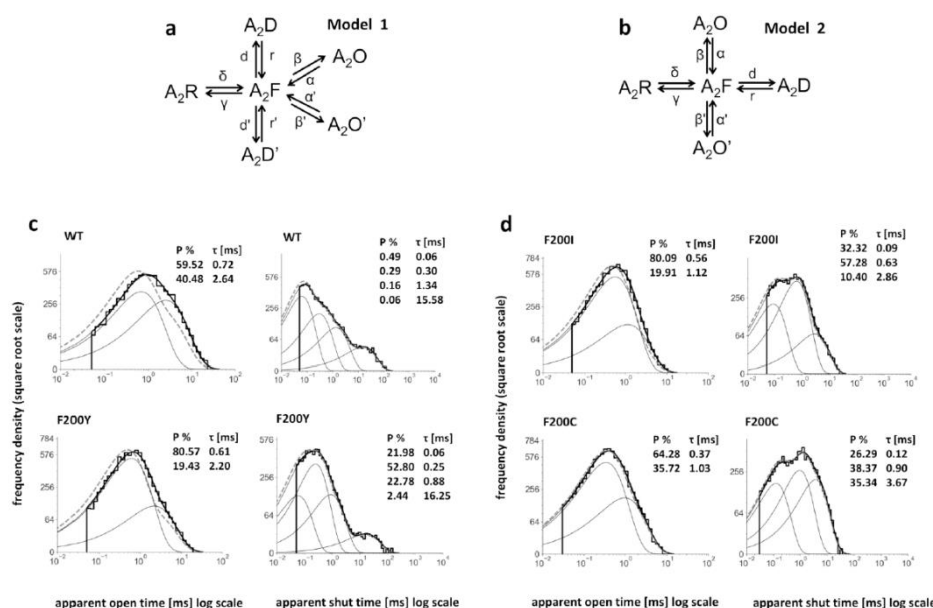


Fig. 10. Simulated frequency density functions of apparent shut and open times for cluster activity fairly reproduce the experimental distributions. (a) Model 1 was used to model the single-channel activity of WT and the F200Y mutant. (b) Model 2 was used to model the single-channel activity of the F200I and F200C mutants. (c) Typical open (left) and shut (right) dwell times distributions for WT (upper graphs) and the F200Y mutant (lower graphs). The insets show the fitting parameters. (d) Typical open (left) and shut (right) dwell times distributions for F200I (upper graphs) and F200C (lower graphs). The insets show the fitting parameters. A_2R , doubly bound receptor; A_2F , flipped state; A_2D/A_2D' , desensitized states; A_2O/A_2O' , open states. The solid gray line indicates each exponential component of the dwell times distribution. The gray dashed line indicates distributions that were determined after correction for missed events.

Table 3

Kinetic rate constants that describe cluster activity for WT and β F200 mutants. Rate constants were determined for a saturating concentration of GABA with Model 1 (WT, F200Y) and Model 2 (F200C, F200I) (Fig. 10). Significant changes in rate constants relative to WT are marked in bold and with an asterisk (*). For each considered case (WT, mutation), the data were obtained from at least four patches.

Kinetic rate constants [ms ⁻¹]	WT	F200Y	F200I	F200C
δ_2	5.17 ± 0.61	9.60 ± 1.16*	3.20 ± 0.45*	2.60 ± 0.13*
γ_2	3.42 ± 0.68	5.96 ± 0.87*	3.60 ± 1.04	3.89 ± 0.61
α_2	1.50 ± 0.28	1.38 ± 0.13	1.70 ± 0.18	2.88 ± 0.50*
β_2	6.31 ± 1.13	6.13 ± 0.65	3.21 ± 0.61*	2.13 ± 0.16*
α_2'	0.51 ± 0.06	0.45 ± 0.07	0.82 ± 0.09*	0.97 ± 0.06*
β_2'	4.35 ± 1.11	2.4 ± 0.5	1.47 ± 0.36*	1.32 ± 0.71*
d_2	0.92 ± 0.25	1.14 ± 0.16	0.42 ± 0.15	1.01 ± 0.39
r_2	0.96 ± 0.17	1.67 ± 0.33	0.39 ± 0.12*	0.39 ± 0.06*
d_2'	0.34 ± 0.10	0.17 ± 0.04	-	-
r_2'	0.21 ± 0.07	0.07 (fixed)	-	-

Additionally, open times were dramatically shortened for the F200C and F200I mutations. However, the effect of the F200Y mutation was qualitatively different from F200I and F200C. The dose-response relationship for the F200Y mutant was shifted to the left, in contrast to F200I and F200C. The F200Y mutation did not increase receptor affinity. We propose that this shift might be attributable to an increase in flipping rate. Similarly, the changes in the time course of macroscopic currents and distributions of single-channel events that were caused by the F200I and F200C mutations would be highly unlikely to be observed if these mutations solely modified binding features of this receptor. Further supporting the robust impact of the F200C mutation on receptor gating, specifically flipping, was the observation that FLU increased the amplitude of currents that were mediated by the F200C

mutants, whereas the opposite effect was observed for WT receptors (Mercik et al., 2007; Mozrzymas et al., 2007) and the F200Y mutant, which presented the closest similarity to WT among the mutants that were considered herein. Such a potentiation of current amplitude by FLU requires that the flipping rate is substantially decreased (also see Jatzcak-Śliwa et al., 2018, where the mechanism of action of FLU was specifically addressed). Interestingly, a similar scenario for a potentiating effect of FLU on responses to saturating [GABA] was recently described by our group for the α_1 F64 mutation (at the LBS on the D loop at the complementary subunit; Szczot et al., 2014). Thus, despite different localization of the C and D loops on different subunits and the distinct structural features of these loops (i.e., the C loop is largely unstructured, whereas the D loop is a part of a rigid β sheet), their mutation leads to robust modification of the flipping (preactivation) process. The impacts of the β_2 F200 and α_1 F64 mutations were clearly distinct. Mutating the β_2 F200 residue resulted in large changes in all gating features, whereas the α_1 F64 mutation affected primarily preactivation. Thus, key residues that are located at the orthosteric LBS are likely strongly involved in receptor gating.

Our major conclusions about the impact of the C loop on GABA_AR gating qualitatively differed from the conclusions that were drawn by Purohit and Auerbach (2013), who performed an elegant single-channel analysis of the AChR and found that even radical manipulation of this loop affected binding rather than gating. This discrepancy most likely resulted from the fact that in distinct Cys-loop receptors (GABA_ARs vs. AChRs), the role of the C loop might be different. One example of such different roles that are played by homologous elements in different Cys-loop receptors is that mutation of the α_1 F64 residue resulted primarily in preactivation impairment in the GABA_AR (Szczot et al., 2014), whereas the homologous residue in α_7 AChR homomers was implicated in rapid desensitization (Gay et al., 2008). However, Mukhtasimova et al. (2009) analyzed activity of the AChR receptor (similar to Purohit and Auerbach, 2013) and reported a causal link between C loop capping and receptor priming (preactivation). Pless and Lynch (2009) applied

voltage-clamp fluorometry and electrophysiology and identified structural changes that were associated with closed flipping transitions in GlyRs. They did not support any clear involvement of C loop movement in encoding efficacy transitions, but these authors did not exclude alternative scenarios, such as an interaction between the C loop and the D and E loops via bound agonist, thus affecting a signal transfer within the macromolecule.

One issue is whether the 100 mM concentration of GABA that missed saturation by a small margin (12%) affected our conclusions that were derived from single-channel recordings. Importantly, the macroscopic and single-channel investigations led to similar conclusions, in which all aspects of gating were affected by the β_2 F200 mutation. Notably, our single-channel analysis was restricted to three components in the shut times distributions, which most likely represent features of the fully bound receptors. For WT GABA_ARs, lowering [GABA] from a saturation concentration (10 mM) to 1 mM did not affect the distributions of these three shut time components, and lowering the concentration further (30 μ M) did not affect the time constants, reducing only the percentages of the fastest ones (data not shown). We expected a similar pattern for the F200C mutant. Additionally, the open times distribution (Fig. 8) clearly indicated that the vast majority of opening events that comprised the distribution were fully bound. Singly bound or spontaneous openings are very characteristic because of their very brief duration ("needle"-like events). The open times distributions that are illustrated in Fig. 8 show that the contribution from not fully bound receptors is negligible at the GABA concentration of 100 mM. Lastly, the macroscopic recordings indicated that responses to 100 and 200 mM GABA did not show any clear differences in time course, indicating that when activated, the kinetic behavior of the receptor at these concentrations was very similar. Altogether, our macroscopic and single-channel analyses consistently indicated a robust effect of the β_2 F200 mutation on receptor gating.

5.2. Possible mechanistic scenarios of the impact of the C loop on GABA_A receptor gating

The important role of the C loop in ligand binding is well established. From a structural perspective, the critical contribution of β_2 F200 and β_2 Y205 residues is emphasized in the context of "aromatic box" formation of the LBS that separates the orthosteric LBS from bulk solution. However, the structural mechanisms that underlie the role of this loop in receptor gating remain largely unknown. Our studies provide solid evidence of the involvement of the C loop in GABA_AR gating but do not provide any direct mechanistic or structural explanations for this role. However, some likely, albeit speculative, scenarios can be suggested for subsequent studies. The C loop connects the β_9 and β_{10} strands. The β_9 strand is beyond the LBS and is connected via the so-called loop 9 with the β_8 strand, which is located on the opposite side of the subunit that contributes to the interface with a preceding subunit (α_1 or γ_2). Notably, both loop 9 and the β_9 strand are known to be involved in channel gating (Hanson and Czajkowski, 2011; Williams et al., 2010). Thus, the β_8 strand is in a position that is readily susceptible to changes that occur at the C loop and participates in the transduction of anticlockwise signaling which, in turn, may contribute to rotation of the extracellular domain (ECD) that is an important step in receptor activation. The concept of the ECD twist was recently described by Masiulis et al. (2019) for GABA_ARs and previously for AChRs (Gupta et al., 2016) and GLIC (Sauguet et al., 2014). Backbone deformation of the C loop through the mutations that were imposed herein likely alters possible coupling of the β_9 strand–loop 9– β_8 strand–preceding subunit, thus affecting intersubunit interactions and receptor gating. In addition to the possible impact of the C loop on lateral intersubunit interactions within the GABA_AR macromolecule, this loop is connected to the transmembrane domain (TMD) via a rigid β_{10} and short β_{10} –M1 helix linker. This structural arrangement facilitates mechanical signal transfer from the LBS toward the receptor gate. Deformation of the C loop may weaken the "stiff" β -strand connection between the LBS and ECD-TMD interface,

which is known to play a critical role in receptor activation (e.g., Cederholm et al., 2009) that in turn affects the receptor gating process. In summary, a profound impact of the C loop mutation on GABA_AR gating may result from interference with intersubunit interactions within the ECD ("horizontal" path) or the hindrance of "vertical" ECD-TMD interactions within a single receptor (principal) subunit.

5.3. Conclusions

In conclusion, based on extensive experimental data, we provide evidence that the C loop of the GABA_AR that is located at the LBS in the ECD contributes to almost all stages of receptor activation, effectively shaping all aspects of receptor gating. Interestingly, mutation of the C loop, particularly the F200C mutation, also affected receptor pharmacology, altering sensitivity of the receptor to the benzodiazepine FLU. The present findings may be particularly helpful for elucidating mechanisms of the pharmacological modulation of GABA_ARs and designing new drugs.

Authorship contribution statement

K.T. participated in performing the experiments, data analysis, and writing the paper. P.T.K. performed the experiments, data analysis, and model simulations for single-channel activity and contributed to writing the paper. M.A.M. performed the *in silico* analysis to enable the choice of mutants, homology modeling, ligand docking, C loop structure modeling, and kinetic simulations for macroscopic currents and contributed to writing the paper. A.D. participated in performing some of the experiments and data analysis. J.W.M. conceived the project, procured financial support, supervised project realization, participated in designing the experiments, data analysis, and model simulations, and wrote and edited the final version of the manuscript.

Declaration of competing interest

None.

Acknowledgements

This work was supported by Polish National Science Centre grant MAESTRO DEC- 2015/18/A/NZ1/00395.

References

- Brickley, S.G., Mody, I., 2012. Extrasynaptic GABAA receptors: their function in the CNS and implications for disease. *Neuron* 73, 23–34. <https://doi.org/10.1016/j.neuron.2011.12.012>.
- Brodzki, M., Rutkowski, R., Jatczak, M., Kisiel, M., Czyzewska, M.M., Mozrzymas, J.W., 2016. Comparison of kinetic and pharmacological profiles of recombinant $\alpha_1\gamma_2$ L and $\alpha_1\beta_2\gamma_2$ L GABAA receptors - a clue to the role of intersubunit interactions. *Eur. J. Pharmacol.* 784, 81–89. <https://doi.org/10.1016/j.ejphar.2016.05.015>.
- Cederholm, J.M.E., Schofield, P.R., Lewis, T.M., 2009. Gating mechanisms in Cys-loop receptors. *Eur. Biophys. J.* 39, 37–49. <https://doi.org/10.1007/s00249-009-0452-y>.
- Cheng, X., Wang, H., Grant, B., Sine, S.M., McCammon, J.A., 2006. Targeted molecular dynamics study of C-loop closure and channel gating in nicotinic receptors. *PLoS Comput. Biol.* 2, e134. <https://doi.org/10.1371/journal.pcbi.0020134>.
- Colquhoun, D., 1998. Binding, gating, affinity and efficacy: the interpretation of structure-activity relationships for agonists and the effects of mutating receptors. *Br. J. Pharmacol.* 125, 923–947. <https://doi.org/10.1038/sj.bjp.0702164>.
- Colquhoun, D., Lape, R., 2012. Allosteric coupling in ligand-gated ion channels. *J. Gen. Physiol.* 140, 599–612. <https://doi.org/10.1085/jgp.201210844>.
- Di Tommaso, P., Moretti, S., Xenarios, I., Orobitg, M., Montanyola, A., Chang, J.M., Taly, J.F., Notredame, C., 2011. T-Coffee: a web server for the multiple sequence alignment of protein and RNA sequences using structural information and homology extension. *Nucleic Acids Res.* 39, 13–17. <https://doi.org/10.1093/nar/gkr245>.
- Downing, S.S., Lee, Y.T., Farb, D.H., Gibbs, T.T., 2005. Benzodiazepine modulation of partial agonist efficacy and spontaneously active GABA(A) receptors supports an allosteric model of modulation. *Br. J. Pharmacol.* 145, 894–906. <https://doi.org/10.1038/sj.bjp.0706251>.
- Farrant, M., Nusser, Z., 2005. Variations on an inhibitory theme: phasic and tonic activation of GABA A receptors. *Nat. Rev. Neurosci.* 6, 215–229. <https://doi.org/10.1038/nrn1625>.

- Gafford, G.M., Guo, J.-D., Flandreau, E.I., Hazra, R., Rainnie, D.G., Ressler, K.J., 2012. Cell-type specific deletion of GABA(A) 1 in corticotropin-releasing factor-containing neurons enhances anxiety and disrupts fear extinction. *Proc. Natl. Acad. Sci.* 109, 16330–16335. <https://doi.org/10.1073/pnas.1119261109>.
- Gay, E.A., Giniatullin, R., Skorinkin, A., Yakel, J.L., 2008. Aromatic residues at position 55 of rat $\alpha 7$ nicotinic acetylcholine receptors are critical for maintaining rapid desensitization. *J. Physiol.* 586, 1105–1115. <https://doi.org/10.1113/jphysiol.2007.149492>.
- Gielen, M.M.C., Lumb, M.J.M., Smart, T.T.G., 2012. Benzodiazepines modulate GABA_A receptors by regulating the preactivation step after GABA binding. *J. Neurosci.* 32, 5707–5715. <https://doi.org/10.1523/JNEUROSCI.5663-11.2012>.
- Gupta, S., Chakraborty, S., Vij, R., Auerbach, A., 2016. A mechanism for acetylcholine receptor gating based on structure, coupling, phi, and flip. *J. Gen. Physiol.* 149, 1–19. <https://doi.org/10.1085/jgp.201611673>.
- Hanson, S.M., Czajkowski, C., 2011. Disulphide trapping of the GABA A receptor reveals the importance of the coupling interface in the action of benzodiazepines. *Br. J. Pharmacol.* 162, 673–687. <https://doi.org/10.1111/j.1476-5381.2010.01073.x>.
- Humphrey, W., Dalke, A., Schulten, K., 1996. VMD: visual molecular dynamics. *J. Mol. Graph.* 14, 33–38. [https://doi.org/10.1016/0263-7855\(96\)00018-5](https://doi.org/10.1016/0263-7855(96)00018-5).
- Jackson, M.B., Wong, B.S., Morris, C.E., Lecar, H., Christian, C.N., 1983. Successive openings of the same acetylcholine receptor channel are correlated in open time. *Biophys. J.* 42, 109–114. [https://doi.org/10.1016/S0006-3495\(83\)84375-6](https://doi.org/10.1016/S0006-3495(83)84375-6).
- Jatczak-Śliwa, M., Terejko, K., Brodzki, M., Michałowski, M.A., Czyżewska, M.M., Nowicka, J.M., Andrzejczak, A., Srinivasan, R., Mozrzymas, J.W., 2018. Distinct modulation of spontaneous and GABA-evoked gating by flurazepam shapes cross-talk between agonist-free and liganded GABA_A receptor activity. *Front. Cell. Neurosci.* 12, 1–18. <https://doi.org/10.3389/fncel.2018.00237>.
- Jonas, P., 1995. Fast application of agonists to isolated membrane patches. In: Sakmann, B., Neher, E. (Eds.), *Single-Channel Recording*. Springer US, Boston, MA, pp. 231–243. https://doi.org/10.1007/978-1-4419-1229-9_10.
- Jones, M.V., Westbrook, G.L., 1995. Desensitized states prolong GABA_A channel responses to brief agonist pulses. *Neuron* 15, 181–191. [https://doi.org/10.1016/0896-6273\(95\)90075-6](https://doi.org/10.1016/0896-6273(95)90075-6).
- Kisiel, M., Jatczak, M., Brodzki, M., Mozrzymas, J.W., 2018b. Spontaneous activity, singly bound states and the impact of alpha1Phe64 mutation on GABA_A receptor gating in the novel kinetic model based on the single-channel recordings. *Neuropharmacology* 131, 453–474. <https://doi.org/10.1016/j.neuropharm.2017.11.030>.
- Kisiel, M., Jatczak-Śliwa, M., Mozrzymas, J.W., 2018a. Protons modulate gating of recombinant $\alpha 1\beta 2\gamma 2$ GABA_A receptor by affecting desensitization and opening transitions. *Neuropharmacology* 146, 300–315. <https://doi.org/10.1016/j.neuropharm.2018.10.016>.
- Krampl, K., Lepier, A., Jahn, K., Franke, C., Bufer, J., 1998. Molecular modulation of recombinant rat $\alpha 1\beta 2\gamma 2$ GABA(A) receptor channels by diazepam. *Neurosci. Lett.* 256, 143–146. [https://doi.org/10.1016/S0304-3940\(98\)00767-8](https://doi.org/10.1016/S0304-3940(98)00767-8).
- Lape, R., Colquhoun, D., Sivillotti, L.G., 2008. On the nature of partial agonism in the nicotinic receptor superfamily. *Nature* 454, 722–727. <https://doi.org/10.1038/nature07139>.
- Lavery, D., Desai, R., Uchański, T., Masiulis, S., Stec, W.J., Malinauskas, T., Zivanov, J., Pardon, E., Steyaert, J., Miller, K.W., Aricescu, A.R., 2019. Cryo-EM structure of the human $\alpha 1\beta 3\gamma 2$ GABA_A receptor in a lipid bilayer. *Nature* 1. <https://doi.org/10.1038/s41586-018-0833-4>.
- Lavoie, A.M., Twyman, R.E., 1996. Direct evidence for diazepam modulation of GABA(A) receptor microscopic affinity. *Neuropharmacology* 35, 1383–1392. [https://doi.org/10.1016/S0028-3908\(96\)00077-9](https://doi.org/10.1016/S0028-3908(96)00077-9).
- Lema, G.M.C., Auerbach, A., 2006. Modes and models of GABA_A receptor gating. *J. Physiol.* 572, 183–200. <https://doi.org/10.1113/jphysiol.2005.099093>.
- Masiulis, S., Desai, R., Uchański, T., Serna Martin, I., Lavery, D., Karia, D., Malinauskas, T., Zivanov, J., Pardon, E., Kotecha, A., Steyaert, J., Miller, K.W., Aricescu, A.R., 2019. GABA_A receptor signalling mechanisms revealed by structural pharmacology. *Nature* 565, 454–459. <https://doi.org/10.1038/s41586-018-0832-5>.
- Mercik, K., Piast, M., Mozrzymas, J.W., 2007. Benzodiazepine receptor agonists affect both binding and gating of recombinant $\alpha 1\beta 2\gamma 2$ gamma-aminobutyric acid-A receptors. *Neuroreport* 18, 781–785. <https://doi.org/10.1097/WNR.0b013e3280c1e2fb>.
- Michałowski, M.A., Kraszewski, S., Mozrzymas, J.W., 2017. Binding site opening by loop C shift and chloride ion-pore interaction in the GABA_A receptor model. *Phys. Chem. Chem. Phys.* 19, 13664–13678. <https://doi.org/10.1039/c7cp00582b>.
- Miller, P., Masiulis, S., Malinauskas, T., Kotecha, A., Rao, S., Chavali, S., De Colibus, L., Pardon, E., Hannan, S., Scott, S., Sun, Z., Frenz, B., Klesse, G., Li, S., Diprose, J., Siebert, A., Esnouf, R., DiMaio, F., Tucker, S., Smart, T., Steyaert, J., Babu, M., Sansom, M., Huiskonen, J., Aricescu, A.R., 2018. Heteromeric GABA_A receptor structures in positively-modulated active states. *bioRxiv* 338343. <https://doi.org/10.1101/338343>.
- Miller, P.S., Aricescu, A.R., 2014. Crystal structure of a human GABA_A receptor. *Nature* 512, 270–275. <https://doi.org/10.1038/nature13293>.
- Miller, P.S., Smart, T.G., 2010. Binding, activation and modulation of Cys-loop receptors. *Trends Pharmacol. Sci.* 31, 161–174. <https://doi.org/10.1016/j.tips.2009.12.005>.
- Mody, I., Pearce, R.A., 2004. Diversity of inhibitory neurotransmission through GABA A receptors. *Trends Neurosci.* 27, 569–575. <https://doi.org/10.1016/j.tins.2004.07.002>.
- Mozrzymas, J.W., Barberis, A., Mercik, K., Zarnowska, E.D., 2003a. Binding sites, singly bound states, and conformation coupling shape GABA-evoked currents. *J. Neurophysiol.* 89, 871–883. <https://doi.org/10.1152/jn.00951.2002>.
- Mozrzymas, J.W., Wójtowicz, T., Piast, M., Lebida, K., Wyrembek, P., Mercik, K., 2007. GABA transient sets the susceptibility of mIPSCs to modulation by benzodiazepine receptor agonists in rat hippocampal neurons. *J. Physiol.* 585, 29–46. <https://doi.org/10.1113/jphysiol.2007.143602>.
- Mozrzymas, J.W., Zarnowska, E.D., Pytel, M., Mercik, K., 2003b. Modulation of GABA A receptors by hydrogen ions reveals synaptic GABA transient and a crucial role of the desensitization process. *J. Neurosci.* 23, 7981–7992. <https://doi.org/10.1523/JNEUROSCI.23-22-07981.2003>.
- Mukhtasimova, N., Lee, W.Y., Wang, H.L., Sine, S.M., 2009. Detection and trapping of intermediate states priming nicotinic receptor channel opening. *Nature* 459, 451–454. <https://doi.org/10.1038/nature07923>.
- Nemecz, Á., Prevost, M.S., Menny, A., Corringer, P.J., 2016. Emerging molecular mechanisms of signal transduction in pentameric ligand-gated ion channels. *Neuron* 90, 452–470. <https://doi.org/10.1016/j.neuron.2016.03.032>.
- Nys, M., Kesters, D., Ulens, C., 2013. Structural insights into Cys-loop receptor function and ligand recognition. *Biochem. Pharmacol.* 86, 1042–1053. <https://doi.org/10.1016/j.bcp.2013.07.001>.
- Padgett, C.L., Hanek, A.P., Lester, H.A., Dougherty, D.A., Lummiss, S.C.R., 2007. Unnatural amino acid mutagenesis of the GABA_A receptor binding site residues reveals a novel cation- π interaction between GABA and beta 2Tyr97. *J. Neurosci.* 27, 886–892. <https://doi.org/10.1523/JNEUROSCI.4791-06.2007>.
- Phulera, S., Zhu, H., Yu, J., Claxton, D.P., Yoder, N., Yoshioka, C., Gouaux, E., 2018. Cryo-EM structure of the benzodiazepine-sensitive $\alpha 1\beta 1\gamma 2\delta$ tri-heteromeric GABA_A receptor in complex with GABA. *Elife* 7, 1–21. <https://doi.org/10.7554/eLife.39383>.
- Pless, S.A., Lynch, J.W., 2009. Magnitude of a conformational change in the glycine receptor $\beta 1\beta 2$ loop is correlated with agonist efficacy. *J. Biol. Chem.* 284, 27370–27376. <https://doi.org/10.1074/jbc.M109.048405>.
- Purohit, P., Auerbach, A., 2013. Loop C and the mechanism of acetylcholine receptor-channel gating. *J. Gen. Physiol.* 141, 467–478. <https://doi.org/10.1085/jgp.201210946>.
- Rudolph, U., Möhler, H., 2006. GABA-based therapeutic approaches: GABA_A receptor subtype functions. *Curr. Opin. Pharmacol.* 6, 18–23. <https://doi.org/10.1016/j.coph.2005.10.003>.
- Rudolph, U., Möhler, H., 2004. Analysis of GABA_A receptor function and dissection of the pharmacology of benzodiazepines and general anesthetics through mouse genetics. *Annu. Rev. Pharmacol. Toxicol.* 44, 475–498. <https://doi.org/10.1146/annurev.pharmtox.44.101802.121429>.
- Šali, A., Blundell, T.L., 1993. Comparative protein modelling by satisfaction of spatial restraints. *J. Mol. Biol.* 234, 779–815. <https://doi.org/10.1006/jmbi.1993.1626>.
- Sauguet, L., Shahsavari, A., Poitevin, F., Huon, C., Menny, A., Nemecz, Á., Haouz, A., Changeux, J.-P.-P., Corringer, P.-J.-P., Delarue, M., Nemecz, A., Haouz, A., Changeux, J.-P.-P., Corringer, P.-J.-P., Delarue, M., 2014. Crystal structures of a pentameric ligand-gated ion channel provide a mechanism for activation. *Proc. Natl. Acad. Sci. U.S.A.* 111, 966–971. <https://doi.org/10.1073/pnas.1314997111>.
- Sieghart, W., Savić, M.M., 2018. International union of basic and clinical pharmacology. CVI: GABA A receptor subtype- and function-selective ligands: key issues in translation to humans. *Pharmacol. Rev.* 70, 836–878. <https://doi.org/10.1124/pr.117.014449>.
- Sigel, E., Steinmann, M.E., 2012. Structure, function, and modulation of GABA_A receptors. *J. Biol. Chem.* 287, 40224–40231. <https://doi.org/10.1074/jbc.R112.386664>.
- Smith, G.B., Olsen, R.W., 1995. Functional domains of GABA A receptors. *Trends Pharmacol. Sci.* 16, 162–168. [https://doi.org/10.1016/S0165-6147\(00\)89009-4](https://doi.org/10.1016/S0165-6147(00)89009-4).
- Szczot, M., Kisiel, M., Czyżewska, M.M., Mozrzymas, J.W., 2014. 1F64 residue at GABA_A receptor binding site is involved in gating by influencing the receptor flipping transitions. *J. Neurosci.* 34, 3193–3209. <https://doi.org/10.1523/JNEUROSCI.2533-13.2014>.
- Thompson, A.J., Lester, H. A., Lummiss, S.C.R., 2010. The structural basis of function in Cys-loop receptors. *Q. Rev. Biophys.* 43, 449–499. <https://doi.org/10.1017/S0033583510000168>.
- Tran, P.N., Laha, K.T., Wagner, D.A., 2011. A tight coupling between $\beta 2Y97$ and $\beta 2F200$ of the GABA_A receptor mediates GABA binding. *J. Neurochem.* 119, 283–293. <https://doi.org/10.1111/j.1471-4159.2011.07409.x>.
- Trott, O., Olson, A.J., 2009. AutoDock Vina: improving the speed and accuracy of docking with a new scoring function, efficient optimization, and multithreading. *J. Comput. Chem.* 49. <https://doi.org/10.1002/jcc.21334>. NA-NA.
- Unwin, N., 2005. Refined structure of the nicotinic acetylcholine receptor at 4 Å resolution. *J. Mol. Biol.* 346, 967–989. <https://doi.org/10.1016/j.jmb.2004.12.031>.
- Venkatachalan, S.P., Czajkowski, C., 2008. A conserved salt bridge critical for GABA(A) receptor function and loop C dynamics. *Proc. Natl. Acad. Sci. U.S.A.* 105, 13604–13609. <https://doi.org/10.1073/pnas.0801854105>.
- Wagner, D.A., Czajkowski, C., 2001. Structure and dynamics of the GABA binding pocket: a narrowing cleft that constricts during activation. *J. Neurosci.* 21, 67–74. <https://doi.org/10.1523/JNEUROSCI.21-01-00067.2001>.
- Waterhouse, A.M., Procter, J.B., Martin, D.M.A., Clamp, M., Barton, G.J., 2009. Jalview Bioinformatics 25, 1189–1191. <https://doi.org/10.1093/bioinformatics/btp033>.
- Williams, C.A., Bell, S.V., Jenkins, A., 2010. A residue in loop 9 of the $\beta 2$ -subunit stabilizes the closed state of the GABA_A receptor. *J. Biol. Chem.* 285, 7281–7287. <https://doi.org/10.1074/jbc.M109.050294>.
- Zhong, W., Gallivan, J.P., Zhang, Y., Li, L., Lester, H.A., Dougherty, D.A., 1998. From ab initio quantum mechanics to molecular neurobiology: a cation- π binding site in the nicotinic receptor. *Proc. Natl. Acad. Sci.* 95, 12088–12093. <https://doi.org/10.1073/pnas.95.21.12088>.
- Zhu, S., Noviello, C.M., Teng, J., Walsh, R.M., Kim, J.J., Hibbs, R.E., 2018. Structure of a human synaptic GABA_A receptor. *Nature* 1. <https://doi.org/10.1038/s41586-018-0255-3>.

3.

„Interaction between GABA_A receptor α_1 and β_2 subunits at the N-terminal peripheral regions is crucial for receptor binding and gating”

Katarzyna Terejko, Michał A. Michałowski, Anna Dominik, Anna Andrzejczak, Jerzy W. Mozrzymas

Biochemical Pharmacology 183 (2021), 114338

doi.org/10.1016/j.bcp.2020.114338



Interaction between GABA_A receptor α_1 and β_2 subunits at the N-terminal peripheral regions is crucial for receptor binding and gating

Katarzyna Terejko^{a,*}, Michał A. Michałowski^{b,a}, Anna Dominik^a, Anna Andrzejczak^b, Jerzy W. Mozrzyński^{a,b,*}

^a Department of Biophysics and Neuroscience, Wrocław Medical University, ul. Chłubińskiego 3A, 50-368 Wrocław, Poland

^b Department of Molecular Physiology and Neurobiology, University of Wrocław, ul. Sienkiewicza 21, 50-335 Wrocław, Poland

ARTICLE INFO

Keywords:

GABA_A receptors
Single-channel analysis
Structure-function
Mutagenesis
Homology modeling

ABSTRACT

Pentameric ligand gated ion channels (pLGICs) are crucial in electrochemical signaling but exact molecular mechanisms of their activation remain elusive. So far, major effort focused on the top-down molecular pathway between the ligand binding site and the channel gate. However, recent studies revealed that pLGIC activation is associated with coordinated subunit twisting in the membrane plane. This suggests a key role of intersubunit interactions but the underlying mechanisms remain largely unknown. Herein, we investigated a “peripheral” subunit interface region of GABA_A receptor where structural modeling indicated interaction between N-terminal α_1 F14 and β_2 F31 residues. Our experiments underscored a crucial role of this interaction in ligand binding and gating, especially preactivation and opening, showing that the intersubunit cross-talk taking place outside (above) the top-down pathway can be strongly involved in receptor activation. Thus, described here intersubunit interaction appears to operate across a particularly long distance, affecting vast portions of the macromolecule.

1. Introduction

The GABA_A receptors (GABA_ARs) mediate fast synaptic inhibitory transmission in the adult mammalian central nervous system (CNS). GABA_ARs are pentameric ligand-gated ion channels (pLGICs) and belong to the Cys-loop receptor superfamily together with glycine receptors (GlyRs), 5-hydroxytryptamine type 3 receptors (5-HT₃Rs) and nicotinic acetylcholine receptors (nAChRs). As many as 20 distinct subunits of GABA_AR have been cloned, explaining a vast heterogeneity of the pentamer composition but the most prevalent is the $\alpha_1\beta_2\gamma_2$ receptor type [1,2]. It is known that activation of GABA_AR and other pLGICs starts at the agonist-binding sites located in the extracellular domain (ECD) region and comprises both “top-down” rearrangements of the macromolecule as well as the anticlockwise rotation of the respective subunits, a phenomenon requiring strong intersubunit interaction and cooperation [3,4]. Several interactions between amino acid residues were implicated in the process of activation of GABA_ARs and other Cys-loop receptors [5–8]. Interestingly, it was found that mutations of residues at the GABA_AR agonist binding site (e.g. loop C [9], loop D [10], loop G [11]) strongly affect not only binding features but also gating transitions of the receptor, including upregulation of the spontaneous activity [12,13]. This is surprising as the

channel gate in the transmembrane domain is particularly distant (approx. 40–50 Å) from the binding sites [14,15]. As already mentioned, receptor activation is associated with the anticlockwise rotation revealing strong lateral interactions between the subunits. It is of note that whereas the “top-down” interactions are typically considered within a single subunit, the rotatory “un-blooming” (as suggested for bacterial pLGIC Gloeobacter ligand-gated ion channel (GLIC) [16], glutamate-gated chloride channel (GluCl) from *C. elegans* [17,18] and supposedly in GlyR [19] and nAChR [20] comprises the whole macromolecule, being thus particularly relevant in the context of conformational transitions. Molecular scenarios underlying the lateral interactions leading to the anticlockwise rotations are even less understood, especially in the context of collective structural subunits rearrangement, than the “top-down” energy transfer from the binding site to the channel gate. However, some examples of studies underscoring importance of interactions between residues that belong to different subunits are available. In GABA_AR, salt-bridge interaction between β_2 Asp163 and α_1 Arg120 located at the top of the binding pocket is formed upon ligand binding to stabilize the bound-closed states of the receptor [21]. Pflanz et al. [22] studied potentiating effect of benzodiazepines (BDZ) and found that electrostatic bond between α_1 Lys104 and γ_2 Asp75 (BDZ binding site is located at the interface between α and γ

* Corresponding authors.

E-mail addresses: katarzyna.terejko@student.umed.wroc.pl (K. Terejko), jerzy.mozrzymski@umed.wroc.pl (J.W. Mozrzyński).

<https://doi.org/10.1016/j.bcp.2020.114338>

Received 25 September 2020; Received in revised form 9 November 2020; Accepted 9 November 2020

Available online 13 November 2020

0006-2952/© 2020 Elsevier Inc. All rights reserved.

subunits) stabilized positive modulation of GABA_AR by these compounds. An interesting example of short-range interactions between adjacent α subunits was reported for GlyR. Namely, the closed state of GlyR is stabilized by the electrostatic interaction between Asp97 and Arg119 and the mutation of Asp97 led to spontaneous channel activity [23]. Additionally, a salt bridge between loop A Glu103 and loop E Arg131 in the binding site region of this receptor shapes the efficacy of gating in an agonist-dependent manner [24]. This evidence indicates that intersubunit interactions can be transmitted over a particularly long distance, affecting thus global macromolecule transitions and related conformational changes. To further explore the impact of intersubunit interactions in GABA_AR and their far-reaching impact on the channel gate, it seems interesting to investigate the residues close to the top of the extracellular domain (e.g. "above" the binding sites) and at subunits' interface. Such a pair of residues was identified by structural studies in $\alpha_1\beta_3\gamma_2$ GABA_AR for two phenylalanine residues α_1 F14 and β_2 F31 localized in the N-terminus region [3] and was confirmed in $\alpha_1\beta_2\gamma_2$ GABA_AR [4].

The major goal of this study was thus to describe the impact of these residues mutations on the channel gating properties by additionally considering the role of interaction between these residues. To this end, macroscopic and single-channel electrophysiology, the double-mutant cycle analysis [25] and disruption of disulfide bridges with dithiothreitol (DTT) were applied. Based on these studies we concluded that in spite of peripheral location, the intersubunit interaction via these residues plays a pivotal role in determining binding and gating properties of GABA_A receptor.

2. Materials and methods

2.1. Transfection and expression of recombinant GABA_AR

The experiments were performed on HEK 293 cells (European Collection of Authenticated Cell Culture, Salisbury, UK) that were cultured as described in detail in Terejko et al. [9]. 48 h prior to an experiment, the cells were transiently transfected using FuGENE HD (Promega, Madison, WI, U.S.) at a 3:1 FuGENE HD:DNA ratio with an adenoviral vector with the pCMV promoter that contained rat cDNA of GABA_AR subunits. For WT and α_1 F14C, the $\alpha_1/\beta_2/\gamma_2$ subunits were mixed in a 1:1:3 ratio and for β_2 F31C and the double mutant in a 1:3:3 ratio in transfection solution, together with 0.5 μ g of enhanced green fluorescent protein (EGFP)-encoding plasmid. An increased amount of the β_2 subunit encoding plasmid in the case of β_2 F31C and the double mutant was used because a very low expression of these receptors was observed when the standard subunit ratio was used. For identification of successfully transfected cells, a visualization with a fluorescence illuminator (470 nm wavelength, COOLLED, Andover, UK) was used (mounted on a modular inverted microscope (Leica DMI8, Wetzlar, Germany)).

2.2. Patch-clamp recordings

Electrophysiological experiments were performed at room temperature (22–23 °C). Macroscopic currents were low-pass-filtered at 10 kHz and recorded from outside-out membrane patches or in the whole-cell configuration (lifted cell mode) at a holding potential of –40 mV using an Axopatch 200B amplifier (Molecular Devices, Sunnyvale, CA, U.S.) and acquired with a Digidata 1550A acquisition card (Molecular Devices, Sunnyvale, CA, U.S.). For signal acquisition, pClamp 10.7 software (Molecular Devices, Sunnyvale, CA, U.S.) was used. Borosilicate glass pipettes (outer diameter, 1.5 mm, inner diameter, 1.0 mm; Hilgenberg, Malsfeld, Germany) were pulled using a P-97 horizontal puller (Sutter Instruments, Novato, CA, U.S.) and filled with intracellular solution that contained 137 mM KCl, 1 mM CaCl₂, 2 mM ATP-Mg, 2 mM MgCl₂, 10 mM K-gluconate, 11 mM EGTA, and 10 mM HEPES, with the pH adjusted to 7.2 with KOH. Pipettes resistance was in the range of 3 to 5 M Ω (pipettes filled with the internal solution). Standard Ringer's solution was used as the external saline, which contained 137 mM NaCl, 5 mM KCl, 2 mM CaCl₂, 1 mM MgCl₂, 10 mM HEPES, and 20 mM glucose, with the pH adjusted to 7.2

with NaOH. Ultrafast perfusion system was used to elicit macroscopic currents. Solutions were supplied simultaneously with a high-precision SP220IZ syringe pump (World Precision Instruments, Inc., Sarasota, FL, U.S.) to the two channels of a theta-glass capillary (Hilgenberg, Malsfeld, Germany) mounted on a piezoelectric-driven translator (Physik Instrumente, Karlsruhe, Germany), as described in detail by Jonas [26] and by our group [10,27,28]. The open tip solution exchange time of the theta-glass capillary ranged from 150 to 300 μ s, depending on its size and speed of flux. Two types of application protocol were used: long, 500 ms application pulse and a short one 2–10 ms pulse which duration was assessed individually for each experiment as minimum time needed to evoke a full current amplitude. For all of the considered mutants, a saturating concentration of GABA was determined as 10 mM GABA. Membrane patches were pre-treated with standard Ringer's solution wash + 1 mM DTT solution for 2–3 min, after which saturating GABA + 1 mM DTT solution was applied (long or short pulse protocol) and followed by 2–3 min wash with Ringer's solution before any next application was performed.

Single-channel recordings were performed in the cell-attached configuration at a holding potential of 100 mV using an Axopatch 200B amplifier (Molecular Devices, Sunnyvale, CA, U.S.) and filtered at 10 kHz with a built-in low-pass Bessel filter. Signals were digitized at 100 kHz sampling rate by a Digidata 1550B acquisition card and Clampex 10.7 software (Molecular Devices, Sunnyvale, CA, U.S.) Pipettes were pulled from thick-wall filamented borosilicate glass capillaries (outer diameter, 1.5 mm; inner diameter, 0.87 mm; Hilgenberg, Malsfeld, Germany) using a P-1000 horizontal puller (Sutter Instruments, Novato, CA, U.S.). Pipettes resistance ranged from 8 to 12 M Ω (filled with the Ringer solution). For noise reduction, the pipettes were coated with Sylgard 184 (DowCorning, Auburn, MI, U.S.) and fire-polished on a microforge. External and intrapipette solution was different from the one used for macroscopic recordings and consisted of 102.7 mM NaCl, 20 mM Na-gluconate, 2 mM KCl, 2 mM CaCl₂, 1.2 mM MgCl₂, 10 mM HEPES, 20 mM TEA-Cl, 14 mM D-(+)-glucose, and 15 mM sucrose (Carl Roth, Karlsruhe, Germany), dissolved in deionized water with the pH adjusted to 7.4 by 2 M NaOH. The amount of the external solution in the dish was kept at a very low level (1 ml in dish of 35 mm diameter), assuring minimal immersion of the recording electrode for noise reduction. Only the patches with resistance > 10 G Ω were considered for further analysis.

All of the chemicals were purchased from Merck (Darmstadt, Germany) unless stated otherwise.

2.3. Macroscopic current analysis and kinetic modeling

Dose-response relationships were determined by fitting the Hill equation:

$$EC = \frac{1}{1 + \left(\frac{EC_{50}}{[GABA]}\right)^{n_h}}$$

to relative current amplitudes of a wide range of non-saturating GABA current amplitudes versus the saturating GABA control (n_h – Hill coefficient).

The dose–response curve For WT receptors presented in Fig. 2A was previously determined by our group in the same way and conditions [29] and in the present study it is used as a reference.

Kinetic analysis was performed exclusively on currents recorded from excised patches, which enabled the fastest solution exchange of the ultrafast perfusion system and thereby the temporal resolution. The current onset was measured as the 10–90% rise time (RT). The time course of macroscopic desensitization differed greatly between WT and the considered mutants (Fig. 2 B) and while in WT and in the double mutant two exponential components were observed, in the single mutants (especially α_1 F14C) fading was so slow that it could be hardly fitted even with a single exponential. In this situation we decided to describe the macroscopic desensitization onset as a total amplitude fraction remaining after 10 ms (abbreviated FR 10). To assess also the extent of

desensitization after long GABA pulses, additionally the FR 500 parameter was determined.

Deactivation kinetics (current relaxation time course after agonist removal) was considered for both long and short application protocols and was described in terms of a mean time constant (τ_{deact}) calculated for either a single exponential fitting or for a sum of two exponentials using the function:

$$I(t) = \sum_{n=1}^f A_n e^{-t/\tau_n}$$

where A_n is the amplitude of the n -th component, and τ_n is the respective time constant. In particular, the mean deactivation time constant for the time course fitted with a sum of two exponentials was calculated:

$$\tau_{\text{deact}} = A_1\% \tau_1 + A_2\% \tau_2$$

where $A_n\%$ is the percentage of the respective component and $A_1\% + A_2\% = 1$.

Kinetic modeling for macroscopic currents was performed using ChannelLab 2.0 software (Synaptosoft, Decatur, GA, U.S.) similarly as described in Terejko et al. [9]; Brodzki et al. [11] and Jatzak-Sliwa et al. [30]. Kinetic model used for WT was the same as in Brodzki et al. [11]. No formal fitting to experimental traces was performed but an extensive trend analysis of possible scenarios was done. The kinetic parameters were varied to best reproduce RT, EC₅₀, FR 10, FR 500 and deactivation. The effect of DTT on the double mutant current responses was simulated based on relative values of the differences between the experimental values versus control.

2.4. Single channel analysis and modeling

Single-channel analysis started with determination of the predominant activity mode for each mutant selected among typically 3–4 different modes. For distinctive clusters of activity, open probability

$$\Delta\Delta G_{\text{coupling}}(\text{parameter}, \text{mutant}_{1,2}) = \Delta\Delta G(\text{parameter}, \text{mutant}_{1,2}) - (\Delta\Delta G(\text{parameter}, \text{mutant}_1) + \Delta\Delta G(\text{parameter}, \text{mutant}_2))$$

(nP_{open} ; n – number of channels within the patch) was calculated using event detection analysis in Clampfit 10.7 software (Molecular Devices, Sunnyvale, CA, U.S.). Predominant mode for WT activity was selected as described by Lena and Auerbach [31] and Kiesel et al. [32]. After determination of the predominant mode for each mutant, single-channel kinetic analysis and modeling were performed using DCprogs pack software that was kindly provided to our group by David Colquhoun. Signals were filtered to obtain a signal-to-noise ratio of at least 15. The final cutoff frequency (f_c) was calculated as following:

$$\frac{1}{f_c} = \frac{1}{f_a} + \frac{1}{f_d}$$

where f_a is the analog filter frequency (typically 10 kHz), and f_d is the digital frequency (offline filtering with 8-pole low-pass Bessel filter by pClamp software). The sampling frequency (f_s) was reduced to $f_s = 10 \times f_c$. Recordings that showed multilevel openings were not considered for the analysis. Selected clusters of the predominant mode of activity were extracted from the traces and stored in separate *.abf files. The clusters were then idealized by a time-course fitting procedure and saved with SCAN software as *.scn files. Subsequently, the files were used to generate distributions of apparent shut and open times using EKDIST software for at least 10,000 events obtained from the idealization. However, for some of the mutated receptors (especially for the β_2 F31C mutant), cluster activity was sparse and the limit of minimum 10,000 events was difficult to achieve but the number of events (usually > 7700) was still sufficient for reliable

analysis. Distributions were fitted typically with four exponential components for shut times and with two for open periods (represented in figures; P% – relative areas, τ – time constants). In some cells a third minor exponential could be detected in the open times distribution but still two exponential fit could be reasonably made and, to enable comparisons, two exponential fit was made in all cases. Bursts were defined with critical time (t_{crit}) that was calculated with EKDIST software from the shut times distribution analysis according to the Clapham & Neher criterion [33], applied to the 3rd and 4th shut time components. For each recording, time resolution was identified which was within the range of 40–70 μ s for open and shut times. The same resolutions were then used in the kinetic modeling based on the single-channel data (stored in *.scn files) using HJCFIT software (from the DCprogs pack), which is based on the maximum likelihood method that enabled optimization of the rate constants. The model used for the simulation contained two open and two desensitized states (as in our recent study – Kiesel et al. [32]). The model was compared in terms of consistency with experimental data and, in case of WT, with our previous reports [9,11,32], at both experimental and 0 μ s resolutions and it was also expected to reproduce key changes between the same parameters in the experimental distributions between WT and the mutants

2.5. Double-mutant cycle analysis

Calculation of coupling constants using double-mutant cycle analysis [25] was performed on EC₅₀ and single channel-based kinetic model rates. The following equation was employed:

$$\Delta\Delta G(\text{parameter}, \text{mutant}) = RT \ln \left(\frac{\text{parameter}_{\text{mutant}}}{\text{parameter}_{\text{WT}}} \right)$$

where R is ideal gas constant (1.987 cal/mol), T is absolute temperature (296 K) and parameter is either EC₅₀ or kinetic model rate (δ_2 , γ_2 , α_2 , β_2 , α_2' , β_2' , d_2 , r_2 , d_2' and r_2'). To calculate the coupling energy the following equation was used:

The higher the deviation of coupling energy from 0 kcal/mol the more functionally dependent are investigated residues. We assumed the significance level of this interaction at ± 0.5 kcal/mol on the basis of previous research [5].

2.6. Data and statistical analysis

The data from the analyses and modeling was stored using Excel 2016 software (Microsoft, Redmont, WA, U.S.). The statistical analysis and data presentation was performed using SigmaPlot 11.0 software (Systat Software, San Jose, CA, U.S.). The analysis included an assessment of distribution normality with the Shapiro-Wilk test and outlier identification with the Grubb's test. For comparisons between the mutants and WT receptors, each time Student's t -test was used for each data set consisting of the results from one mutant versus WT (control). Alternatively, Mann-Whitney U test was used for the data that failed the normality or equal variance test. For the analysis of the effects of DTT application on the double mutant, a paired, two-sided t -test was used.

2.7. Sequence and structure analysis and modeling

Sequence alignment was performed using T-Coffe web server [34] and manually refined with Jalview [35]. Visualization of the sequence alignment was prepared in Jalview as well. All protein structures were downloaded from Protein Data Bank [36], for homology modeling respective structures were employed: 6I53, 6HUK, 6HUP, 6HUO, 6HUJ

and 6HUG [3,37]. On the basis of each template three types of models were created: wild type, double cysteine mutant (α_1 F14C β_2 F31C γ_2) and double cysteine mutant with forced disulfide bond. One hundred models of each type for each template were created. To build these models, MODELLER package [38] with in house Python scripts was used. Disulfide bond was introduced by DISU patch in MODELLER configuration. Model analysis was done in VMD [39] and in house Python scripts. To prepare model and structures visualization VMD was used as well.

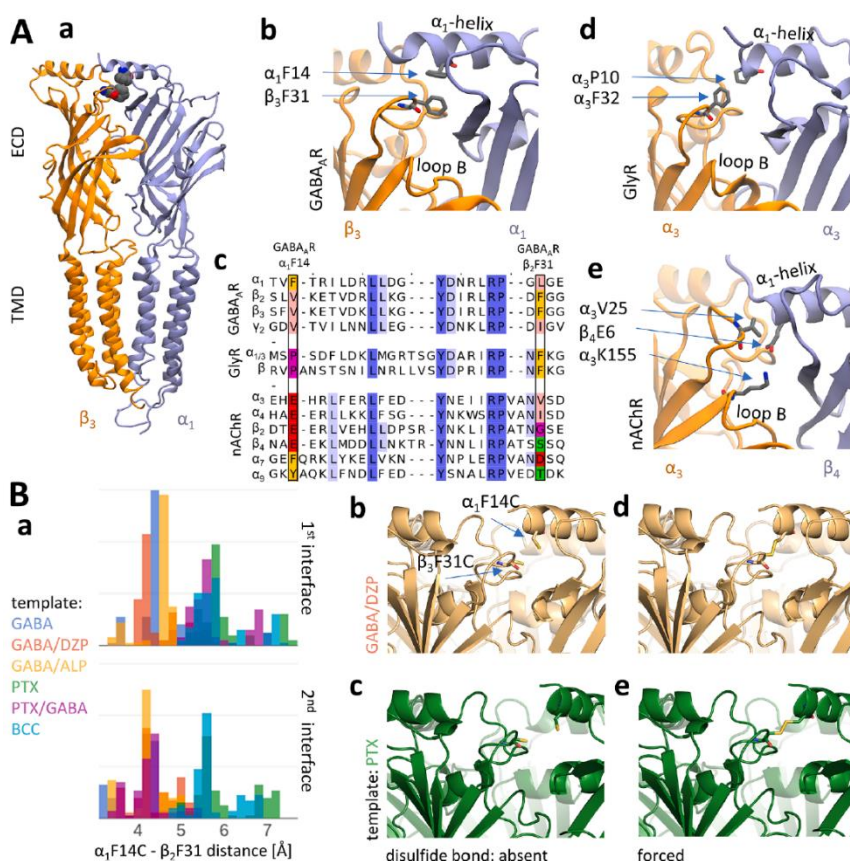
3. Results

3.1. Structural considerations of N-terminus ECD region subunit interface

Structure and sequence alignment of proteins that belong to the pLGIC family was performed to examine whether the interaction between α_1 F14 (α_1 F15 for human) and β_3 F31 identified by structural studies in $\alpha_1\beta_3\gamma_2$ GABA_AR [3] (Fig. 1A-a,b) is present in $\alpha_1\beta_2\gamma_2$ assembly (most commonly expressed in the mammalian CNS). In case of the GABA_AR subunits, this residue pair is preserved in α and β subunit interfaces, but only when β is the principal subunit. On the other hand, it is absent in each of the interfaces involving γ subunit (Fig. 1A-c). Thus, the phenylalanine interaction is present only at GABA binding site forming interfaces. In another prominent member of the pLGICs – GlyR, at position homologous to α_1 F14, proline is present whereas second phenylalanine is preserved. Interestingly, in case of homomeric GlyRs this Pro-Phe pair is predicted at each subunit interface (Fig. 1A-c,d). Addition of the β subunit to the receptor assembly would also probably preserve this structural arrangement (as proline and phenylalanine are present at respective positions). On the contrary, in nAChR (cationic

pLGIC) in subunits forming heteromeric assemblies ($\alpha_{3,4}$ and $\beta_{2,4}$) at position homologous to α_1 F14, glutamic acid residue is found (Fig. 1A-c). In addition, its charged group is oriented toward another charged residue (K155 in α_3) from the loop B region (Fig. 1A-e). In both GABA_AR and GlyR, the α_1 -helix is positioned more distantly from loop B than in nAChR, preventing this type of interaction. In nAChR subunits forming homomeric assemblies ($\alpha_{7,9}$), at position homologous to α_1 F14, residues with aromatic side chains are present, but not at β_3 F31 homologous position. This indicates that the putative interaction between phenylalanine residues in the top region of the ECD is expected to be specific for subunit cooperation in GABA_AR.

As residues α_1 F14 and β_3 F31 are located in close vicinity to each other in $\alpha_1\beta_3\gamma_2$ GABA_AR, homology modeling was employed to test, whether these residues are similarly positioned in $\alpha_1\beta_2\gamma_2$ GABA_AR and to check, if after double cysteine mutation (α_1 F14C β_2 F31C γ_2), formation of the disulfide bond between them is possible. If so, WT and the double cysteine mutant would be expected to bear some functional similarities observable using electrophysiological tools (assuming at least partial functional substitution of the phenyl ring interaction by the disulfide bridge) in contrast to single (α_1 F14C $\beta_2\gamma_2$ or α_2 F31C γ_2) mutants. This would confirm that these phenylalanine residues are crucial for intersubunit cooperation involved in receptor functioning. Homology models were created using various structural templates – with GABA molecule bound (referred as GABA template), GABA and diazepam (GABA/DZP), GABA and alprazolam (GABA/ALP), picrotoxin (PTX), picrotoxin and GABA (PTX/GABA) and bicuculline (BCC) [3,37]. On the basis of each template, two variants of α_1 F14C β_2 F31C γ_2 models were created: one with the disulfide bond forced between introduced cysteines and one without this constrain. Interestingly, in models without forced bond, two clusters of models emerged: first, with distance between cysteine residues of ~4 Å and



second one with distance longer than ~ 5 Å (Fig. 1B-a). Models based on templates with bound GABA or GABA and positive modulator were found in the first group (example in Fig. 1B-b), whereas the ones based on templates with channel blocker or antagonist were in the second one (example in Fig. 1B-c). Models based on GABA/PTX template showed mixed behavior – at first β_2/α_1 interface cysteine residues were located distantly, whereas at the second interface they were as close as in agonist/modulator type models. However, after forcing the disulfide bond, the distance between the cysteines was reduced to ~ 2 Å in each model variant (example in Fig. 1B-d,e). This indicates, that formation of the disulfide bond between introduced cysteine residues is possible in GABA_AR at each functional state, but would be more probable in agonist/modulator bound state and could possibly exert a stabilizing effect on the active conformation.

As modeling studies indicated a possibility of forming the disulfide bond in case of the double mutant, in the next step electrophysiological recordings from WT and single and double cysteine mutants of $\alpha_1\beta_2\gamma_2$ GABA_AR were performed to verify these hypotheses.

3.2. Impact of mutations on macroscopic current responses

The impact of the investigated mutations on receptor functioning was first assessed for agonist potency by determining the dose–response relationships (Fig. 2A). In both cases of the $\alpha_1\beta_2\gamma_2$ (F14C) and

$\alpha\beta_2\gamma_2$ (F31C) single mutants, it was rightward shifted when compared to WT [29]. However, surprisingly, EC₅₀ for the double mutant $\alpha_1\beta_2\gamma_2$ (F14CF31C) was almost identical to that for WT (Fig. 2A, inset). These data show that both of the mutations reduce the agonist potency but in the case of the double mutant a reversal of this effect is taking place. The rightward shift of the dose–response relationships could suggest a reduction in affinity but it needs to be considered that such effect could be also due to alterations in the gating properties [28,40]. Thus, to get an insight into the impact of the considered mutations on receptor gating, we analyzed the kinetics of current responses elicited by saturating GABA for the mutant and WT (Fig. 2B-a). Interestingly, each of the single mutations increased rise time (RT) of currents evoked by saturating GABA (for WT: 0.45 ± 0.04 ms, $n = 7$, for F14C: 3.97 ± 1.04 ms, $n = 6$, $p = 0.001$; for F31C: 1.50 ± 0.08 ms, $n = 4$, $p = 0.001$). However, for the double mutant F14CF31C, the slow down of current onset was still significant with respect to WT (0.85 ± 0.09 ms, $n = 4$, $p = 0.001$; Fig. 2B-b; C) but this difference was markedly smaller than in the case of each of the single mutations (Fig. 2B-b; C).

Upon prolonged saturating GABA application, current traces exhibited fading that reflected the macroscopic desensitization. As shown in Fig. 2B-a, currents mediated by WT receptors showed the largest both rate and extent of desensitization. As explained in Methods,

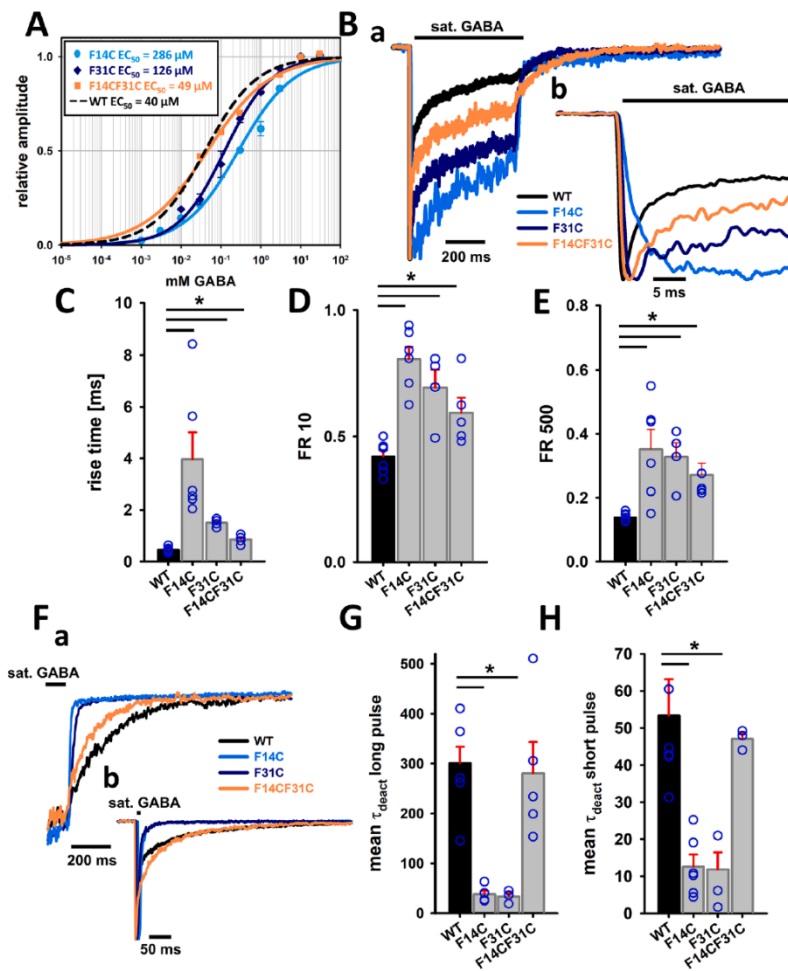


Fig. 2. Macroscopic current responses mediated by GABA_ARs are strongly affected by the F14C and F31C mutations but the impact of the double mutation is weak. A. Dose–response relationships determined for all of the considered mutants after normalization to maximum current amplitudes elicited by saturating GABA and fitted with the Hill equation. Black dashed line represents the dose–response relationship determined by Brodzki et al. [29] as the standard reference for WT. EC₅₀ values are presented in the inset. Hill coefficient for WT: $n_h = 0.67$, for F14C: $n_h = 0.63$, for F31C: $n_h = 0.74$ and for F14CF31C: $n_h = 0.55$. B. (a) Examples of typical normalized traces for WT (black) and the mutants: F14C (blue), F31C (navy) and F14CF31C (orange) evoked by a 500 ms of saturating GABA pulse. Note profoundly different extent of desensitization and the deactivation rates. Thick black line above the traces represents the agonist application (b) Typical normalized traces close to the current peak for WT (black) and the F14C (blue), F31C (navy), and F14CF31C (orange) mutants elicited by a long saturating agonist pulse. Note the differences in the duration of the current onset and reduced extent of desensitization after 10 ms for the mutants. C. Statistics for mean values of rise time for WT and the mutants. D. Statistics for mean FR 10 values. E. Statistics for mean FR 500 values. The FR 10 and FR 500 parameters describe the percentage of current remaining after 10 (D) and 500 ms (E), respectively during prolonged (500 ms) GABA application. F. Examples of typical normalized traces that show distinct deactivation kinetics for WT (black), the F14C (blue), F31C (navy), and F14CF31C (orange) mutants. (a) Deactivation after a long (500 ms) pulse and (b) after a short (2–10 ms) pulse of saturating GABA. G. Statistics for deactivation kinetics (mean τ_{deact} ; a deactivation time constant) for currents which were evoked by a long pulse and H. statistics for mean τ_{deact} after a short pulse. Statistically significant difference between each mutant compared with WT are indicated with asterisks.

fading for the mutants was so slow that it could not be reliably fitted with exponential functions and for this reason the FR 10 parameter was used (percentage of amplitude 10 ms after the peak). Accordingly, the FR 10 parameter was the smallest for WT (FR 10: 0.42 ± 0.02 , $n = 7$) and for the single mutations, markedly larger FR 10 values were determined (for F14C: 0.81 ± 0.05 , $n = 6$, $p < 0.001$ and for F31C: 0.69 ± 0.07 , $n = 4$, $p = 0.001$; Fig. 2B-b; D). Again, for the double mutant, a trend of reversal of the effect toward WT phenotype was observed (FR 10 for F14CF31C: 0.059 ± 0.06 , $n = 5$, $p = 0.012$; Fig. 2B-b; D). Similar tendency was observed for FR 500 (for WT: 0.14 ± 0.01 , $n = 7$; for F14C: 0.35 ± 0.06 , $n = 6$, $p = 0.014$; for F31C: 0.33 ± 0.04 , $n = 4$, $p = 0.006$; for F14CF31C: 0.27 ± 0.04 , $n = 4$, $p = 0.003$, Fig. 2E). Deactivation, which reflects current relaxation after the agonist removal, described by the mean time constant (τ_{deact}), was highly accelerated for the F14C and F31C mutants but not for the F14CF31C double mutant when compared to WT (for long GABA pulses, Fig. 2F-a, mean τ_{deact} for WT: 301 ± 32.54 ms, $n = 7$; for F14C: 38.21 ± 6.85 ms, $n = 5$, $p < 0.001$; for F31C: 33.61 ± 7.81 ms, $n = 3$, $p < 0.001$, for F14CF31C: 208.44 ± 62.63 ms, $n = 5$, $p > 0.05$; for short GABA application, Fig. 2F-b, mean τ_{deact} for WT: 53 ± 9.83 ms, $n = 6$; for F14C: 12.58 ± 3.3 ms, $n = 6$, $p = 0.002$; for F31C: 11.84 ± 4.61 ms, $n = 3$, $p = 0.024$, for F14CF31C: 47.08 ± 1.57 ms, $n = 3$, $p > 0.05$; Fig. 2F-a,b; G and H). Taking altogether, this analysis revealed that each of the F14C and F31C mutations strongly affected receptor gating but when both mutations are concomitantly present, a clear reversal toward WT phenotype is observed.

3.3. Disruption of the disulfide bond with DTT in the F14CF31C mutant alters current time course

To test the role of the putative disulfide bond between cysteine residues which substituted the phenylalanine residues in the double mutant F14CF31C, DTT effect on the current kinetics elicited by saturating GABA (Fig. 3A-a) was assessed. The administration of DTT on excised patches in pre-treatment protocol (see Methods) resulted in a significant

increase in the amplitude of currents mediated by the doubly mutated receptors (relative mean amplitude for GABA + DTT vs. GABA: 1.18 ± 0.03 , $n = 4$, $p = 0.015$, Fig. 3A-b; B). This effect was not observed in analogous experiments on WT receptors (relative mean amplitude for GABA + DTT vs. GABA: 0.91 ± 0.07 , $n = 4$, $p = 0.175$, Fig. 3B). Rise time and desensitization (rate and extent) were not affected by DTT either in the case of the F14CF31C or in WT receptors (data not shown). However, DTT caused a significant acceleration of deactivation for currents mediated by the F14CF31C mutants (relative mean τ_{deact} for GABA + DTT vs. GABA for long pulse: 0.66 ± 0.09 , $n = 4$, $p = 0.036$ and for short pulse: 0.48 ± 0.06 , $n = 4$, $p = 0.048$; Fig. 3C-a,b; D; E). Again, this effect was absent in the case of control experiments on WT receptors (relative mean τ_{deact} for GABA + DTT vs. GABA in long pulse: 0.97 ± 0.12 , $n = 4$, $p = 0.667$ and short pulse: 0.96 ± 0.02 , $n = 3$, $p = 0.117$; Fig. 3D; E), indicating that the effects of DTT were specific only to the F14CF31C double mutant. Thus, the disruption of the disulfide bond in F14CF31C led to a phenotype that, in terms of deactivation kinetics, seemed closer to the single mutation in which a significant acceleration of deactivation was observed (Fig. 2F, G, H).

3.4. Kinetic modeling of mutated receptors macroscopic responses

As an attempt to provide a mechanistic interpretation of the effects that were observed in macroscopic experiments, a modeling based on trend analysis (see Methods) was performed. Using the kinetic scheme, recently proposed by our group [11] (Fig. 4A), we were able to fairly reproduce the dose-response relationships and the time course of current responses to saturating GABA for WT receptors and the considered mutants (Fig. 4B). The general strategy was to reproduce mutation-related alterations in kinetics of current responses and in the dose-response relationships (Fig. 2A, 4C-a,b,c) by making minimum variations in the rate constants. Since the largest kinetic changes were observed for the F14C mutant, we started with the fit for these receptors. In order to reproduce a particularly large reduction of macroscopic

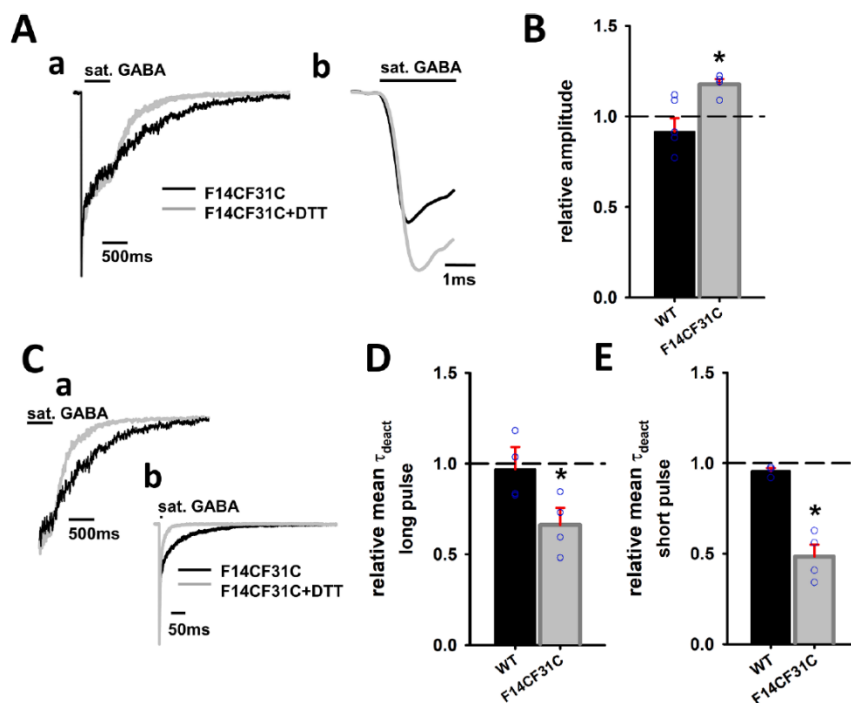


Fig. 3. DTT alters the time course of currents elicited by saturating GABA for F14CF31C but not for WT. A. Typical currents mediated by the F14CF31C double mutant and evoked by saturating GABA (black line) and by the agonist applied in the presence of 1 mM DTT (grey line) (a) Normalized current traces for long (500 ms) agonist application. Note a clear DTT effect on the deactivation phase. (b) Typical current trace elicited by a short GABA pulse. Note that in both conditions (a and b) DTT strongly accelerated deactivation time course. D-E. Statistics for mean relative τ_{deact} for WT and the F14CF31C mutant after long and short pulses. Statistically significant relative differences between GABA + DTT vs. GABA are indicated with asterisks.

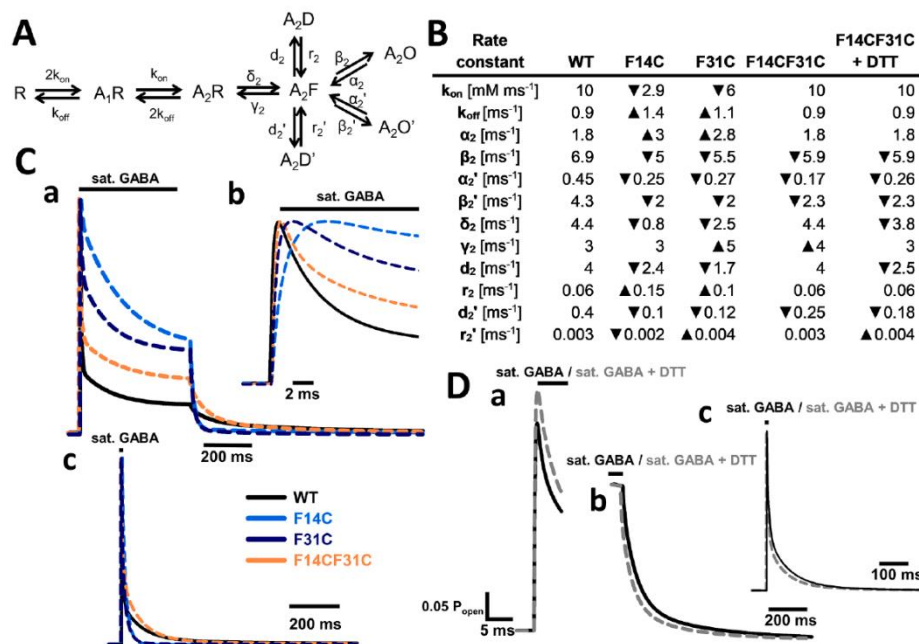


Fig. 4. Kinetic scheme modeling of macroscopic current responses reveals an impact of the F14C and F31C mutations on GABA_AR binding and gating. **A.** A scheme of the kinetic model (“flipped Jones-Westbrook model”) from Brodzki et al. [11] with two open and two desensitized states. R – unbound state; A₁R – singly bound state; A₂R – doubly bound state; A₂F – flipped state (preactivation); A₂O and A₂O’ – open states; A₂D and A₂D’ – desensitized states. **B.** Rate constants for WT [11] and for the considered mutants. Note that only in the case of the F14C and F31C mutants, changes in binding and unbinding rates (k_{on} and k_{off}) were found. The effect of DTT on F14CF31C was also considered (last column). **C.** Simulated traces for WT (black), the F14C (blue), F31C (navy) and F14CF31C (orange) mutants. **(a)** Superimposed and normalized simulated traces of responses to a long pulse of saturating GABA. Thick black line above the trace represents the agonist application. **(b)** Same as in **(a)** in the expanded time scale to visualize differences in rise time for the respective mutants. **(c)** Superimposed and normalized simulated traces of responses to a short pulse of saturating GABA that reproduce large differences between WT and the mutants in deactivation kinetics. **D.** Simulated traces for F14CF31C upon saturating GABA application (black) and co-application with 1 mM DTT (grey). **(a)** Simulated increase of current amplitude in the presence of DTT, resulting mainly from the reduction of the desensitization rates d_2 and d_2' . **(b–c)** Acceleration of deactivation kinetics in both long **(b)** and short **(c)** pulses of simulated traces in the presence of DTT application. (For interpretation of the references to colour in this figure legend, the reader is referred to the web version of this article.)

desensitization and marked slow down of rise time (Fig. 4C-a,b), the desensitization rates d_2 and d_2' were reduced but this modification turned out to be insufficient to simulate a slow, one-exponential desensitization time course observed for this mutant. A concomitant large reductions in the onset and desensitization rates clearly required additionally a reduction of the flipping rate δ_2 . However, these modifications together led to acceleration of deactivation kinetics beyond what observed experimentally, but it could be corrected by a reduction of the closing rate α_2' (Fig. 4C-a,c). Additional improvement in reproducing the kinetics of macroscopic currents, mainly the relationship between the current peak and the amplitude after 500 ms (FR 500), was achieved by reducing the opening rates β_2 and β_2' (Fig. 4B). These modifications of the rate constants controlling gating together with a decrease in affinity (reduced k_{on} and increased k_{off}) allowed to reproduce the rightward shift of the dose–response curve. Qualitatively, reproduction of kinetic behavior of the F31C mutant required modifications of the same rate constants (although quantitatively smaller) with the exception that, for this mutant, additionally the unflipping rate γ_2 had to be increased (Fig. 4B). There was yet another scenario in which deactivation (Fig. 4C-a,c) was correctly reproduced along with a large reduction of macroscopic desensitization, which was a strong decrease of the unbinding rate k_{off} . This option, however, led to a major leftward shift of the dose–response relationships for the mutants and was dismissed.

As expected, in the case of the double F14CF31C mutant, some gating rate constants were altered to a smaller extent than in the single mutants (Fig. 4B). However, some of the rates which were changed in the single

mutants, did not show any alteration with respect to WT receptors in the double mutant (Fig. 4B). Indeed, in F14CF31C, flipping δ_2 , closing α_2 , desensitization d_2 and binding/unbinding k_{on}/k_{off} were unaltered with respect to WT (Fig. 4B). We also sought for interpretation of the results of the disulfide bond disruption in the double mutant by application of DTT (Fig. 3). A decrease of the desensitization rates d_2 and d_2' as well as a slight reduction of δ_2 were sufficient to fairly reproduce the effects of DTT treatment: an increase of current amplitude and acceleration of deactivation phase with respect to the double mutant (Fig. 4D-a,b,c). As emphasized in previous studies [28,41–43], in conditions of agonist saturation, in the bifurcated (Jones and Westbrook-like) models, a reduced entry to desensitized state(s) increases the occupancy of the open states (resulting in increased current amplitude). Taking altogether, these model simulations demonstrate that both the F14C and F31C mutations strongly affect both binding and gating of $\alpha_1\beta_2\gamma_2$ receptors. Moreover, the double cysteine mutation of these residues alleviates this impact most likely because the disulfide bonds between cysteine residues are able to mimic, at least partially, the interaction between phenylalanine residues in WT receptors.

3.5. The analysis and model simulations of single-channel activity

To further address the question of specific role of F14C, F31C and their interaction in GABA_AR gating, we performed a detailed analysis of single-channel activity that was recorded for each single mutant and the double mutant at saturating GABA concentration (10 mM). The activity

of the mutants took the form of clusters, however, different activity modes were present and the predominant one (Fig. 5A) was selected for the analysis (see Methods). The mutants significantly varied in terms of the burst activity within the clusters which is reflected by the differences in P_{open} for bursts (P_{open} for WT: 0.70 ± 0.03 , $n = 6$; P_{open} for F14C: 0.32 ± 0.06 , $n = 6$, $p < 0.001$; P_{open} for F31C: 0.28 ± 0.03 , $n = 4$, $p = 0.001$; P_{open} for F14CF31C: 0.59 ± 0.02 , $n = 4$, $p = 0.021$; Fig. 5B). The burst were also significantly shorter for F14C when compared to WT (burst length for WT: 139.93 ± 22.04 ms, $n = 6$; for F14C: 19.89 ± 5.07 ms, $n = 6$, $p = 0.003$) but for F31C (158.11 ± 61.84 ms, $n = 4$) and for F14CF31C: (140.45 ± 50.4 , $n = 4$; Fig. 5C) no significant difference ($p > 0.05$) with respect to WT was observed. The distributions of open and shut times for the mutants clearly differed from WT but the largest differences were observed for the single mutants (F14C and F31C, Fig. 5D, Table 1). All of the percentages of the four shut time components were significantly altered and there was a general trend of a marked slow down of these components (Table 1). The weighted averages of shut and open times were also significantly different from WT, as τ_{mean} for shut times indicated that closing was longer but the mean open

time was significantly shorter for the F14C and F31C mutants. Interestingly, shut time τ_{mean} for F31C was nearly twofold shorter than for F14C while the opposite relation was revealed for the mean open times for these mutants. These observations indicate thus a trend of gradualness of the mutation effect on the single-channel kinetics (Table 1).

The F14CF31C double mutation strongly affected the percentage of the first ($P_1\%$) and third ($P_3\%$) shut time component and only τ_2 time constant was significantly changed when compared to WT. The shut time τ_{mean} was still significantly increased but no difference in mean open time was observed (Table 1), which altogether, again indicated a non-additive effect of the two mutations on receptor activity.

Single-channel data was then used to perform a kinetic modeling and simulations. The framework adapted for the simulations was the model from Kisiel et al. [32] with two open and two desensitized states (Fig. 6A). A set of mean kinetic rate constants for transitions between the states was obtained from the simulations (Fig. 6B). Simulations of distributions of shut and open times generated from the model for WT and each considered mutant were also used to validate the results of modeling (Fig. 6C). The comparisons between the mutants vs. WT

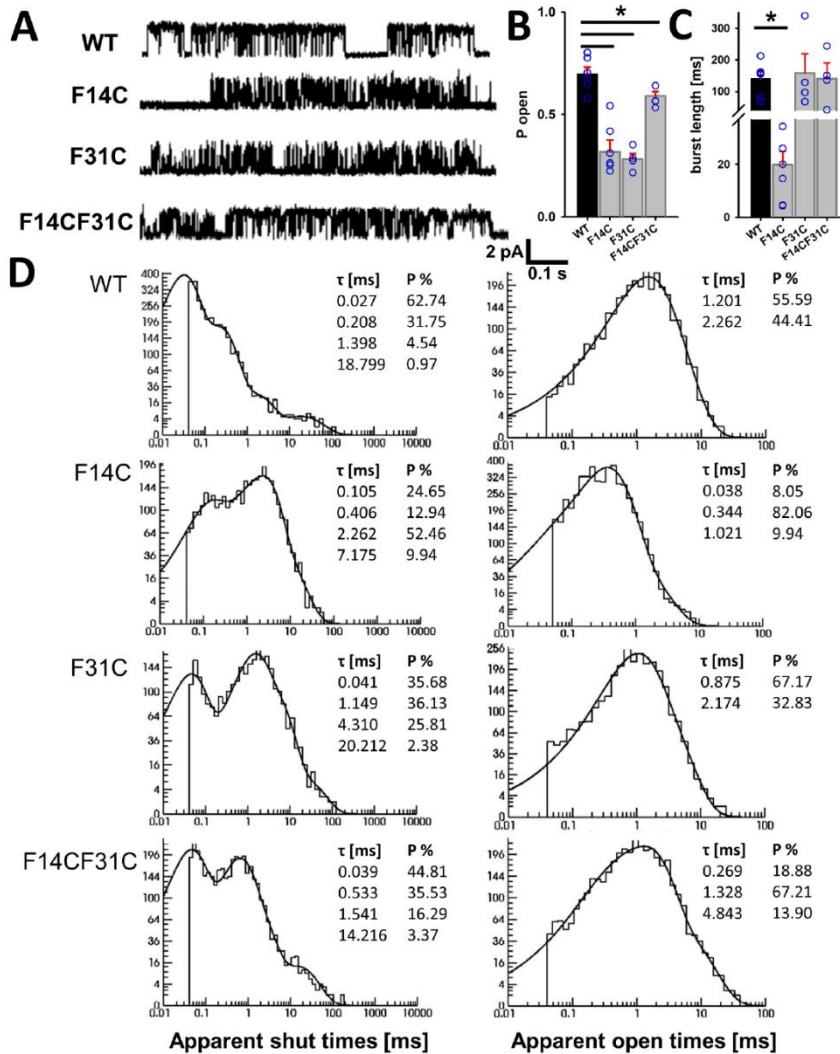


Fig. 5. at F14 and F31 affect single-channel kinetics. A. Examples of typical clusters of single-channel activity (the predominant mode) for WT, the F14C, F31C and F14CF31C mutants. B. Statistics for mean open probability (P_{open}) that were calculated for bursts. C. Statistics for mean burst length. D. Examples of typical distributions of apparent shut and open times for WT and each considered mutant. The distributions were fitted with probability density functions at 0 μ s resolution and the respective parameters (time constant and percentage of each component) are presented in the insets. For statistics see Table 1. The asterisks indicate statistically significant difference between the mutant and WT.

Table 1

Values of shut times and mean open time parameters for WT and the mutants, determined from dwell time distributions, τ – time constant, P% – percentage for each component: without brackets – experimental parameters; normal brackets – simulated with experimental resolution; square brackets – simulated with 0 μ s resolution. Parameters for the mutants that significantly differed from WT are highlighted in **bold** with an asterisk (*) and the corresponding *p* value.

Shut times:	τ_1 [ms]	P ₁ %	τ_2 [ms]	P ₂ %	τ_3 [ms]	P ₃ %	τ_4 [ms]	P ₄ %	Shut time τ_{mean} [ms]	Mean open time [ms]
WT	0.04 ± 0.003 (0.06 ± 0.01) [0.06 ± 0.01]	0.59 ± 0.03 (0.48 ± 0.03) [0.52 ± 0.03]	0.26 ± 0.02 (0.33 ± 0.02) [0.32 ± 0.03]	0.31 ± 0.02 (0.35 ± 0.02) [0.33 ± 0.03]	1.56 ± 0.08 (1.71 ± 0.14) [1.69 ± 0.16]	0.09 ± 0.02 (0.15 ± 0.02) [0.14 ± 0.02]	21.72 ± 1.91 (21.26 ± 2.33) [21.25 ± 2.86]	0.01 ± 0.002 (0.01 ± 0.001) [0.01 ± 0.001]	0.40 ± 0.06 (0.59 ± 0.06) [0.52 ± 0.05]	1.87 ± 0.34 (1.25 ± 0.14) [0.78 ± 0.07]
F14C	0.08 ± 0.02* P = 0.002	0.26 ± 0.05* P < 0.001	0.90 ± 0.04* P = 0.002	0.19 ± 0.04* P = 0.007	4.73 ± 1.02* P = 0.002	0.41 ± 0.08* P = 0.002	15.56 ± 3.66 (17.48 ± 3.81) [17.20 ± 3.81]	0.14 ± 0.04* P = 0.004	3.86 ± 0.81* P = 0.002 (4.33 ± 0.89)	0.41 ± 0.1* P = 0.002 (0.50 ± 0.11)
F31C	0.05 ± 0.01 (0.06 ± 0.01) [0.06 ± 0.01]	0.25 ± 0.04* P < 0.001	1.04 ± 0.18* P = 0.001	0.43 ± 0.05* P = 0.048	4.23 ± 0.63* P = 0.01	0.30 ± 0.03* P < 0.001	23.77 ± 3.19 (24.24 ± 3.35) [24.21 ± 3.36]	0.02 ± 0.01* P = 0.036	2.10 ± 0.18* P < 0.001 (2.18 ± 0.22)	0.89 ± 0.14* P = 0.01 (0.83 ± 0.11)
F14CF31C	0.04 ± 0.003 (0.05 ± 0.01) [0.05 ± 0.01]	0.40 ± 0.08* P = 0.036	0.59 ± 0.03* P < 0.001	0.41 ± 0.05 (0.43 ± 0.06) [0.42 ± 0.06]	1.99 ± 0.3 (2.01 ± 0.3) [1.98 ± 0.3]	0.17 ± 0.03* P = 0.02	19.81 ± 1.95 (17.07 ± 1.79) [17.05 ± 1.79]	0.02 ± 0.01 (0.02 ± 0.01) [0.02 ± 0.01]	0.85 ± 0.07* P = 0.01 (0.90 ± 0.07)	1.59 ± 0.2 (1.04 ± 0.11) [0.77 ± 0.03]

revealed that both closing α_2 and α_2' rates were significantly increased and the opening rate β_2 was markedly decreased for the F14C mutant. Preactivation step was significantly affected but only the flipping rate δ_2 was altered (decreased). Additionally, the F14C mutation caused an increase of desensitization d_2 and d_2' rates (Fig. 6B). The kinetic modeling for the F31C mutant also revealed significant changes in the rate constants with respect to WT. Namely, opening and closing rates (β_2 and α_2) were decreased and increased, respectively. Moreover, flipping transition δ_2 decreased and unflipping γ_2 increased while the resensitization rate r_2 increased with no changes in d_2 and d_2' (Fig. 6B). However, most interestingly, in the case of the F14CF31C mutant, most of the kinetic rate constants remained unaffected with respect to WT, except for the closing α_2 and unflipping γ_2 rates (Fig. 6B), confirming the experimental observations (both macroscopic and single-channel) that the double mutation affects receptor gating to a smaller extent than the single ones. Moreover, these qualitatively and quantitatively different impacts of single and double mutations further indicate the lack of additivity of effects induced by single mutations. This issue was pursued using double-mutant cycle analysis (Methods, Fig. 6B). Interestingly, a particularly strong coupling $\Delta\Delta G$ (−1.70 kcal/mol) calculated for EC₅₀ values was found, which can be ascribed to a strong interaction between F14 and F31 in the binding step. In addition, a significant coupling above ± 0.5 kcal/mol was found for all opening and closing rates, desensitization d_2 and r_2 and the flipping δ_2 rates (Fig. 6B) revealing strong interaction between F14 and F31 also in the gating transitions.

4. Discussion

In the present study we demonstrate that two phenylalanine residues α_1 F14 and β_2 F31 mediate particularly effective intersubunit interaction which shapes both binding and gating of GABA_AR. The strong impact of the residues mutations to cysteine on receptor gating is intriguing as both of these residues are located very distantly from the channel gate (−75 Å) which operates at the channel pore i.e. markedly farther than from the binding site to the channel gate (−50 Å). The following evidence argues for the notion that the key mechanism underlying our

observations is related to the intersubunit interaction between the two phenylalanine residues. Whereas single cysteine mutations of α_1 F14 or β_2 F31 cause dramatic changes in the channel binding and gating, the double mutation results in a reversal of these effects toward WT phenotype. This observation indicates that the disulfide bridge between the two cysteine residues is able to mimic, at least at a good qualitative level, the interactions between α_1 F14 and β_2 F31 in WT receptor. This view is further supported by the observation that disruption of the disulfide bridges with DTT partially restores the single mutant phenotype, confirming that indeed, the bonds between the cysteines are in play in the case of the double mutant. Our structural analyses provided further indications that formation of the disulfide bridges in the double mutant is indeed possible, especially in the case of GABA-activated receptor. Moreover, a marked functional interdependence between α_1 F14 or β_2 F31 residues is further demonstrated by the double-mutant cycle analysis which was carried out for both EC₅₀ and for the gating rate constants (see Methods). Notably, this analysis provided evidence that both binding and also several aspects of gating (opening/closing, desensitization and flipping) are dependent on interaction between these two residues, suggesting a global effect on the channel macromolecule. It is interesting to note that our data suggest that formation of intersubunit bond between the two phenylalanine residues is more efficient in shaping the functional properties of the receptor than local structural changes related to substitution of Phe by Cys. Indeed, mimicking the bond between α_1 F14 or β_2 F31 by the disulfide bridge (in double mutant) reverses most of the kinetic alterations observed in single mutants in spite of the fact that substitution of Phe by Cys substantially alters local macromolecule structure. These alterations are mainly due to the lack of attractive interaction between Phe and Cys, which prevents subunit interface tightening. Thus, in this particular case, the impact of intersubunit interactions appears to be by far superior than that resulting from local structural changes within the subunits due to residue substitutions.

Considering also other examples of intersubunit interaction for GABA_ARs and other Cys-loop receptors [21–24], the picture emerges that intersubunit interactions are associated with long range

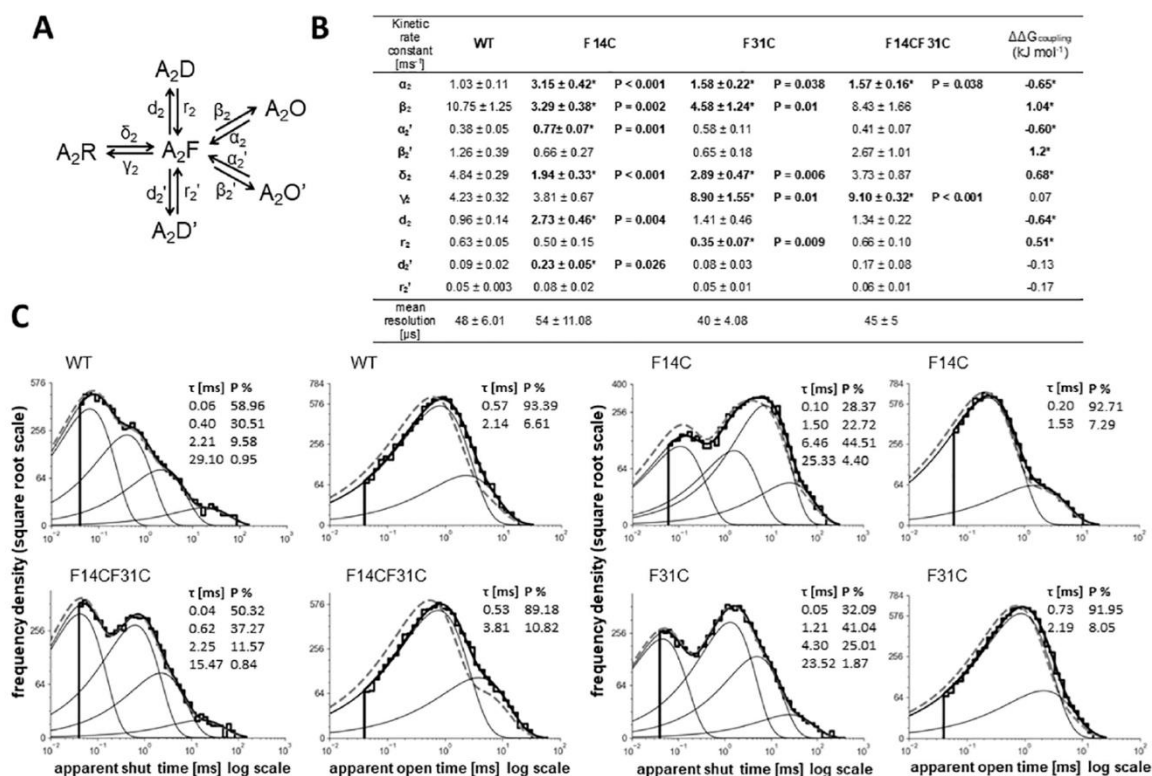


Fig. 6. Single-channel modeling reveals the impact of the mutation on distinct gating transitions. Double-mutant cycle analysis confirms coupling between F14 and F31. A. Scheme of the kinetic model from Kisiel et al. [32] used for the modeling and simulations of the cluster activity; A_2R – doubly bound receptor; A_2F – flipped state; A_2O and A_2O' – open states; A_2D and A_2D' – desensitized states. B. Mean values of the kinetic rate constants determined from 6 patches (WT, F14C) and 4 patches (F31C, F14CF31C), describing the impact of the mutation on the specific gating transitions. Significant changes in the rate constants relative to WT are marked in bold with an asterisk (*) and the corresponding p value is disclosed. The last column refers to the coupling energy $\Delta\Delta G$ calculated for the rate constants in the double-mutant cycle analysis. Change in the $\Delta\Delta G$ indicating a significant coupling between the two residues ($\Delta\Delta G > 0.5$ kcal/mol) is also marked in bold and with an asterisk (*). C. Examples of simulated frequency density functions of apparent shut and open times for cluster activity of WT and the mutants (insets present time constants and percentages of the components). Solid gray thin lines outline exponential components in the dwell time distributions for apparent shut and open times. Gray thick dashed lines show distributions obtained when applying the corrections for missed events.

interactions within the channel macromolecule giving rise, typically, to a multifaceted effects on the channel functioning, comprising effects on binding and various aspects of gating. However, it needs to be stressed that also mutations within single subunit bearing none or weak interactions with residues within other subunits might also have a long range impact. Indeed, our recent studies revealed that mutations located at or in the close vicinity of the binding site, may also have a diversified impact on receptor gating in spite of a long distance between the binding site and the channel gate [9–11,41]. It seems thus that the mechanical signal spreading from the binding sites runs essentially in two major directions: vertical (“top-down”) and the lateral one and both of them are involved in shaping several different aspects of receptor functioning rather than some singular gating features.

In order to make the information on changes in the rate constants caused by the considered mutations as precise as possible, we based our analysis on both macroscopic and single-channel experiments (Figs. 4 and 6). Importantly, the two approaches yielded a number of converging predictions: 1) the single mutations resulted in a very consistent decrease in the flipping rate δ_2 but this effect was absent in the double mutant; 2) the unflipping rate γ_2 was significantly increased in the case of the F31C mutant but not for F14C; 3) in addition to flipping, the analyses revealed major impact of mutations on opening/closing transitions although this effect showed some differences in transitions into

two different open states. The opening rate β_2 was consistently decreased.

Although, these results of macroscopic and single-channel modeling are in general agreement, there are also some differences which require a comment: 1) in the case of the second open state, macroscopic and single-channel analyses indicated a decrease in β_2' but α_2' was predicted to be increased in the single-channel analysis whereas the macroscopic investigation indicated a decrease in the value of this rate constant. The reason for this discrepancy related to the closing rate α_2' is not clear. It appears more intuitive that effective weakening of receptor efficacy (decreased access to the open state A_2O') is achieved by a decrease in the opening and an increase in the closing rate, as predicted by the single-channel analysis. We may speculate that in the macroscopic analysis the estimation of the α_2' parameter might have been affected by a profound desensitization (see also below) consisting of several components and the rate constant for one of them could be comparable to the closing rate α_2' 2) another discrepancy between macroscopic and single-channel analysis is related to the estimation of mutants' impact on rate constants describing desensitization. The macroscopic analysis indicated a substantial decrease in the desensitization rates, compatible with markedly reduced fading of currents mediated by the mutants but the opposite was found in the single-channel analysis. It needs to be stressed, however, that macroscopic and single-channel recordings were performed in

different conditions: steady-state vs. non-equilibrium at which receptor functioning is likely to be shaped by distinct sets of conformational transitions. In the agonist “jumps” experiments, vast majority of receptors desensitize within a few milliseconds but slower components were also reported: ~100 ms [43–45] and in the range of seconds [44,46]. It is thus possible that in our single-channel recordings we observe only a remnant of desensitization, revealed as two low percentage components in the shut times distributions. Importantly, a similar observation regarding distinct estimations of desensitization rates in macroscopic and single-channel recordings was made in our recent study concerning the impact of α_1 F64 residue mutation [42] and an analogous interpretation of this apparent discrepancy was proposed.

It is noteworthy that the double-mutant cycle analysis indicated most consistently the coupling between α_1 F14 and β_2 F31 for flipping and opening rate constants, further indicating that the interaction between these residues plays the major role upon receptor activation. The reason for which the transitions in the opposite direction (unflipping and closing) are associated with weaker coupling is unknown and will require more insight into the molecular scenarios of conformational transitions of GABA_ARs.

The issue of intersubunit interactions seems particularly interesting in the context of different physiological roles and pharmacological properties of GABA_ARs assembled from different subunit types [47,48]. For instance, administration of benzodiazepines selectively affecting GABA_ARs that contain different α subunits may give rise to different effects such as sedation, anxiolysis, amnesia etc. [49–51]. It seems thus that a further progress in understanding the impact of intersubunit interactions on GABA_ARs properties is likely to indicate new avenues in designing modulatory drugs of clinical relevance. Interestingly, in the GlyRs, analogous residues F32 and P10 are a part of the allosteric binding site of a new class of pharmacological analgesic potentiators recently reported by Huang et al. [52]. This finding thus encourages the studies of the impact of the considered α_1 F14 and β_2 F31 mutations in the context of pharmacological modulation of GABA_ARs.

In conclusion, we provide evidence for a novel intersubunit interaction in GABA_ARs which occurs in the periphery of the N-terminal region in the ECD. This intersubunit cross-talk appears to result in particularly long-distance transduction of the activation signal, capable to affect binding and majority of gating steps of the receptor.

CRedit authorship contribution statement

Katarzyna Terejko: Investigation, Methodology, Formal analysis, Data curation, Visualization, Writing - original draft. **Michał A. Michałowski:** Investigation, Formal analysis, Software, Visualization, Writing - original draft. **Anna Dominik:** Investigation. **Anna Andrzejczak:** Investigation. **Jerzy W. Mozrzymas:** Conceptualization, Funding acquisition, Methodology, Project administration, Resources, Supervision, Validation, Writing - original draft, Writing - review & editing.

Acknowledgement

Research carried out in the frame of this project was supported by Polish National Science Centre grant MAESTRO DEC 2015/18/A/NZ1/00395.

Declarations of interest

The authors declare no conflict of interest.

References

- [1] W. Sieghart, M.M. Savić, E.H. Ohlstein, International union of basic and clinical pharmacology. CVI: GABA A receptor subtype- and function-selective ligands: key issues in translation to humans, *Pharmacol. Rev.* 70 (4) (2018) 836–878, <https://doi.org/10.1124/pr.117.014449>.
- [2] R.M. McKernan, P.J. Whiting, Which GABA_A-receptor subtypes really occur in the brain? *Trends Neurosci.* 19 (4) (1996) 139–143, [https://doi.org/10.1016/S0166-2236\(96\)80023-3](https://doi.org/10.1016/S0166-2236(96)80023-3).
- [3] S. Masiulis, R. Desai, T. Uchański, I. Serna Martin, D. Laverty, D. Karia, T. Malinauskas, J. Zivanov, E. Pardon, A. Kotecha, J. Steyaert, K.W. Miller, A. R. Aricescu, GABA_A receptor signalling mechanisms revealed by structural pharmacology, *Nature* 565 (7740) (2019) 454–459, <https://doi.org/10.1038/s41586-018-0832-5>.
- [4] J.J. Kim, A. Gharpure, J. Teng, Y. Zhuang, R.J. Howard, S. Zhu, C.M. Novello, R. M. Walsh Jr, E. Lindahl, R.E. Hibbs, Shared structural mechanisms of general anaesthetics and benzodiazepines, *Nature* 585 (7824) (2020) 303–308, <https://doi.org/10.1038/s41586-020-2654-5>.
- [5] P.N. Tran, K.T. Laha, D.A. Wagner, A tight coupling between β_2 Y97 and β_2 F200 of the GABA_A receptor mediates GABA binding, *J. Neurochem.* 119 (2011) 283–293, <https://doi.org/10.1111/j.1471-4159.2011.07409.x>.
- [6] T.L. Kash, A. Jenkins, J.C. Kelley, J.R. Trudell, N.L. Harrison, Coupling of agonist binding to channel gating in the GABA_A receptor, *Nature* 421 (6920) (2003) 272–275, <https://doi.org/10.1038/nature01280>.
- [7] W.Y. Lee, S.M. Sine, Principal pathway coupling agonist binding to channel gating in nicotinic receptors, *Nature* 438 (7065) (2005) 243–247, <https://doi.org/10.1038/nature04156>.
- [8] S. Scott, J.W. Lynch, A. Keramidas, Correlating structural and energetic changes in glycine receptor activation, *J. Biol. Chem.* 290 (9) (2015) 5621–5634, <https://doi.org/10.1074/jbc.M114.616573>.
- [9] K. Terejko, P.T. Kaczor, M.A. Michałowski, A. Dąbrowska, J.W. Mozrzymas, The C loop at the orthosteric binding site is critically involved in GABA_A receptor gating, *Neuropharmacology* 166 (2020) 107903, <https://doi.org/10.1016/j.neuropharm.2019.107903>.
- [10] M. Szczot, M. Kisiel, M.M. Czyżewska, J.W. Mozrzymas, α_1 F64 residue at GABA_A receptor binding site is involved in gating by influencing the receptor flipping transitions, *J. Neurosci.* 34 (9) (2014) 3193–3209, <https://doi.org/10.1523/JNEUROSCI.2533-13.2014>.
- [11] M. Brodzki, M.A. Michałowski, M. Gos, J.W. Mozrzymas, Mutations of α_1 F45 residue of GABA_A receptor loop G reveal its involvement in agonist binding and channel opening/closing transitions, *Biochem. Pharmacol.* 177 (2020) 113917, <https://doi.org/10.1016/j.bcp.2020.113917>.
- [12] J.G. Newell, R.A. McDevitt, C. Czajkowski, Mutation of glutamate 155 of the GABA_A receptor β_2 subunit produces a spontaneously open channel: a trigger for channel activation, *J. Neurosci.* 24 (2004) 11226–11235, <https://doi.org/10.1523/JNEUROSCI.3746-04.2004>.
- [13] V.I. Torres, D.S. Weiss, Identification of a tyrosine in the agonist binding site of the homomeric ρ_1 γ -aminobutyric acid (GABA) receptor that, when mutated, produces spontaneous opening, *J. Biol. Chem.* 277 (46) (2002) 43741–43748, <https://doi.org/10.1074/jbc.M202007200>.
- [14] J.M.E. Cederholm, P.R. Schofield, T.M. Lewis, Gating mechanisms in Cys-loop receptors, *Eur. Biophys. J.* 39 (1) (2009) 37–49, <https://doi.org/10.1007/s00249-009-0452-y>.
- [15] P.S. Miller, T.G. Smart, Binding, activation and modulation of Cys-loop receptors, *Trends Pharmacol. Sci.* 31 (4) (2010) 161–174, <https://doi.org/10.1016/j.tips.2009.12.005>.
- [16] L. Sauguet, A. Shahsavari, F. Poitevin, C. Huon, A. Menny, A. Nemeč, A. Haouz, J.-P. Changeux, P.-J. Corringer, M. Delarue, Crystal structures of a pentameric ligand-gated ion channel provide a mechanism for activation, *Proc. Natl. Acad. Sci.* 111 (3) (2014) 966–971, <https://doi.org/10.1073/pnas.1314997111>.
- [17] T. Althoff, R.E. Hibbs, S. Banerjee, E. Gouaux, X-ray structures of GluCl in apo states reveal a gating mechanism of Cys-loop receptors, *Nature* 512 (7514) (2014) 333–337, <https://doi.org/10.1038/nature13669>.
- [18] N.E. Martin, S. Malik, N. Calimet, et al., Un-gating and allosteric modulation of a pentameric ligand-gated ion channel captured by molecular dynamics, *PLoS Comput. Biol.* 13 (2017) 1–25, <https://doi.org/10.1371/journal.pcbi.1005784>.
- [19] A. Nemeč, M. Prevost, A. Menny, P.-J. Corringer, Emerging molecular mechanisms of signal transduction in pentameric ligand-gated ion channels, *Neuron* 90 (3) (2016) 452–470, <https://doi.org/10.1016/j.neuron.2016.03.032>.
- [20] A. Taly, M. Delarue, T. Grutter, M. Nilges, N. Le Novère, P.-J. Corringer, J.-P. Changeux, Normal mode analysis suggests a quaternary twist model for the nicotinic receptor gating mechanism, *Biophys. J.* 88 (6) (2005) 3954–3965, <https://doi.org/10.1529/biophysj.104.050229>.
- [21] K.T. Laha, D.A. Wagner, A state-dependent salt-bridge interaction exists across the β/α intersubunit interface of the GABA_A receptor, *Mol. Pharmacol.* 79 (2011) 662–671, <https://doi.org/10.1124/mol.110.068619>.
- [22] Natasha C. Pflanz, Anna W. Daszkowski, Garrett L. Cornelison, James R. Trudell, S. John Mihic, An intersubunit electrostatic interaction in the GABA A receptor facilitates its responses to benzodiazepines, *J. Biol. Chem.* 293 (21) (2018) 8264–8274, <https://doi.org/10.1074/jbc.RA118.002128>.
- [23] Jelena Todorovic, Brian T. Welsh, Edward J. Bertaccini, James R. Trudell, S. John Mihic, Disruption of an intersubunit electrostatic bond is a critical step in glycine receptor activation, *PNAS* 107 (17) (2010) 7987–7992, <https://doi.org/10.1073/pnas.1001845107>.
- [24] Fatemah Safar, Elliot Hurdiss, Marios Erotocritou, Timo Greiner, Remigijus Lape, Mark W. Irvine, Guangyu Fang, David Jane, Rilei Yu, Marc A. Dąmgen, Philip C. Biggin, Lucia G. Sivilotti, The startle disease mutation E103K impairs activation of human homomeric α_1 glycine receptors by disrupting an intersubunit salt bridge across the agonist binding site, *J. Biol. Chem.* 292 (12) (2017) 5031–5042, <https://doi.org/10.1074/jbc.M116.767616>.

- [25] Amnon Horowitz, Double-mutant cycles: a powerful tool for analyzing protein structure and function, *Fold Des.* 1 (6) (1996) R121–R126, [https://doi.org/10.1016/S1359-0278\(96\)00056-9](https://doi.org/10.1016/S1359-0278(96)00056-9).
- [26] P. Jonas, Fast application of agonists to isolated membrane patches, in: B. Sakmann, E. Neher (Eds.), *Single-Channel Recording*, Springer US, Boston, MA, 1995, pp. 231–243.
- [27] J.W. Mozrzymas, T. Wójtowicz, M.M. Piast, et al., GABA transient sets the susceptibility of mIPSCs to modulation by benzodiazepine receptor agonists in rat hippocampal neurons, *J. Physiol.* 585 (2007) 29–46, <https://doi.org/10.1113/jphysiol.2007.143602>.
- [28] Jerzy W. Mozrzymas, Andrea Barberis, Katarzyna Mercik, Ewa D. Zarnowska, Binding sites, singly bound states, and conformation coupling shape GABA-evoked currents, *J. Neurophysiol.* 89 (2) (2003) 871–883, <https://doi.org/10.1152/jn.00951.2002>.
- [29] Marek Brodzki, Radosław Rutkowski, Magdalena Jatzczak, Magdalena Kisiel, Marta M. Czyżewska, Jerzy W. Mozrzymas, Comparison of kinetic and pharmacological profiles of recombinant $\alpha 1\gamma 2$ and $\alpha 1\beta 2\gamma 2$ GABAA receptors – a clue to the role of intersubunit interactions, *Eur. J. Pharmacol.* 784 (2016) 81–89, <https://doi.org/10.1016/j.ejphar.2016.05.015>.
- [30] M. Jatzczak-Sliwa, K. Terejko, M. Brodzki, et al., Distinct modulation of spontaneous and GABA-evoked gating by flurazepam shapes cross-talk between agonist-free and liganded GABAA receptor activity, *Front Cell Neurosci* 12 (2018) 1–18, <https://doi.org/10.3389/fncel.2018.00237>.
- [31] G.M.C. Lema, A. Auerbach, Modes and models of GABA_A receptor gating, *J. Physiol.* 572 (2006) 183–200, <https://doi.org/10.1113/jphysiol.2005.099093>.
- [32] Magdalena Kisiel, Magdalena Jatzczak, Marek Brodzki, Jerzy W. Mozrzymas, Spontaneous activity, singly bound states and the impact of alpha 1 Phe64 mutation on GABA A R gating in the novel kinetic model based on the single-channel recordings, *Neuropharmacology* 131 (2018) 453–474, <https://doi.org/10.1016/j.neuropharm.2017.11.030>.
- [33] D.E. Clapham, E. Neher, Substance P reduces acetylcholine-induced currents in isolated bovine chromaffin cells, *J. Physiol.* 347 (1984) 255–277, <https://doi.org/10.1113/jphysiol.1984.sp015065>.
- [34] P. Di Tommaso, S. Moretti, I. Xenarios, M. Orobítg, A. Montanyola, J.-M. Chang, J.-F. Taly, C. Notredame, T-Coffee: a web server for the multiple sequence alignment of protein and RNA sequences using structural information and homology extension, *Nucleic Acids Res.* 39 (suppl) (2011) W13–W17, <https://doi.org/10.1093/nar/gkr245>.
- [35] A.M. Waterhouse, J.B. Procter, D.M.A. Martin, M. Clamp, G.J. Barton, Jalview Version 2—a multiple sequence alignment editor and analysis workbench, *Bioinformatics* 25 (9) (2009) 1189–1191, <https://doi.org/10.1093/bioinformatics/btp033>.
- [36] H.M. Berman, J. Westbrook, Z. Feng, et al., The protein data bank, *Nucleic Acids Res.* 28 (2000) 235–242, <https://doi.org/10.1093/nar/28.1.235>.
- [37] Duncan Lavery, Rooma Desai, Tomasz Uchański, Simonas Masiulis, Wojciech J. Stec, Tomas Malinauskas, Jasenko Zivanov, Els Pardon, Jan Steyaert, Keith W. Miller, A. Radu Aricescu, Cryo-EM structure of the human $\alpha 1\beta 3\gamma 2$ GABAA receptor in a lipid bilayer, *Nature* 565 (7740) (2019) 516–520, <https://doi.org/10.1038/s41586-018-0833-4>.
- [38] B. Webb, A. Sali, Comparative protein structure modeling using MODELLER, 2014.
- [39] William Humphrey, Andrew Dalke, Klaus Schulten, VMD: visual molecular dynamics, *J. Mol. Graph.* 14 (1) (1996) 33–38, [https://doi.org/10.1016/0263-7855\(96\)00018-5](https://doi.org/10.1016/0263-7855(96)00018-5).
- [40] D. Colquhoun, Binding, gating, affinity and efficacy: the interpretation of structure-activity relationships for agonists acid of the effects of mutating receptors, *Br. J. Pharmacol.* 125 (1998) 923–947, <https://doi.org/10.1038/sj.bjp.0702164>.
- [41] M. Jatzczak-Sliwa, M. Kisiel, M.M. Czyżewska, et al., GABAA receptor $\beta 2E155$ residue located at the agonist-binding site is involved in the receptor gating, *Front Cell Neurosci* 14 (2020) 1–18, <https://doi.org/10.3389/fncel.2020.00002>.
- [42] Magdalena Kisiel, Magdalena Jatzczak-Sliwa, Jerzy W. Mozrzymas, Protons modulate gating of recombinant $\alpha 1\beta 2\gamma 2$ GABAA receptor by affecting desensitization and opening transitions, *Neuropharmacology* 146 (2019) 300–315, <https://doi.org/10.1016/j.neuropharm.2018.10.016>.
- [43] Mathew V. Jones, Gary L. Westbrook, Desensitized states prolong GABAA channel responses to brief agonist pulses, *Neuron* 15 (1) (1995) 181–191, [https://doi.org/10.1016/0896-6273\(95\)90075-6](https://doi.org/10.1016/0896-6273(95)90075-6).
- [44] K.F. Haas, R.L. Macdonald, GABA(A) receptor subunit $\gamma 2$ and δ subtypes confer unique kinetic properties on recombinant GABA(A) receptor currents in mouse fibroblasts, *J. Physiol.* 514 (1999) 27–45, <https://doi.org/10.1111/j.1469-7793.1999.027af.x>.
- [45] Jerzy W. Mozrzymas, Andrea Barberis, Krystyna Michalak, Enrico Cherubini, Chlorpromazine inhibits miniature GABAergic currents by reducing the binding and by increasing the unbinding rate of GABA A receptors, *J. Neurosci.* 19 (7) (1999) 2474–2488, <https://doi.org/10.1523/JNEUROSCI.19-07-02474.1999>.
- [46] A.H. Lagrange, E.J. Botzlikakis, R.L. Macdonald, Enhanced macroscopic desensitization shapes the response of $\alpha 4$ subtype-containing GABAA receptors to synaptic and extrasynaptic GABA, *J. Physiol.* 578 (2007) 655–676, <https://doi.org/10.1113/jphysiol.2006.122135>.
- [47] U. Rudolph, H. Mohler, GABA-based therapeutic approaches: GABAA receptor subtype functions, *Curr. Opin. Pharmacol.* 6 (1) (2006) 18–23, <https://doi.org/10.1016/j.coph.2005.10.003>.
- [48] U. Rudolph, H. Mohler, GABAA receptor subtypes: therapeutic potential in down syndrome, affective disorders, schizophrenia, and autism, *Annu. Rev. Pharmacol. Toxicol.* 54 (2014) 483–507, <https://doi.org/10.1016/j.pestbp.2011.02.012>.
- [49] U. Rudolph, H. Möhler, Analysis of GABAA receptor function and dissection of the pharmacology of benzodiazepines and general anesthetics through mouse genetics, *Annu. Rev. Pharmacol. Toxicol.* 44 (2004) 475–498, <https://doi.org/10.1146/annurev.pharmtox.44.101802.121429>.
- [50] Teijo I. Saari, Mikko Uusi-Oukari, Joumi Ahonen, Klaus T. Olkkola, Markku Koulu, Enhancement of GABAergic activity: neuropharmacological effects of benzodiazepines and therapeutic use in anesthesiology, *Pharmacol. Rev.* 63 (1) (2011) 243–267, <https://doi.org/10.1124/pr.110.002717>.
- [51] Werner Sieghart, Unraveling the function of GABAA receptor subtypes, *Trends Pharmacol. Sci.* 21 (11) (2000) 411–413, [https://doi.org/10.1016/S0165-6147\(00\)01564-9](https://doi.org/10.1016/S0165-6147(00)01564-9).
- [52] Xin Huang, Paul L Shaffer, Shawn Ayube, Howard Bregman, Hao Chen, Sonya G Lehto, Jason A Luther, David J Matson, Stefan I McDonough, Klaus Michelsen, Matthew H Plant, Stephen Schneider, Jeffrey R Simard, Yohannes Teffera, Shuyan Yi, Maosheng Zhang, Erin F DiMauro, Jacinthe Gingras, Crystal structures of human glycine receptor $\alpha 3$ bound to a novel class of analgesic potentiators, *Nat. Struct. Mol. Biol.* 24 (2) (2017) 108–113, <https://doi.org/10.1038/nsmb.3329>.
- [53] Anant Gharpure, Jinfeng Teng, Yuxuan Zhuang, Colleen M. Novello, Richard M. Walsh Jr., Rico Cabuco, Rebecca J. Howard, Nurulain T. Zaveri, Erik Lindahl, Ryan E. Hibbs, Agonist selectivity and ion permeation in the $\alpha 3\beta 4$ ganglionic nicotinic receptor, *Neuron* 104 (3) (2019) 501–511.e6, <https://doi.org/10.1016/j.neuron.2019.07.030>.

PODSUMOWANIE I WNIOSKI

Domena zewnątrzkomórkowa (ang. „*extracellular domain*”, ECD) to, jeśli idzie o statyczną strukturę, jeden z lepiej poznanych fragmentów receptora GABA_A ze względu na dobrą rozdzielczość przestrzenną uzyskanych struktur dla tego obszaru (Kim i wsp., 2020; Masiulis i wsp., 2019; Zhu i wsp., 2018). Jednakże sama wiedza na temat struktury nie dostarcza odpowiedzi na temat konkretnej roli poszczególnych jej elementów w funkcjonowaniu receptorów. Wyniki zaprezentowane w niniejszej rozprawie doktorskiej dostarczają nowych informacji na temat relacji między wybranymi rejonami ECD a ich funkcją w procesie aktywacji receptorów GABA_A, który pełni kluczową rolę w kształtowaniu kinetyki prądów hamujących IPSCs i przez to w procesach hamowania w ośrodkowym układzie nerwowym.

Zarówno reszty aromatyczne α_1 F14 i β_2 F31 w okolicy N-końca łańcucha aminokwasów u szczytu ECD, jak i pętla C, na przykładzie reszty β_2 F200, są zaangażowane w procesy odbywające się w znaczącej odległości, czyli wiązanie neuroprzekaźnika w miejscu wiązania, preaktywację a także bramkowanie kanału jonowego w oddalonej o ok. 50-75 Å domenie transbłonowej (ang. „*transmembrane domain*”, TMD). Ma to szczególnie istotne znaczenie w przypadku pętli C, o wysoce konserwatywnej strukturze w receptorach pLGIC, dla której postulowano przede wszystkim rolę ograniczoną jedynie do wiązania agonisty, ze względu na jej lokalizację w miejscu wiązania (Pless i Lynch, 2009; Purohit i Auerbach, 2013), chociaż istniały także wczesne przesłanki sugerujące inne funkcje pętli C w receptorze acetylocholinowy nAChR (Mukhtasimova i wsp., 2009). Przedstawione w rozprawie wyniki wykazują jednoznacznie, że w przypadku receptora GABA_A, zasadniczo wszystkie etapy aktywacji są zależne od skuteczności „nakrywania” (ang. „*capping*”) miejsca wiązania przez pętlę C. Podobnie mutacje fenyloalanin α_1 F14 i β_2 F31 upośledzają większość etapów aktywacji, pomimo peryferyjnej lokalizacji na szczycie ECD, który jest obszarem dotychczas bardzo mało poznany w receptorze GABA_A. Dowiedziona istotna rola tych aminokwasów, ale także znaczenie oddziaływania zachodzącego pomiędzy nimi na styku dwóch podjednostek w funkcjonowaniu receptora, może w przyszłości wyznaczyć nowe kierunki badań farmakologicznych. Jak wykazano dla receptora glicyny, w analogicznym obszarze P10 i F32 rozpoznano miejsce wiązania dla nowej klasy związków farmakologicznych o działaniu analgetycznym (Huang i wsp., 2016).

Przedstawione wyniki wskazują na to, że transdukcja sygnału prowadzącego do aktywacji jest zatem zjawiskiem niezwykle złożonym i nie należy przyjmować, że odbywa się w jednym kierunku od miejsca wiązania do bramki kanału jonowego. Dodatkowo, oddziaływanie pomiędzy α_1F14 i β_2F31 dowodzi, że sygnał ten rozchodzi się także lateralnie w obrębie różnych podjednostek. Zastosowanie punktowej mutagenety badanych aminokwasów pozwoliło jednoznacznie wykazać, że prawidłowe funkcjonowanie receptora zależy od wielu czynników, a pojedyncza reszta aminokwasowa nie pełni wybiórczej roli w aktywacji, może natomiast dotyczyć różnych aspektów tego procesu.

Drugim zagadnieniem poruszonym w niniejszej rozprawie jest mechanizm modulacji aktywności receptora GABA_A przez benzodiazepiny. Jak wykazuje stanowiący niniejszą rozprawę cykl publikacji, flurazepam w wysokim stopniu moduluje etap preaktywacji, czego dowodzą zarówno eksperymenty z użyciem agonisty GABA jak i częściowego agonisty, kwasu piperydino-4-sulfonowego (P4S). Zastosowane mutacje kluczowej dla preaktywacji reszty fenyloalaninowej w miejscu wiązania α_1F64 , spowodowało zmianę wrażliwości badanych receptorów na flurazepam poprzez zwiększenie amplitudy wywołanych prądów w warunkach wysycenia. Mechanizm działania benzodiazepin obejmuje przyspieszenie wejścia w stan preaktywacji, które w przypadku receptorów typu dzikiego dzieje się na tyle szybko, że opisywany efekt nie jest możliwy do zaobserwowania. Benzodiazepiny powodują zatem większą stabilizację dalszych etapów aktywacji poprzez przyspieszenie spowolnionych na skutek mutacji kinetycznych stałych czasowych desensytyzacji i resensytyzacji, co wykazano zarówno dla α_1F64 i wspomnianej wcześniej β_2F200 .

Zaprezentowane badania stanowią potwierdzenie postawionej we wstępie hipotezy: wybrane mutacje kluczowych aminokwasów aromatycznych w domenie zewnątrzkomórkowej receptora GABA_A wykazują istotny wpływ zarówno na wiązanie agonisty i na bramkowanie kanału jonowego. Interpretacja mechanistyczna, która tłumaczyłaby molekularne mechanizmy tego zjawiska nie została jeszcze w pełni opracowana i wymaga dalszych szczegółowych badań nad procesem aktywacji receptora. Można przypuszczać jednak, że zastosowanie mutacji poprzez substytucję pojedynczych aminokwasów powoduje lokalne zaburzenia trzeciorzędowej struktury białka, wynikające z zerwania występujących tam licznych oddziaływań elektrostatycznych lub π -kationowych. Tego typu oddziaływania w strukturze mają na celu zapewnienie prawidłowej orientacji aminokwasów względem siebie w łańcuchu oraz stabilizację wiązania cząsteczek do receptora.

Podsumowując, otrzymane wyniki w znacznym stopniu przyczyniły się do rozwoju wiedzy na temat aktywacji receptorów GABA_A w kontekście relacji pomiędzy jego strukturą i funkcją wraz z uwzględnieniem modulatorowych mechanizmów działania benzodiazepin, istotnych w dziedzinie badań nad inhibicją GABA-ergiczną. Uzyskane wyniki oparto na rozległych badaniach obejmujących wysokiej rozdzielczości techniki elektrofizjologiczne poparte metodami *in silico*, m. in. modelowaniem kinetycznym, wykorzystując tym samym najnowsze metody badawcze. Zdobyta wiedza może w przyszłości zostać wykorzystana podczas projektowania nowych związków farmakologicznych oddziałujących z receptorem GABA_A lub także w medycynie i fizjologii do zrozumienia mechanizmów patofizjologicznych niektórych chorób układu nerwowego.

BIBLIOGRAFIA

- Althoff Thorsten, Ryan E. Hibbs, Surajit Banerjee i Eric Gouaux. 2014. “X-Ray Structures of GluCl in Apo States Reveal a Gating Mechanism of Cys-Loop Receptors.” *Nature* 512 (7514): 333–37. <https://doi.org/10.1038/nature13669>.
- Berezhnoy Dmytro, Yves Nyfeler, Anne Gonthier, Maurice Goeldner i Erwin Sigel. 2004. “On the Benzodiazepine Binding Pocket in GABA A Receptors.” *Biochemistry* 279 (5): 3160–68. <https://doi.org/10.1074/jbc.M311371200>.
- Brickley Stephen G. i Istvan Mody. 2012. “Extrasynaptic GABAA Receptors: Their Function in the CNS and Implications for Disease.” *Neuron* 73 (1): 23–34. <https://doi.org/10.1016/j.neuron.2011.12.012>.
- Brodzki Marek, Michał A. Michałowski, Michalina Gos i Jerzy W. Mozrzymas. 2020. “Mutations of α 1F45 Residue of GABAA Receptor Loop G Reveal Its Involvement in Agonist Binding and Channel Opening/Closing Transitions.” *Biochemical Pharmacology* 177: 113917. <https://doi.org/10.1016/j.bcp.2020.113917>.
- del Castillo J. i B. Katz. 1957. “Interaction at End-Plate Receptors between Different Choline Derivatives.” *Proceedings of the Royal Society of London. Series B, Containing Papers of a Biological Character. Royal Society (Great Britain)* 146 (924): 369–81. <https://doi.org/10.1098/rspb.1957.0018>.
- Cederholm Jennie M.E., Peter R. Schofield i Trevor M. Lewis. 2009. “Gating Mechanisms in Cys-Loop Receptors.” *European Biophysics Journal* 39 (1): 37–49. <https://doi.org/10.1007/s00249-009-0452-y>.
- Chen Xiumin, Angelo Keramidas i Joseph W. Lynch. 2017. “Physiological and Pharmacological Properties of Inhibitory Postsynaptic Currents Mediated by A5 β 1 γ 2, A5 β 2 γ 2 and A5 β 3 γ 2 GABAA Receptors.” *Neuropharmacology* 125: 243–53. <https://doi.org/10.1016/j.neuropharm.2017.07.027>.
- Cheng Xiaolin, Hailong Wang, Barry Grant, Steven M. Sine i J. Andrew McCammon. 2006. “Targeted Molecular Dynamics Study of C-Loop Closure and Channel Gating in Nicotinic Receptors.” *PLoS Computational Biology* 2 (9): e134. <https://doi.org/10.1371/journal.pcbi.0020134>.

- Cherubini Enrico. 2012. "Phasic GABA A-Mediated Inhibition," no. Md: 1–21.
https://www.ncbi.nlm.nih.gov/books/NBK98155/pdf/Bookshelf_NBK98155.pdf.
- Cherubini Enrico i Fiorenzo Conti. 2001. "Generating Diversity at GABAergic Synapses." *Trends in Neurosciences* 24 (3): 155–62. [https://doi.org/10.1016/S0166-2236\(00\)01724-0](https://doi.org/10.1016/S0166-2236(00)01724-0).
- Colquhoun D. 1998. "Binding, Gating, Affinity and Efficacy: The Interpretation of Structure-Activity Relationships for Agonists Acid of the Effects of Mutating Receptors." *British Journal of Pharmacology* 125 (5): 923–47. <https://doi.org/10.1038/sj.bjp.0702164>.
- Colquhoun David i Remigijus Lape. 2012. "Allosteric Coupling in Ligand-Gated Ion Channels." *The Journal of General Physiology* 140 (6): 625–34.
<https://doi.org/10.1085/jgp.201210849>.
- Corringer Pierre Jean, Frédéric Poitevin, Marie S. Prevost, Ludovic Sauguet, Marc Delarue i Jean Pierre Changeux. 2012. "Structure and Pharmacology of Pentameric Receptor Channels: From Bacteria to Brain." *Structure* 20 (6): 941–56.
<https://doi.org/10.1016/j.str.2012.05.003>.
- Dixon Christine L., Neil L. Harrison, Joseph W. Lynch i Angelo Keramidis. 2015. "Zolpidem and Eszopiclone Prime $\alpha 1\beta 2\gamma 2$ GABAA Receptors for Longer Duration of Activity." *British Journal of Pharmacology*. <https://doi.org/10.1111/bph.13142>.
- Downing Scott S, Yan T. Lee, David H Farb i Terrell T. Gibbs. 2005. "Benzodiazepine Modulation of Partial Agonist Efficacy and Spontaneously Active GABA(A) Receptors Supports an Allosteric Model of Modulation." *British Journal of Pharmacology* 145 (7): 894–906. <https://doi.org/10.1038/sj.bjp.0706251>.
- Du Juan, Wei Lü, Shenping Wu, Yifan Cheng i Eric Gouaux. 2015. "Glycine Receptor Mechanism Illuminated by Electron Cryo- Microscopy" 344 (6188): 1173–78.
<https://doi.org/10.1038/nature14853>.Glycine.
- Farrant Mark i Zoltan Nusser. 2005. "Variations on an Inhibitory Theme: Phasic and Tonic Activation of GABA(A) Receptors." *Nature Reviews. Neuroscience* 6 (March): 215–29.
<https://doi.org/10.1038/nrn1625>.
- Farrar Sophie J., Paul J. Whiting, Timothy P. Bonnert i Ruth M. McKernan. 1999. "Stoichiometry of a Ligand-Gated Ion Channel Determined by Fluorescence Energy Transfer." *Journal of Biological Chemistry* 274 (15): 10100–104.

<https://doi.org/10.1074/jbc.274.15.10100>.

- Gielen, Mc Marc C, Michael J Mj Lumb, i Tg Trevor G Smart. 2012. “Benzodiazepines Modulate GABAA Receptors by Regulating the Preactivation Step after GABA Binding.” *The Journal of Neuroscience : The Official Journal of the Society for Neuroscience* 32 (17): 5707–15. <https://doi.org/10.1523/JNEUROSCI.5663-11.2012>.
- Glykys Joseph i Istvan Mody. 2007. “Activation of GABAA Receptors: Views from Outside the Synaptic Cleft.” *Neuron* 56 (5): 763–70. <https://doi.org/10.1016/j.neuron.2007.11.002>.
- Hanson Susan M. i Cynthia Czajkowski. 2008. “Cellular/Molecular Structural Mechanisms Underlying Benzodiazepine Modulation of the GABA A Receptor” 28 (13): 3490–99. <https://doi.org/10.1523/JNEUROSCI.5727-07.2008>.
- Horovitz Amnon. 1996. “Double-Mutant Cycles: A Powerful Tool for Analyzing Protein Structure and Function.” *Folding and Design* 1 (6): 121–26. [https://doi.org/10.1016/S1359-0278\(96\)00056-9](https://doi.org/10.1016/S1359-0278(96)00056-9).
- Huang Xin, Paul L. Shaffer, Shawn Ayube, Howard Bregman, Hao Chen, Sonya G. Lehto, Jason A. Luther i wsp. 2016. “Crystal Structures of Human Glycine Receptor A3 Bound to a Novel Class of Analgesic Potentiators.” *Nature Structural & Molecular Biology*, no. December: 1–9. <https://doi.org/10.1038/nsmb.3329>.
- Jacob Tija C., Guido Michels, Liliya Silayeva, Julia Haydon, Francesca Succol i Stephen J. Moss. 2012. “Benzodiazepine Treatment Induces Subtype-Specific Changes in GABA(A) Receptor Trafficking and Decreases Synaptic Inhibition.” *Proceedings of the National Academy of Sciences of the United States of America* 109 (45): 18595–600. <https://doi.org/10.1073/pnas.1204994109>.
- Jaczak-Śliwa Magdalena, Katarzyna Terejko, Marek Brodzki, Michał A. Michałowski, Marta M. Czyzewska, Joanna M. Nowicka, Anna Andrzejczak, Rakenduvadhana Srinivasan i Jerzy W. Mozrzymas. 2018. “Distinct Modulation of Spontaneous and GABA-Evoked Gating by Flurazepam Shapes Cross-Talk Between Agonist-Free and Liganded GABAA Receptor Activity.” *Frontiers in Cellular Neuroscience* 12 (August): 1–18. <https://doi.org/10.3389/fncel.2018.00237>.
- Jonas Peter. 1995. “Fast Application of Agonists to Isolated Membrane Patches.” In *Single-Channel Recording*, edytowany przez: Bert Sakmann i Erwin Neher, 231–43. Boston,

- MA: Springer US. https://doi.org/10.1007/978-1-4419-1229-9_10.
- Jones Mathew V. i Gary L. Westbrook. 1995. “Desensitized States Prolong GABAA Channel Responses to Brief Agonist Pulses.” *Neuron* 15 (1): 181–91.
[https://doi.org/10.1016/0896-6273\(95\)90075-6](https://doi.org/10.1016/0896-6273(95)90075-6).
- Kim Jeong Joo, Anant Gharpure, Jinfeng Teng, Yuxuan Zhuang, Rebecca J. Howard, Shaotong Zhu, Colleen M. Noviello, Richard M. Walsh, Erik Lindahl i Ryan E. Hibbs. 2020. “Shared Structural Mechanisms of General Anaesthetics and Benzodiazepines.” *Nature* 585 (7824): 303–8. <https://doi.org/10.1038/s41586-020-2654-5>.
- Kisiel Magdalena, Magdalena Jatczak, Marek Brodzki i Jerzy W. Mozrzymas. 2018. “Spontaneous Activity, Singly Bound States and the Impact of Alpha1Phe64 Mutation on GABAAR Gating in the Novel Kinetic Model Based on the Single-Channel Recordings.” *Neuropharmacology* 131: 453–74.
<https://doi.org/10.1016/j.neuropharm.2017.11.030>.
- Krampfl K., A. Lepier, K. Jahn, C. Franke, and J. Bufler. 1998. “Molecular Modulation of Recombinant Rat $\alpha 1\beta 2\gamma 2$ GABA(A) Receptor Channels by Diazepam.” *Neuroscience Letters* 256 (3): 143–46. [https://doi.org/10.1016/S0304-3940\(98\)00767-8](https://doi.org/10.1016/S0304-3940(98)00767-8).
- Laha Kurt T. i David A. Wagner. 2011. “A State-Dependent Salt-Bridge Interaction Exists across the β/α Intersubunit Interface of the GABAA Receptor.” *Molecular Pharmacology* 79 (4): 662–71. <https://doi.org/10.1124/mol.110.068619>.
- Lape Remigijus, David Colquhoun i Lucia G. Sivilotti. 2008. “On the Nature of Partial Agonism in the Nicotinic Receptor Superfamily.” *Nature* 454 (7205): 722–27.
<https://doi.org/10.1038/nature07139>.
- Lavery Duncan, Rooma Desai, Tomasz Uchański, Simonas Masiulis, Wojciech J. Stec, Tomas Malinauskas, Jasenko Zivanov i wsp. 2019. “Cryo-EM Structure of the Human A1 β 3 γ 2 GABAA Receptor in a Lipid Bilayer.” *Nature*, 1.
<https://doi.org/10.1038/s41586-018-0833-4>.
- Lavoie A. M. i R. E. Twyman. 1996. “Direct Evidence for Diazepam Modulation of GABA(A) Receptor Microscopic Affinity.” *Neuropharmacology* 35 (9–10): 1383–92.
[https://doi.org/10.1016/S0028-3908\(96\)00077-9](https://doi.org/10.1016/S0028-3908(96)00077-9).
- Martin Nicolas E., Siddharth Malik, Nicolas Calimet, Jean Pierre Changeux i Marco Cecchini.

2017. “Un-Gating and Allosteric Modulation of a Pentameric Ligand-Gated Ion Channel Captured by Molecular Dynamics.” *PLoS Computational Biology* 13 (10): 1–25.
<https://doi.org/10.1371/journal.pcbi.1005784>.
- Masiulis Simonas, Rooma Desai, Tomasz Uchański, Itziar Serna Martin, Duncan Lavery, Dimple Karia, Tomas Malinauskas i wsp. 2019. “GABAA Receptor Signalling Mechanisms Revealed by Structural Pharmacology.” *Nature*.
<https://doi.org/10.1038/s41586-018-0832-5>.
- McKernan Ruth M. i Paul J. Whiting. 1996. “Which GABAA-Receptor Subtypes Really Occur in the Brain?” *Trends in Neurosciences* 19 (4): 139–43.
[https://doi.org/10.1016/S0166-2236\(96\)80023-3](https://doi.org/10.1016/S0166-2236(96)80023-3).
- Mercik Katarzyna, Michał Piast i Jerzy W. Mozrzymas. 2007. “Benzodiazepine Receptor Agonists Affect Both Binding and Gating of Recombinant $\alpha 1\beta 2\gamma 2$ Gamma-Aminobutyric Acid-A Receptors.” *NeuroReport* 18 (8): 781–85.
<https://doi.org/10.1097/WNR.0b013e3280c1e2fb>.
- Michałowski M. A., S. Kraszewski i J. W. Mozrzymas. 2017. “Binding Site Opening by Loop C Shift and Chloride Ion-Pore Interaction in the GABAA Receptor Model.” *Physical Chemistry Chemical Physics* 19 (21): 13664–78. <https://doi.org/10.1039/c7cp00582b>.
- Miller Paul S. i A. Radu Aricescu. 2014. “Crystal Structure of a Human GABAA Receptor.” *Nature* 512 (7514): 270–75. <https://doi.org/10.1038/nature13293>.
- Miller Paul S. i Trevor G. Smart. 2010. “Binding, Activation and Modulation of Cys-Loop Receptors.” *Trends in Pharmacological Sciences* 31 (4): 161–74.
<https://doi.org/10.1016/j.tips.2009.12.005>.
- Mody Istvan i Robert A. Pearce. 2004. “Diversity of Inhibitory Neurotransmission through GABA A Receptors.” *Trends in Neurosciences* 27 (9): 569–75.
<https://doi.org/10.1016/j.tins.2004.07.002>.
- Möhler Hanns. 2015. “The Legacy of the Benzodiazepine Receptor: From Flumazenil to Enhancing Cognition in down Syndrome and Social Interaction in Autism.” *Advances in Pharmacology* 72: 1–36. <https://doi.org/10.1016/bs.apha.2014.10.008>.
- Mortensen Martin, Uffe Kristiansen, Bjarke Ebert, Bente Frølund, Povl Krogsgaard-Larsen i Trevor G Smart. 2004. “Activation of Single Heteromeric GABA(A) Receptor Ion

- Channels by Full and Partial Agonists.” *The Journal of Physiology* 557 (Pt 2): 389–413.
<https://doi.org/10.1113/jphysiol.2003.054734>.
- Mozrzymas Jerzy W., Andrea Barberis, Katarzyna Mercik i Ewa D. Żarnowska. 2003.
“Binding Sites, Singly Bound States, and Conformation Coupling Shape GABA-Evoked Currents.” *Journal of Neurophysiology* 89 (2): 871–83.
<https://doi.org/10.1152/jn.00951.2002>.
- Mozrzymas Jerzy W., Andrea Barberis, Krystyna Michalak i Enrico Cherubini. 1999.
“Chlorpromazine Inhibits Miniature GABAergic Currents by Reducing the Binding and by Increasing the Unbinding Rate of GABA(A) Receptors.” *Journal of Neuroscience* 19 (7): 2474–88. <https://doi.org/10.1523/jneurosci.19-07-02474.1999>.
- Mozrzymas Jerzy W., Tomasz Wójtowicz, Michał Piast, Katarzyna Lebida, Paulina Wyrembek i Katarzyna Mercik. 2007. “GABA Transient Sets the Susceptibility of MIPSCs to Modulation by Benzodiazepine Receptor Agonists in Rat Hippocampal Neurons.” *Journal of Physiology* 585 (1): 29–46.
<https://doi.org/10.1113/jphysiol.2007.143602>.
- Mukhtasimova Nuriya, Won Yong Lee, Hai Long Wang i Steven M. Sine. 2009. “Detection and Trapping of Intermediate States Priming Nicotinic Receptor Channel Opening.” *Nature* 459 (7245): 451–54. <https://doi.org/10.1038/nature07923>.
- Nemecz Akos, Marie S. Prevost, Anaïs Menny, Pierre-Jean Corringer i wsp. 2016. “Emerging Molecular Mechanisms of Signal Transduction in Pentameric Ligand-Gated Ion Channels.” *Neuron* 90 (3): 452–70. <https://doi.org/10.1016/j.neuron.2016.03.032>.
- Padgett C. L., A. P. Hanek, H. A. Lester, D. A. Dougherty i S. C. R. Lummis. 2007.
“Unnatural Amino Acid Mutagenesis of the GABA A Receptor Binding Site Residues Reveals a Novel Cation - π Interaction between GABA and Beta2 Tyr97.” *Journal of Neuroscience* 27 (4): 886–92. <https://doi.org/10.1523/JNEUROSCI.4791-06.2007>.
- Papke David, Giovanni Gonzalez-Gutierrez i Claudio Grosman. 2011. “Desensitization of Neurotransmitter-Gated Ion Channels during High-Frequency Stimulation: A Comparative Study of Cys-Loop, AMPA and Purinergic Receptors.” *Journal of Physiology* 589 (7): 1571–85. <https://doi.org/10.1113/jphysiol.2010.203315>.
- Pless Stephen A. i Joseph W. Lynch. 2009. “Magnitude of a Conformational Change in the Glycine Receptor B1-B2 Loop Is Correlated with Agonist Efficacy.” *Journal of*

- Biological Chemistry* 284 (40): 27370–76. <https://doi.org/10.1074/jbc.M109.048405>.
- Plested Andrew J.R. 2014. “Don’t Flip out: AChRs Are Primed to Catch and Hold Your Attention.” *Biophysical Journal* 107 (1): 8–9. <https://doi.org/10.1016/j.bpj.2014.05.021>.
- Purohit Prasad i Anthony Auerbach. 2013. “Loop C and the Mechanism of Acetylcholine Receptor–Channel Gating.” *The Journal of General Physiology* 141 (4): 467–78. <https://doi.org/10.1085/jgp.201210946>.
- Rajendra Sundran, Joseph W. Lynch i Peter R. Schofield. 1997. “The Glycine Receptor.” *Pharmacology and Therapeutics* 73 (2): 121–46. [https://doi.org/10.1016/S0163-7258\(96\)00163-5](https://doi.org/10.1016/S0163-7258(96)00163-5).
- Rudolph Uwe i Hanns Möhler. 2014. “GABAA Receptor Subtypes: Therapeutic Potential in Down Syndrome, Affective Disorders, Schizophrenia, and Autism.” *Annu Rev Pharmacol Toxicol* 54: 483–507. <https://doi.org/10.1016/j.pestbp.2011.02.012>.Investigations.
- Rudolph Uwe i Hanns Möhler. 2004. “Analysis of GABAA Receptor Function and Dissection of the Pharmacology of Benzodiazepines and General Anesthetics Through Mouse Genetics.” *Annual Review of Pharmacology and Toxicology* 44 (1): 475–98. <https://doi.org/10.1146/annurev.pharmtox.44.101802.121429>.
- Rudolph Uwe i Hanns Möhler. 2006. “GABA-Based Therapeutic Approaches: GABAA Receptor Subtype Functions.” *Current Opinion in Pharmacology* 6 (1 SPEC. ISS.): 18–23. <https://doi.org/10.1016/j.coph.2005.10.003>.
- Rüsch Dirk i Stuart A. Forman. 2005. “Classic Benzodiazepines Modulate the Open-Close Equilibrium in Alpha1beta2gamma2L Gamma-Aminobutyric Acid Type A Receptors.” *Anesthesiology* 102 (4): 783–92. <https://doi.org/00000542-200504000-00014> [pii].
- Sauguet Ludovic, Azadeh Shahsavari, Frédéric Poitevin, Christèle Huon, Anaïs Menny, Àkos Némecz, Ahmed Haouz i wsp. 2014. “Crystal Structures of a Pentameric Ligand-Gated Ion Channel Provide a Mechanism for Activation.” *Proceedings of the National Academy of Sciences of the United States of America* 111 (3): 966–71. <https://doi.org/10.1073/pnas.1314997111>.
- Seljeset, Sandra, Duncan Laverty, i Trevor G. Smart. 2015. “Inhibitory Neurosteroids and the GABAA Receptor.” *Advances in Pharmacology* 72: 165–87.

<https://doi.org/10.1016/bs.apha.2014.10.006>.

- Sieghart Werner. 2000. “Unraveling the Function of GABA(A) Receptor Subtypes.” *Trends in Pharmacological Sciences* 21 (11): 411–13. [https://doi.org/10.1016/S0165-6147\(00\)01564-9](https://doi.org/10.1016/S0165-6147(00)01564-9).
- Sieghart Werner i Miroslav M. Savić. 2018. “International Union of Basic and Clinical Pharmacology. CVI: GABA A Receptor Subtype- and Function-Selective Ligands: Key Issues in Translation to Humans.” edytowany przez: Eliot H. Ohlstein. *Pharmacological Reviews* 70 (4): 836–78. <https://doi.org/10.1124/pr.117.014449>.
- Sigel Erwin i Michael E. Steinmann. 2012. “Structure, Function, and Modulation of GABAA Receptors.” *Journal of Biological Chemistry* 287 (48): 40224–31. <https://doi.org/10.1074/jbc.R112.386664>.
- Smith G B i Richard W. Olsen. 1995. “Functional Domains of GABA A Receptors.” *Trends in Pharmacological Sciences* 16 (5): 162–68. [https://doi.org/10.1016/S0165-6147\(00\)89009-4](https://doi.org/10.1016/S0165-6147(00)89009-4).
- Szczot Marcin, Magdalena Kisiel, Marta M. Czyzewska i Jerzy W. Mozrzymas. 2014. “ α 1F64 Residue at GABA(A) Receptor Binding Site Is Involved in Gating by Influencing the Receptor Flipping Transitions.” *The Journal of Neuroscience : The Official Journal of the Society for Neuroscience* 34 (9): 3193–3209. <https://doi.org/10.1523/JNEUROSCI.2533-13.2014>.
- Terejko Katarzyna, Przemysław T. Kaczor, Michał A. Michałowski, Agnieszka Dąbrowska i Jerzy W. Mozrzymas. 2020. “The C Loop at the Orthosteric Binding Site Is Critically Involved in GABAA Receptor Gating.” *Neuropharmacology* 166 (November 2019): 107903. <https://doi.org/10.1016/j.neuropharm.2019.107903>.
- Terejko Katarzyna, Michał A. Michałowski, Anna Dominik, Anna Andrzejczak i Jerzy W. Mozrzymas. 2021. “Interaction between GABAA Receptor α 1 and β 2 Subunits at the N-Terminal Peripheral Regions Is Crucial for Receptor Binding and Gating.” *Biochemical Pharmacology* 183 (November 2020): 114338. <https://doi.org/10.1016/j.bcp.2020.114338>.
- Thompson Andrew J., Henry A. Lester i Sarah C.R. Lummis. 2010. *The Structural Basis of Function in Cys-Loop Receptors. Quarterly Reviews of Biophysics*. Vol. 43. <https://doi.org/10.1017/S0033583510000168>.

Venkatachalan Srinivasan P. i Cynthia Czajkowski. 2008. “A Conserved Salt Bridge Critical for GABA(A) Receptor Function and Loop C Dynamics.” *Proceedings of the National Academy of Sciences of the United States of America* 105 (36): 13604–9. <https://doi.org/10.1073/pnas.0801854105>.

Wagner David A. i Cynthia Czajkowski. 2001. “Structure and Dynamics of the GABA Binding Pocket : A Narrowing Cleft That Constricts during Activation” 21 (1): 67–74. <https://doi.org/10.1523/JNEUROSCI.21-01-00067.2001>.

Zhu Chunyan, Li Chen, Liming Ou, Qingshan Geng, Wei Jiang, Xing Lv, Xiang Wu i wsp. 2019. “Mechanism of gating and partial agonist action in the glycine receptor” *bioRxiv* 786632. <https://doi.org/10.1101/786632>.

Zhu Shaotong, Colleen M. Noviello, Jinfeng Teng, Richard M. Walsh, Jeong Joo Kim i Ryan E. Hibbs. 2018. “Structure of a Human Synaptic GABAA Receptor.” *Nature* 559 (7712): 67–72. <https://doi.org/10.1038/s41586-018-0255-3>.

WYKAZ RYCIN

Ryc. 1 <i>Wizualizacja wybranych elementów strukturalnych receptora GABA_A typu $\alpha_1\beta_2\gamma_2$.</i>	8
Ryc. 2 <i>Przykładowe przebiegi czasowe prądów przewodzonych przez receptory GABA_A typu $\alpha_1\beta_2\gamma_2$, wywołane podaniem wysycającego stężenia agonisty (10 mM GABA).....</i>	11
Ryc. 3 <i>Schemat opisujący wiązanie cząsteczki agonisty do receptora</i>	11
Ryc. 4 <i>Schemat klasycznego mechanizmu aktywacji receptora, proponowany przez del Castillo i Katz (1957)</i>	12
Ryc. 5 <i>Schemat modelu kinetycznego uwzględniający wszystkie kluczowe stany, w których może przebywać receptor GABA_A podczas procesu aktywacji w warunkach wysycenia, wraz ze stałymi kinetycznymi definiującymi szybkości przejść pomiędzy nimi</i>	13

ZAŁĄCZNIKI

1. Dorobek naukowy

Wykaz publikacji

Pełne prace

1. Magdalena Jatczak-Śliwa, **Katarzyna Terejko**, Marek Brodzki, Michał A. Michałowski, Marta M. Czyżewska, Joanna M. Nowicka, Anna Andrzejczak, Rakenduvadhana Srinivasan, Jerzy W. Mozrzymas: Distinct Modulation of Spontaneous and GABA-Evoked Gating by Flurazepam Shapes Cross-Talk Between Agonist-Free and Liganded GABA_A Receptor Activity.

Front Cell Neurosci 12:1–18. (2018)

IF: 3.900

Pkt. MNiSW/KBN: 35.00

2. **Katarzyna Terejko**, Przemysław T. Kaczor, Michał A. Michałowski, Agnieszka Dąbrowska, Jerzy W. Mozrzymas: The C loop at the orthosteric binding site is critically involved in GABA_A receptor gating.

Neuropharmacology 166:107903. (2020)

IF: 4.431

Pkt. MNiSW/KBN: 140.00

3. **Katarzyna Terejko**, Michał A. Michałowski, Anna Dominik, Anna Andrzejczak, Jerzy W. Mozrzymas: Interaction between GABA_A receptor α_1 and β_2 subunits at the N-terminal peripheral regions is crucial for receptor binding and gating.

Biochem Pharmacol 183:114338. (2021)

IF: 4.960

Pkt. MNiSW/KBN: 100.00

Konferencje naukowe

1. **Terejko K.**, Sowa J., Hess G., "Unraveling electrophysiological diversity of the rat dorsal raphe nucleus neurons with the use of cluster analysis", 6th International Conference Aspects of Neuroscience, 25-27 listopada 2016, Warszawa, Polska; plakat

2. **Terejko K.** "Jeden mózg i dwie półkule - komunikacja międzypółkulowa i integrowanie informacji", BIOMED Interdyscyplinarność przyszłością nauki, 7-9 kwietnia 2017, Zieloniec, Polska; wystąpienie

3. **Terejko K.**, Brodzki M., Jatczak-Śliwa M., Andrzejczak A., Nowicka J., Mozrzymas J.W.; „Flurazepam enhances spontaneous activity of alpha1beta2gamma2L GABA_A receptors, both wild-type and mutated at the alpha1F64 residue in the agonist binding site”; 7th Conference Aspects of Neuroscience, 24-26 listopada 2017, Warszawa, Polska; plakat

4. Terejko K., Jatzak-Śliwa M., Brodzki M., Czyżewska M., Michałowski M., Nowicka J., Andrzejczak A., Srinivasan R., Mozrzymas J.W.; „Complex effect of benzodiazepines on GABA_A receptor mechanism of activation”; NEURONUS, 20-22 kwietnia 2018, Kraków, Polska; plakat

5. Jatzak-Śliwa M., Terejko K., Brodzki M., Michałowski M., Czyżewska M., Nowicka J., Andrzejczak A., Srinivasan R., Mozrzymas J.W.; „Flurazepam modulates gating of spontaneous and agonist-evoked GABA_A receptor activity via distinct mechanisms”; 11th Electrophysiological Conference, 25-26 maja 2018, Warszawa, Polska; wystąpienie

6. Terejko K., Dąbrowska A., Mozrzymas J.W.; „Rola beta2 F200 w obrębie struktury pętli C receptora GABA_A w etapie wiązania ligandu i bramkowania”; IX Symposium "Współczesna myśl techniczna w naukach medycznych i biologicznych, 22-23 czerwca 2018, Wrocław, Polska; plakat

7. Brodzki M., Jatzak-Śliwa M., Terejko K., Michałowski M., Nowicka J., Andrzejczak A., Srinivasan R., Mozrzymas J.W.; „Robust impact of flurazepam on spontaneous activity of GABA_A receptors indicates modulation of gating transitions by benzodiazepines”; 11th FENS Forum of Neuroscience, 7-11 lipca 2018, Berlin, Niemcy; plakat

8. Terejko K., Michałowski M., Dąbrowska A., Mozrzymas J.W.; „Point mutation at beta2 subunit loop C (F200) affects both binding and gating of the GABA_A receptor” 8th International Conference Aspects of Neuroscience, 23-25 listopada 2018, Warszawa, Polska; wystąpienie

9. Terejko K., Kaczor P. T., Michałowski M., Dąbrowska A., Mozrzymas J.W.; „ GABA_A beta2 subunit loop C shapes binding and gating properties of receptor activation”, 14th International Congress of the Polish Neuroscience Society, 28-30 sierpnia 2019, Katowice, Polska; plakat

10. Terejko K., Michałowski M.A., Dominik A., Andrzejczak A., Mozrzymas J.W.; „Extracellular domain intersubunit interaction of aromatic residues α F14 and β F31 substantially modulates GABA_AR gating.”, NEURONUS, 8-11 grudnia 2020, konferencja online; plakat

ŁĄCZNY IMPACT FACTOR: 13.291 (LICZBA PRAC: 3)

	Liczba punktów MNiSW/KBN
Do roku 2018	35.00
Do roku 2020	140.00
Do roku 2021	100.00
Razem:	275.00

2. Oświadczenia współautorów

mgr Anna Andrzejczak

Wrocław, 7.12.2020

Uniwersytet Wrocławski

Katedra Fizjologii i Neurobiologii Molekularnej

ul. Sienkiewicza 21, 50-335 Wrocław

obecnie:

Laboratorium Genetyki i Epigenetyki Chorób Człowieka

Zakład Terapii Doświadczalnej

Instytut Immunologii i Terapii Doświadczalnej PAN

Weigla 12, 53-114 Wrocław

OŚWIADCZENIE

Oświadczam, że w pracy:

Magdalena Jatczak-Śliwa, Katarzyna Terejko, Marek Brodzki, Michał A. Michałowski, Marta M. Czyżewska, Joanna M. Nowicka, Anna Andrzejczak, Rakenduvadhana Srinivasan, Jerzy W. Mozrzymas: **Distinct Modulation of Spontaneous and GABA-Evoked Gating by Flurazepam Shapes Cross-Talk Between Agonist-Free and Liganded GABA_A Receptor Activity.**

Front Cell Neurosci 12:1–18. (2018) <https://doi.org/10.3389/fncel.2018.00237>

Mój udział polegał na uzyskaniu części wyników eksperymentalnych poprzez prowadzenie rejestracji aktywności spontanicznej zmutowanych receptorów GABA_A w pozycji α_1F64 (α_1F64A oraz α_1F64C) w obecności flurazepamu i/lub pikrotoksyny oraz prądów wywołanych podaniem wysycającego stężenia agonisty w obecności flurazepamu z wykorzystaniem systemu do szybkiej perfuzji BioLogic wraz z analizą uzyskanych danych.

Oświadczam, że w pracy:

Katarzyna Terejko, Michał A. Michałowski, Anna Dominik, Anna Andrzejczak, Jerzy W. Mozrzymas: **Interaction between GABA_A receptor α_1 and β_2 subunits at the N-terminal peripheral regions is crucial for receptor binding and gating.**

Biochem Pharmacol 183:114338. (2021) <https://doi.org/10.1016/j.bcp.2020.114338>

Mój udział polegał na uzyskaniu 50% wyników eksperymentalnych związanych z badaniem krzywej „dawka-odpowiedź” poprzez prowadzenie rejestracji techniką *patch-clamp* makroskopowych prądów przewodzonych przez pojedynczo zmutowane receptory GABA_A w pozycjach α_1F14 i β_2F31 oraz podwójnie zmutowane w tych pozycjach, pod wpływem podania różnych stężeń agonisty wraz z analizą amplitudy uzyskanych odpowiedzi prądowych.



mgr Marek Brodzki
Uniwersytet Wrocławski
Katedra Fizjologii i Neurobiologii Molekularnej
ul. Sienkiewicza 21, 50-335 Wrocław

Wrocław, 9.12.2020

OŚWIADCZENIE

Oświadczam, że w pracy:

Magdalena Jatczak-Śliwa, Katarzyna Terejko, Marek Brodzki, Michał A. Michałowski, Marta M. Czyżewska, Joanna M. Nowicka, Anna Andrzejczak, Rakenduvadhana Srinivasan, Jerzy W. Mozrzymas: **Distinct Modulation of Spontaneous and GABA-Evoked Gating by Flurazepam Shapes Cross-Talk Between Agonist-Free and Liganded GABA_A Receptor Activity.**

Front Cell Neurosci 12:1–18. (2018) <https://doi.org/10.3389/fncel.2018.00237>

Mój udział polegał na uzyskaniu części wyników eksperymentalnych poprzez prowadzenie rejestracji aktywności spontanicznej pojedynczych kanałów jonowych receptorów GABA_A typu dzikiego oraz zmutowanych w pozycji α_1F64 w obecności flurazepamu oraz aktywności pojedynczych kanałów jonowych wywołanej podaniem wysycającego stężenia agonisty i pod wpływem modulacji przez flurazepam wraz z analizą uzyskanych danych, ponadto:

- analizie statystycznej otrzymanych danych;
- uczestnictwie w pisaniu części metodologicznej publikacji;
- przygotowaniu figur nr 2 oraz częściowo 5 i 6 w publikacji.



dr Marta M. Czyżewska
Uniwersytet Medyczny im. Piastów Śląskich we Wrocławiu
Katedra i Zakład Biofizyki i Neurobiologii
ul. T. Chałubińskiego 3a, 50-368 Wrocław

Wrocław, 8.12.2020

OŚWIADCZENIE

Oświadczam, że w pracy:

Magdalena Jatzak-Śliwa, Katarzyna Terejko, Marek Brodzki, Michał A. Michałowski, Marta M. Czyżewska, Joanna M. Nowicka, Anna Andrzejczak, Rakenduvadhana Srinivasan, Jerzy W. Mozrzyk: **Distinct Modulation of Spontaneous and GABA-Evoked Gating by Flurazepam Shapes Cross-Talk Between Agonist-Free and Liganded GABA_A Receptor Activity.**

Front Cell Neurosci 12:1–18. (2018) <https://doi.org/10.3389/fncel.2018.00237>

Mój udział polegał na uzyskaniu części wyników eksperymentalnych poprzez prowadzenie rejestracji techniką *patch-clamp* makroskopowych prądów wywołanych podaniem agonisty receptora GABA_A- kwasu γ -aminomasłowego oraz częściowego agonisty tego receptora - kwasu piperidyno-4-sulfonowego, także w obecności modulatora flurazepamu, na receptory GABA_A typu dzikiego, analizie uzyskanych danych oraz przygotowaniu figury nr 5 w publikacji.



mgr Agnieszka Dąbrowska

Uniwersytet Medyczny im. Piastów Śląskich we Wrocławiu
Katedra i Zakład Biofizyki i Neurobiologii
ul. T. Chałubińskiego 3a, 50-368 Wrocław

Wrocław, 4.12.2020

OŚWIADCZENIE

Oświadczam, że w pracy:

Katarzyna Terejko, Przemysław T. Kaczor, Michał A. Michałowski, Agnieszka Dąbrowska,
Jerzy W. Mozrzyk: **The C loop at the orthosteric binding site is critically involved in
GABA_A receptor gating.**

Neuropharmacology 166:107903. (2020),

<https://doi.org/10.1016/j.neuropharm.2019.107903>

Mój udział polegał na uzyskaniu części wyników eksperymentalnych poprzez prowadzenie rejestracji techniką *patch-clamp* prądów przewodzonych przez zmutowane receptory GABA_A w pozycji β_2 F200 pod wpływem podania wysycającego stężenia agonisty i modulacji przez flurazepam, analizie uzyskanych danych oraz przygotowaniu figury nr 4 w publikacji.



mgr Anna Dominik

Wrocław, 4.12.2020

Uniwersytet Medyczny im. Piastów Śląskich we Wrocławiu
Katedra i Zakład Biofizyki i Neurobiologii
ul. T. Chałubińskiego 3a, 50-368 Wrocław

OŚWIADCZENIE

Oświadczam, że w pracy:

Katarzyna Terejko, Michał A. Michałowski, Anna Dominik, Anna Andrzejczak, Jerzy W. Mozrzymas: **Interaction between GABA_A receptor α_1 and β_2 subunits at the N-terminal peripheral regions is crucial for receptor binding and gating.**

Biochem Pharmacol 183:114338. (2021) <https://doi.org/10.1016/j.bcp.2020.114338>

Mój udział polegał na uzyskaniu części wyników eksperymentalnych poprzez prowadzenie rejestracji techniką *patch-clamp* prądów przewodzonych przez podwójnie zmutowane receptory GABA_A w pozycjach $\alpha_1F14\beta_2F31$ pod wpływem podania wysycającego stężenia agonisty oraz z użyciem ditiotreitolu, analizie uzyskanych danych oraz przygotowaniu figury nr 3 w publikacji.



mgr inż. Magdalena Jatczak-Śliwa
Uniwersytet Wrocławski
Katedra Fizjologii i Neurobiologii Molekularnej
ul. Sienkiewicza 21, 50-335 Wrocław

Wrocław, 15.12.2020

OŚWIADCZENIE

Oświadczam, że w pracy:

Magdalena Jatczak-Śliwa, Katarzyna Terejko, Marek Brodzki, Michał A. Michałowski, Marta M. Czyżewska, Joanna M. Nowicka, Anna Andrzejczak, Rakenduvadhana Srinivasan, Jerzy W. Mozrzyk: **Distinct Modulation of Spontaneous and GABA-Evoked Gating by Flurazepam Shapes Cross-Talk Between Agonist-Free and Liganded GABA_A Receptor Activity.**

Front Cell Neurosci 12:1–18. (2018) <https://doi.org/10.3389/fncel.2018.00237>

Mój udział polegał na uzyskaniu części wyników eksperymentalnych poprzez prowadzenie rejestracji aktywności spontanicznej receptorów GABA_A typu dzikiego oraz zmutowanych w pozycji α_1F64 w obecności flurazepamu i/lub pikrotoksyny oraz prądów wywołanych podaniem wysycającego stężenia agonisty w obecności flurazepamu z wykorzystaniem systemu do szybkiej perfuzji BioLogic wraz z analizą uzyskanych danych, ponadto:

- analizie statystycznej otrzymanych danych;
- uczestnictwie w projektowaniu paradygmatu badawczego;
- uczestnictwie w pisaniu części metodologicznej w publikacji;
- uczestnictwie w pisaniu rozdziałów dotyczących wyników w publikacji;
- przygotowaniu figur nr 1 i 3 w publikacji;
- pełnieniu funkcji autora korespondencyjnego.

Magdalena Jatczak-Śliwa

dr inż. Przemysław T. Kaczor

Uniwersytet Medyczny im. Piastów Śląskich we Wrocławiu
Katedra i Zakład Biofizyki i Neurobiologii
ul. T. Chałubińskiego 3a, 50-368 Wrocław

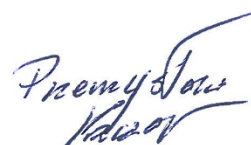
Wrocław, 8.12.2020

OŚWIADCZENIE

Oświadczam, że w pracy pt. „**The C loop at the orthosteric binding site is critically involved in GABA_A receptor gating.**” autorstwa Katarzyny Terejko, Przemysława T. Kaczora, Michała A. Michałowskiego, Agnieszki Dąbrowskiej i Jerzego W. Mozrzymasa **Neuropharmacology 166:107903. (2020),**
<https://doi.org/10.1016/j.neuropharm.2019.107903>

Mój udział polegał na uzyskaniu wyników eksperymentalnych odnoszących się do aktywności na poziomie pojedynczych kanałów jonowych (*single-channel, cell-attached*) receptorów typu GABA_A zmutowanych (substytucja reszty fenyloalaninowej na pozycji β_2 F200 na reszty tyrozynową, izoleucynową i cysteinową) oraz typu dzikiego (WT), ponadto:

- analizie statystycznej tak otrzymanych danych;
- modelowaniu kinetycznym i symulacjach nagrań/rejestracji *single-channel*;
- przygotowaniu figur nr 8, 9, 10, tabel 1, 2, 3;
- uczestnictwie w pisaniu części metodologicznej oraz rozdziałów 4.6 i 4.7 w wyżej wymienionej publikacji.



mgr inż. Michał A. Michałowski

Wrocław, 9.12.2020

Uniwersytet Medyczny im. Piastów Śląskich we Wrocławiu
Katedra i Zakład Biofizyki i Neurobiologii
ul. T. Chałubińskiego 3a, 50-368 Wrocław
Uniwersytet Wrocławski
Katedra Fizjologii i Neurobiologii Molekularnej
ul. Sienkiewicza 21, 50-335 Wrocław

OŚWIADCZENIE

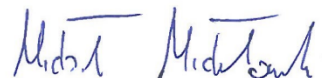
Oświadczam, że w pracy:

Magdalena Jatczak-Śliwa, Katarzyna Terejko, Marek Brodzki, Michał A. Michałowski, Marta M. Czyżewska, Joanna M. Nowicka, Anna Andrzejczak, Rakenduvadhana Srinivasan, Jerzy W. Mozrzymas: **Distinct Modulation of Spontaneous and GABA-Evoked Gating by Flurazepam Shapes Cross-Talk Between Agonist-Free and Liganded GABA_A Receptor Activity.**

Front Cell Neurosci 12:1–18. (2018) <https://doi.org/10.3389/fncel.2018.00237>

Mój udział polegał na uzyskaniu wyników *in silico* polegających na modelowaniu homologicznym, symulacjach dokowania ligandu do receptora GABA_A, trendowym modelowaniu kinetycznym makroskopowych odpowiedzi prądowych, ponadto:

- uczestnictwie w pisaniu części metodologicznej publikacji;
- przygotowaniu rozdziału „Model Simulations”;
- przygotowaniu figur nr 7, 8 i 9 w publikacji.



Oświadczam, że w pracy:

Katarzyna Terejko, Przemysław T. Kaczor, Michał A. Michałowski, Agnieszka Dąbrowska, Jerzy W. Mozrzymas: **The C loop at the orthosteric binding site is critically involved in GABA_A receptor gating.**

Neuropharmacology 166:107903. (2020),

<https://doi.org/10.1016/j.neuropharm.2019.107903>

Mój udział polegał na analizie *in silico*, będącej u podstaw wyboru zastosowanych mutacji receptora GABA_A, uzyskaniu wyników *in silico* polegających na modelowaniu homologicznym, symulacjach dokowania ligandu do receptora, modelowaniu struktury pętli C receptora, trendowym modelowaniu kinetycznym makroskopowych odpowiedzi prądowych, ponadto

- uczestnictwie w pisaniu części metodologicznej publikacji;
- przygotowaniu rozdziałów 4.1, 4.4 i 4.5;
- przygotowaniu figur nr 1, 5, 6 i 7 w publikacji.



Oświadczam, że w pracy:

Katarzyna Terejko, Michał A. Michałowski, Anna Dominik, Anna Andrzejczak, Jerzy W. Mozrzyk: **Interaction between GABA_A receptor α_1 and β_2 subunits at the N-terminal peripheral regions is crucial for receptor binding and gating.**

Biochem Pharmacol 183:114338. (2021) <https://doi.org/10.1016/j.bcp.2020.114338>

Mój udział polegał na analizie *in silico* będącej u podstawy wyboru zastosowanych mutacji receptora GABA_A, uzyskaniu wyników *in silico* polegających na porównaniu sekwencji genetycznych różnych receptorów pLGIC, modelowaniu homologicznym oraz analizie powstawania mostków disiarczkowych w podwójnie zmutowanym receptorze GABA_A w pozycjach α_1 F14 β_2 F31, ponadto:

- przeprowadzeniu obliczeniowej analizy termodynamicznej „*mutant cycle analysis*”
- uczestnictwie w pisaniu części metodologicznej publikacji;
- przygotowaniu rozdziału 3.1;
- przygotowaniu figury nr 1 w publikacji.



Prof. dr hab. Jerzy W. Mozrzykas
Uniwersytet Medyczny im. Piastów Śląskich we Wrocławiu
Katedra i Zakład Biofizyki i Neurobiologii
ul. T. Chałubińskiego 3a, 50-368 Wrocław

Wrocław, 27.01.2021

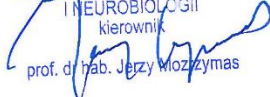
OŚWIADCZENIE

Oświadczam, że w pracy:

Magdalena Jatczak-Śliwa, Katarzyna Terejko, Marek Brodzki, Michał A. Michałowski, Marta M. Czyżewska, Joanna M. Nowicka, Anna Andrzejczak, Rakenduvadhana Srinivasan, Jerzy W. Mozrzykas: **Distinct Modulation of Spontaneous and GABA-Evoked Gating by Flurazepam Shapes Cross-Talk Between Agonist-Free and Liganded GABA_A Receptor Activity.**

Front Cell Neurosci 12:1–18. (2018) <https://doi.org/10.3389/fncel.2018.00237>

Mój udział polegał na opracowaniu i koncepcji projektów grantowych OPUS DEC-2013/11/B/NZ3/00983 oraz MAESTRO DEC-2015/18/A/NZ1/00395 będących podstawą dla przeprowadzonych badań oraz uzyskaniu finansowania z Narodowego Centrum Nauki, nadzorze i konsultacjach merytorycznych związanych z realizacją założeń badawczych, udziale w projektowaniu metodologii eksperymentalnych, analizie danych oraz pisaniu pierwotnej wersji artykułu oraz na redagowaniu jego statecznej wersji.

Uniwersytet Medyczny we Wrocławiu
KATEDRA I ZAKŁAD BIOFIZYKI
I NEUROBIOLOGII
kierownik

prof. dr hab. Jerzy Mozrzykas


Oświadczam, że w pracy:

Katarzyna Terejko, Przemysław T. Kaczor, Michał A. Michałowski, Agnieszka Dąbrowska, Jerzy W. Mozrzykas: **The C loop at the orthosteric binding site is critically involved in GABA_A receptor gating.**

Neuropharmacology 166:107903. (2020),

<https://doi.org/10.1016/j.neuropharm.2019.107903>

Mój udział polegał na opracowaniu i koncepcji projektu grantowego MAESTRO DEC-2015/18/A/NZ1/00395 będącego podstawą dla przeprowadzonych badań oraz uzyskaniu finansowania z Narodowego Centrum Nauki, nadzorze i konsultacjach merytorycznych związanych z realizacją założeń badawczych, udziale w projektowaniu metodologii eksperymentalnych, analizie danych oraz pisaniu pierwotnej wersji artykułu oraz na redagowaniu jego statecznej wersji.

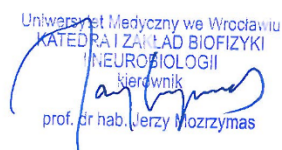
Uniwersytet Medyczny we Wrocławiu
KATEDRA I ZAKŁAD BIOFIZYKI
I NEUROBIOLOGII
kierownik

prof. dr hab. Jerzy Mozrzykas

Oświadczam, że w pracy:

Katarzyna Terejko, Michał A. Michałowski, Anna Dominik, Anna Andrzejczak, Jerzy W. Mozrzyk: **Interaction between GABA_A receptor α_1 and β_2 subunits at the N-terminal peripheral regions is crucial for receptor binding and gating.**

Biochem Pharmacol 183:114338. (2021) <https://doi.org/10.1016/j.bcp.2020.114338>

Mój udział polegał na opracowaniu i koncepcji projektu grantowego MAESTRO DEC-2015/18/A/NZ1/00395 będącego podstawą dla przeprowadzonych badań oraz uzyskaniu finansowania z Narodowego Centrum Nauki, nadzorze i konsultacjach merytorycznych związanych z realizacją założeń badawczych, udziale w projektowaniu metodologii eksperymentalnych, analizie danych oraz pisaniu pierwotnej wersji artykułu oraz na redagowaniu jego statecznej wersji.

Uniwersytet Medyczny we Wrocławiu
KATEDRA I ZAKŁAD BIOFIZYKI
NEUROBIOLOGII
Kierownik

prof. dr hab. Jerzy W. Mozrzyk

mgr inż. Joanna M. Nowicka
Uniwersytet Medyczny im. Piastów Śląskich we Wrocławiu
Katedra i Zakład Biofizyki i Neurobiologii
ul. T. Chałubińskiego 3a, 50-368 Wrocław

Wrocław, 8.12.2020

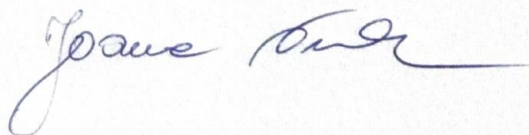
OŚWIADCZENIE

Oświadczam, że w pracy:

Magdalena Jatczak-Śliwa, Katarzyna Terejko, Marek Brodzki, Michał A. Michałowski, Marta M. Czyżewska, Joanna M. Nowicka, Anna Andrzejczak, Rakenduvadhana Srinivasan, Jerzy W. Mozrzymas: **Distinct Modulation of Spontaneous and GABA-Evoked Gating by Flurazepam Shapes Cross-Talk Between Agonist-Free and Liganded GABA_A Receptor Activity.**

Front Cell Neurosci 12:1–18. (2018) <https://doi.org/10.3389/fncel.2018.00237>

Mój udział polegał na uzyskaniu części wyników eksperymentalnych poprzez prowadzenie techniką *patch-clamp* rejestracji z wykorzystaniem systemu do szybkiej perfuzji BioLogic, aktywności spontanicznej receptora GABA_A typu dzikiego pod wpływem modulacji przez flurazepam wraz ze wstępną analizą uzyskanych danych.



mgr Rakenduvadhana Srinivasan

Helsinki, 6.12.2020

Uniwersytet Wrocławski

Katedra Fizjologii i Neurobiologii Molekularnej

ul. Sienkiewicza 21, 50-335 Wrocław

obecnie:

University of Helsinki

Laboratory of Neurobiology,

Faculty of Biological and Environmental Sciences, Biokeskus 3,

Viikinkaari 1, Helsinki 00790

OŚWIADCZENIE

Oświadczam, że w pracy:

Magdalena Jatczak-Śliwa, Katarzyna Terejko, Marek Brodzki, Michał A. Michałowski, Marta M. Czyżewska, Joanna M. Nowicka, Anna Andrzejczak, Rakenduvadhana Srinivasan, Jerzy W. Mozrzymas: **Distinct Modulation of Spontaneous and GABA-Evoked Gating by Flurazepam Shapes Cross-Talk Between Agonist-Free and Liganded GABA_A Receptor Activity.** *Front Cell Neurosci* 12:1–18. (2018) <https://doi.org/10.3389/fncel.2018.00237>

Mój udział polegał na uzyskaniu części wyników eksperymentalnych poprzez prowadzenie rejestracji aktywności pojedynczych kanałów jonowych zmutowanych receptorów GABA_A w pozycji α_1F64C .



Rakenduvadhana Srinivasan 6.12.20